Thermal degradation of packaging plastic waste and its conversion into fuel by pyrolysis

Thesis submitted in partial fulfilment of the

requirements for the degree of

Doctor of Philosophy

by

Pallab Das

(136107016)

Department of Chemical Engineering

Indian Institute of Technology Guwahati

Guwahati – 781039

Assam, India

October, 2019

Thermal degradation of packaging plastic waste and its conversion into fuel by pyrolysis

Pallab Das

Department of Chemical Engineering
Indian Institute of Technology Guwahati
Guwahati – 781039, Assam, India

STATEMENT

I do hereby declare that the content embodied in this thesis entitled "**Thermal degradation of packaging plastic waste and its conversion into fuel by pyrolysis**" is the result of investigations carried out by me at the Department of Chemical Engineering, Indian Institute of Technology Guwahati, India, under the guidance of **Dr. Pankaj Tiwari**. In keeping with the general practice of reporting scientific observations, due acknowledgements have been made wherever the work described is based on the finding of other investigators.

Date: Pallab Das

Department of Chemical Engineering
Indian Institute of Technology Guwahati
Guwahati – 781039, Assam, India

CERTIFICATE

It is to certify that thesis entitled "**Thermal degradation of packaging plastic waste and its conversion into fuel by pyrolysis**" submitted by **Mr. Pallab Das (Roll no.: 136107016)** for the award of the degree of Doctor of Philosophy has been carried out under my guidance and supervision. The work documented in this thesis has not been submitted any other University or Institute for the award of any degree.

Date:

(Dr. Pankaj Tiwari)
Associate Professor
Department of Chemical Engineering
Indian Institute of Technology Guwahati
Guwahati – 781039, Assam, India

Dedicated to my

Parents

ACKNOWLEDGEMENTS

Firstly and foremost, I would like to express my sincere gratitude to my supervisor **Dr. Pankaj Tiwari** for the continuous support during my Ph. D. study and related research, for his patience, motivation and immense knowledge. I like to thank him for encouraging my research and for enabling me to develop as a research scientist. His advice on both my research as well as my career has been priceless. His uncompromising approaches to complete the experimental part, analysis of the data and preparation of the manuscripts have helped me a lot in completing my research objectives.

I would also thank my doctoral committee members Prof. Vimal Katiyar, Prof. G. Pugazhenti from the Department of Chemical Engineering and Prof. A. S. Achalkumar from the Department of Chemistry at Indian Institute of Technology Guwahati for their valuable comments and suggestions towards the improvement of my research works. I would also like to thank Prof. Ramagopal Uppaluri for his valuable advice and help.

I am also thankful to all the faculty members, staff members, and scientific members in the Department of Chemical Engineering for their cooperation in analytical laboratory and others. I would also like to extend my acknowledgement to the Department of Science and Technology (DST), New Delhi for their financial support.

I am thankful to the Central Instrument Facility (CIF) of Indian Institute of Technology Guwahati for allowing me to carry out the crucial analyses, which have been very important in this research work. In this regard, I would like to acknowledge all the members of CIF for their assistance. I am thankful to the Centre of Excellence for Sustainable Polymers (CoE-SUSPOL) at Indian Institute of Technology Guwahati for providing the virgin plastic samples and also allow me to use the research facilities whenever needed. I am also thankful

to the Centre for energy, Indian Institute of Technology, Guwahati and the scientific officers of the centre for the help in using the bomb calorimeter. Special thanks to Deborshi Baruah of Centre for Energy (IITG), for his valuable time and help.

I would also like to thank all the members and co-researchers of Energy Conversion Technology Laboratory (ECTL) for their help and support. Special thanks to Dr. Rahul Saha, Dr. Ali Reshad, Bhargav Baruah for their regular help, support and encouragement during highs and lows of my stay at IIT Guwahti. I would also like to thank my fellow from the Department of Chemical Engineering Abhishek Shukla, Atanu Kumar Paul, Dr. Rajkumar Das, Jitendra Singh Rawat, Chittaranjan Barek, Robinson Timung, Monica Singh, Narendran S, Gaurhari Chakraborty, Dr. Anand Bharti, Shasanka Sekhar Borkotoky, Dr. Babool Prashad, Medha Mili, Dr. Rahul Patwa, Somen Mondal for their fruitful discussion, friendly behaviour and assistance. A special thanks to my best friends of life Pranjal Sarkar and Santu Kundu for their support and encouragement throughout my PhD.

Last but not the least; I would like to thank my parents and my family for their patience and unconditional support throughout the PhD as well the journey of my life. Their love, courage, care and sacrifice have made it possible for me to come so far.

ABSTRACT

Plastics are standard group of synthetic materials, produced from high molecular weight organic molecules mixed with different additives etc. Modern plastics have extensive use due to its high tensile strength, durability, lightweight, flexibility and low cost of production. The global production of plastics keeps on increasing and so does the waste generation. It has been estimated that over 8300 million metric tons (MMT) of virgin plastic has been manufactured till date and approximately 6300 MMT of plastic waste has been generated. The lifetime span of plastic products varies from weeks for packaging to several years for building appliances. Packaging plastics are major contributor to the vastly generated plastic waste. It has been estimated that around 80% of the waste plastic generated has been accumulated in landfills and in the natural habitats like rivers and oceans.

Plastics are produced mostly form fossil fuel resources and possess high calorific value as a solid waste. Useful chemicals and fuels can be produced from the plastic waste. Packaging plastics, used containers, used toothbrush and broken plastic utensils are very common in the dry solid waste that is generated in any household. These plastics are also abundantly present in municipal solid waste (MSW).

The common composition of the plastic waste are low and high density polyethylene (LDPE and HDPE), polypropylene (PP), polystyrene (PS), and polyethylene terephthalate (PET), and polyvinylchloride (PVC), Poly(methyl methacrylate) (PMMA) along with the rubber tyre, polymer composites etc. The primary objective

of this research is to develop an innovative, cost sa[]vvy, naturally benevolent and economical process to recover targeted value-added product from packaging plastic waste by pyrolysis.

Plastic samples were collected from household solid waste as well as virgin samples were procured from the market. Polyolefins such as LDPE, HDPE and PP were chosen for both thermogravimetric analysis (TGA) and lab scale pyrolysis to produce fuel. Virgin polylactic acid (PLA) and polyethylene terephthalate from waste soft drink bottles (PET-SDB) were also considered to study their degradation behaviour under thermal process like pyrolysis.

The non-isothermal TGA analysis under inert (N_2) atmosphere was carried out at seven heating rates ranging from 5 °C/min to 50 °C/min between the temperature range of 30 – 700 °C. The TGA analysis provided the information of possible degradation range of individual materials, their onset temperature (T_o), peak degradation temperature (T_m) and degradation data for kinetic analysis. Isoconversional methods like Friedman, Kissinger-Akahira-Sunnose (KAS), Ozawa-Flynn-Wall (OFW), Staring and advance isoconversional method (AIC) were used to calculate the variable activation energy (E_α). The reaction model $\left(f(\alpha)\right)$ was calculated with the help of Criados' masterplot technique. The pre-exponential factor (A_α) was calculated by substituting E_α and $\left(f(\alpha)\right)$ and experimental values of $\left(d\alpha/dt\right)$ in the Arrhenius equation for each conversion values by applying the isoconversional principle for multi heating rate data. To validate the kinetic data

simulated TGA plots (conversion vs temperature) were constructed by solving the differential rate equation numerically. Kinetic parameters obtain from AIC method gave the best-fitted linearity coefficient between experimental and simulated conversion vs temperature data. The range of activation energy from the AIC method were found in the range of 170 – 231 kJ/mol, 143 -233 kJ/mol, 133 – 173 kJ/mol, 99 – 116 kJ/mol and 198 – 226 kJ/mol for LDPE, HDPE, PP, PLA and PET-SDB respectively. The isothermal TGA data were processed according to McCallum method and the variable activation energy values were reported up to the conversion it reached under the isothermal period at lowest temperature. To understand the composition of the evolve gases generated during the plastic degradation a thermogravimetry (TG) coupled with Fourier transform infrared soectroscopy (FTIR) data was generated for all the plastic samples at a heating rate of 10 °C/min. Real time evolve gas analysis during thermal degradation helped in choosing the right type of material for lab-scale pyrolysis.

Virgin and waste samples of LDPE, HDPE and PP were converted into plastic derived oil (PDO), gases and solid residue by low temperature (300 °C to 400 °C) slow pyrolysis (long isothermal holding time) in a semi-batch reactor (fast heating rate was employed to heat the furnace from ambient to final temperature). The PDO samples obtained had shown variation in their compositions and fuel properties based on the pyrolysis temperature. PDOs from the pyrolysis of PP has high octane number (~92) and low viscosity. Noticeably, PDO samples obtained at low temperature pyrolysis are lighter with low viscosity, octane number and having high

calorific value. ^{1}H NMR analysis revealed that the oil samples mostly consists of paraffinic and olefinic hydrocarbon. Simulated distillation (SimDist) of PDO indicates that the liquid products resemble characteristic closer to middle distillate of petroleum fraction having very low pour point and flash point. The temperature with long pyrolysis time also influenced the evolved gas composition and yield. Trace amount of hydrogen, carbon monoxide, and carbon dioxide were present in the gaseous product along with various hydrocarbon gases ranging from C_1–C_5. Further, the concept of slow pyrolysis of the packaging plastics was explored by decreasing the heating rate to 1 °C/min to a final temperature of 400 °C (reactor temperature). The product samples (liquid/gas) were collected at regular intervals based on their inception. Product analysis revealed that the quality of the PDOs could be controlled by manipulating the temperature either by decreasing heating rate or increasing the total heating time (isothermal/non-isothermal). Presence of polypropylene in the feed resulted in the production of PDOs with branch-chain hydrocarbon components with high isoparaffin index, high H/C ratio and high research octane number (RON). The PDOs obtained (for all feed studied) at the early stages of the degradation process have light hydrocarbon liquid fractions belonging to light and middle distillate of petroleum (C_6 – C_{20}). The yield of both light and middle fractions decreased as the pyrolysis reactor temperature reached the maximum value (~400 °C). Gas evolution pattern depends on both pyrolysis temperature and the feed composition. Propylene was found more dominating among other major components

of gases like methane, ethane, ethylene, propane, n-butane, 1-butene, isobutylene and n-pentane etc.

The thesis develops the in-depth understanding of pyrolysis of packaging plastic waste and the degradation characteristic under non-isothermal and isothermal heating. The concept of slow pyrolysis at low temperature introduced a new area in the field of thermal treatment of plastics. Both isothermal and Non-isothermal slow pyrolysis of polyolefins (LDPE, HDPE and PP) provided a detail understanding of the influence of reaction temperature on the product distribution. The utilization of slow pyrolysis as an alternative approach to produce targeted value added product (gasoline/diesel) from plastic waste is significant considering the plastic disposal and management issues. More investigations with respect to streamlining the process condition, process design and prudent assessment are required to scale up the process. This study provides valuable insights, which may help designing and optimizing pyrolysis process plant to convert packaging plastic waste into valuable fuel.

Table of Contents

List of Tables

Chapter 1

Chapter 2

Chapter 3

Chapter 4

Chapter 5

Appendix A

List of Figures

Chapter 1

Chapter 2

Chapter 4

Chapter 5

Appendix A

ACRONYMS AND NOMENCLATURE

A	Pre-exponential factor (1/min)
AIC	Advance isoconversional method (-)
Al_2O_3	Aluminium oxide (alumina) (-)
API	American petroleum institute (-)
ASTM	American society for testing and materials (-)
CPCB	Central pollution control board (-)
DTG	Differential thermal gravimetric (-)
E	Activation energy (kJ/mol)
$f(\alpha)$	Reaction mechanism (-)
FBP	Fluidised bed pyrolysis (-)
FTIR	Fourier transform infrared spectrometry (-)
$g(\alpha)$	Integral form of rate equation (-)
GCV	Gross calorific value (kJ/kg)
HDPE	High density polyethylene (-)
HHV	Higher heating value (kJ/kg)
i	Various temperature program (ranging from 1 to n, n being the total number of temperature program) (-)
I	Symbol represents integral function (-)
ICTAC	International committee of thermal analysis and calorimetry (-)
IP	Induction period (-)
j	Suffix represents the temperature program other than i^{th} program, $i \neq j$ (-)
KAS	Kissinger-Akahira-Sunnose (-)

KV	Kinematic viscosity (-)
LDPE	Low density polyethylene (-)
LHV	Lower heating value (kJ/m^3)
MMT	Million metric tonne (-)
MSW	Municipal solid waste (-)
NHV	Net calorific value (MJ/m^3)
NiO	Nickel oxide (-)
OFW	Ozawa-Flynn-Wall (-)
PDO	Plastic derived oil (-)
PE	Polyethylene (-)
PET-SDB	Polyethylene terephthalate from waste soft drink bottles (-)
PLA	Polylactic acid (-)
PP	Polypropylene (-)
R	Universal gas constant (8.314 J/mol/K)
T	Temperature (°C)
t	Time (min)
TDP	Tonnes per day (-)
T_e	End degradation temperature (°C)
TGA	Thermal Gravimetric Analysis (-)
T_m	Maximum degradation temperature (°C)
T_o	Onset degradation temperature (°C)
T_α	Distributed temperature with conversion (°C)
t_α	Time corresponding any particular conversion (α)
ULSD	Ultra low sulphur diesel (-)
W	Weight of sample at any temperature during degradation(mg)
W_0	Initial weight of the sample (mg)

W_∞	Residual weight (mg)
$Z(\alpha)$	$f(\alpha) \times g(\alpha)$
ZSM5	Zeolite socony mobil–5 (-)
α	Conversion (-)
Φ	Minimization function of E_α

Chapter 1

INTRODUCTION AND LITERATURE REVIEW

Polymers and plastics
Plastic waste
Disposal techniques of plastic wastes
Pyrolysis
Objectives
Thesis organisation

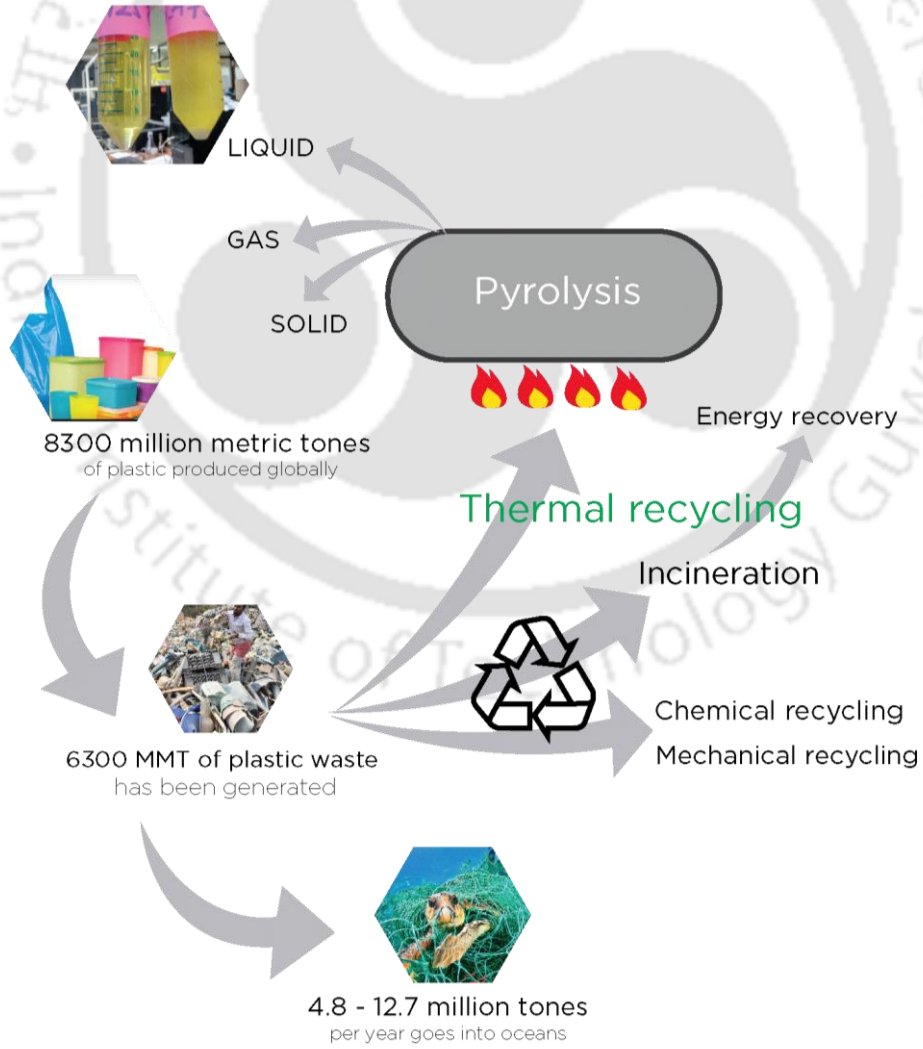

1 Introduction and literature review

1.1 Introduction

Over the years, the scientific community has come up with many breakthrough inventions and discoveries. The vast majority of those discoveries explain our existence in the universe and others just help to make our life easier. From the invention of the printing press in the 15th century to the modern day invention of lithium-ion battery, many such pioneer inventions constantly helping humankind to evolve socially and intellectually. One such technological breakthrough occurred in the dawn of the 20th century when scientist Jeo Baekeland (1907) invented a resin (Bakelite) from phenol and formaldehyde [1]. The bakelite resin can be moulded into various articles with high strength and durability. Bakelite, until today, has been used in many items including billiard balls, heat resistant layers, machine parts etc. This prompted the generation of different polymers with enhanced quality in other laboratories. Within a few decades, both polymer/plastic production increased and the new polymer manufacturing technologies were developed around the world. The plastic became a part of daily life and associated with numerous human activity. During the course of the plastic age human population also increased in many folds. With better technology, communication and modern urban lifestyle the demand of many consumer goods like that of plastic products are also increasing at a faster rate.

On the other hand, the depletion of fuel reserves in recent time increases the demand for renewable energy and efficient utilization of the available resources including waste. The waste can be considered as 'renewable' source since the amount of waste generation is rising day by day and complete waste recycling is still not achievable [2,3]. The waste can be capable of being replenished and not exhausted by its use.

Current global estimation of municipal solid waste (MSW) generation is approximately around 1.3 billion tonnes per year and it is expected to increase up to 2.2 billion tonnes by the year 2025 [4]. The global MSW generation rate is estimated to be in the range of 1.2 – 1.42 kg per person per day [4]. The waste generation rate is significantly influenced by economic development, industrial growth, public habits, and local climate. In general, higher the economic development and urbanisation, more is the solid waste generation [4]. The composition of MSW also varies region to region based on the economic and social background. The MSW approximate composition of India and Globally is shown in Fig. 1.1. These composition data were collected from the urban development series papers published inWorld bank [4] and the report published in the central pollution control board (CPCB), India in 2016 [5,6]. However, in both the cases the major portion of the wastes are the organic waste, which are biodegradable, and modern landfilling is a preferable choice of disposal. On the other hand the papers, glass, metals have good recycle values (mechanical/chemical). Around 10% of the waste consists of plastic waste [7].

The properties of plastic, which influence its disposal, are [7,8]:

i. Non-biodegradable nature of most of the plastics.

ii. Source material such as petroleum resources or biomass.

iii. Density of the plastic products as it effects the volume of the trash.

However, most of the plastics (commodity) is recycled into substandard products by applying minor chemical and mechanical processes. The packaging plastics are major contributor to any plastic waste stream. Packaging plastics are non-homogeneous, occupies large volume (lightweight), and are less suitable for chemical and mechanical recycling. Thermal treatments like combustion, incineration, and pyrolysis are some of the familiar processes to convert the plastic waste into useful fuel, chemical and thermal energy to produce power [9].

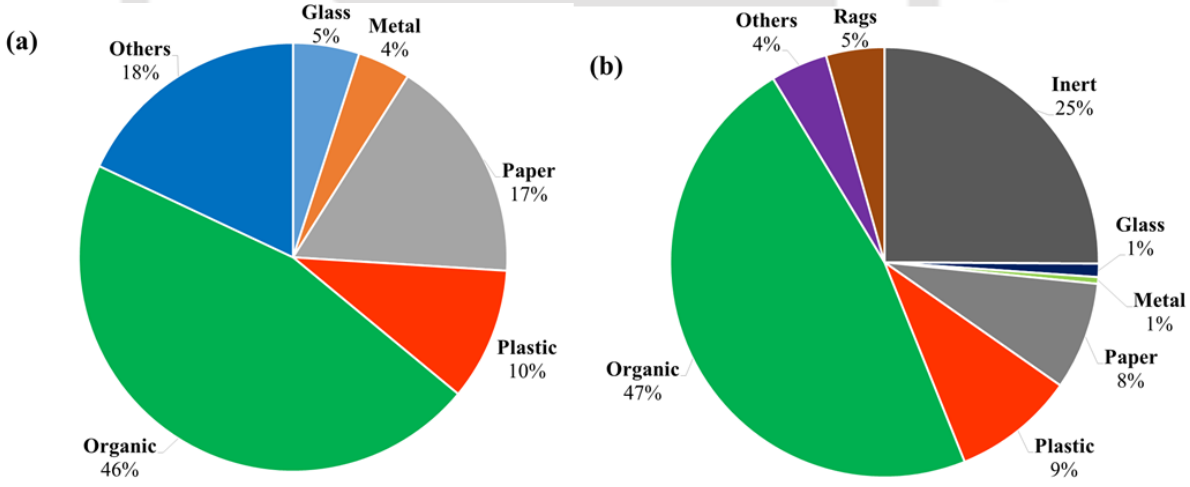

Fig. 1. 1: MSW composition of (a) global and (b) India

1.2 Plastic waste and its environmental impact

Plastics are standard groups of synthetic or natural materials produced from high molecular weight polymer chains consist of carbon as a sole or major element mixed

with other polymers and additives, which influence its physical and chemical properties. Plastics are highly durable, strong, elastic, and less expensive to produce, which make these material an ideal choice for packaging and storage applications. The plastics are very useful because of its large range of physical and chemical attributes like strength, durability, lightweight, flexibility, resistance to the extremity (thermal, electrical and chemical) and their ability to mould into different shapes [10]. The global production of plastics keeps on increasing and so does the waste generation. The worldwide production of plastics (polymer resins, fibre etc.) in the year 2015 was 381 million metric tons (MT) and production has been increased by 75% since the year 2000 [11]. The per capita consumption of plastics in India is around 11 kg/year (2016) whereas average global consumption is 28 kg/year [6]. The major share of plastic consumption is in the packaging application (~44%) and the growth in the production of packaging plastics has been accelerated due to global shift from reusable to single-use containers [11]. As a result, the presence of plastic waste in the municipal solid waste (MSW) increases from less than 1% in 1960 to more than 10% in recent years [8]. The life span of plastics products varies from weeks for packaging to several years for building appliances [7,12].

Municipal plastic waste primarily consists of low-density polyethylene (LDPE), high-density polyethylene (HDPE), poly(ethylene terephthalate) (PET), polypropylene (PP), polystyrene (PS), and poly(vinyl chloride) (PVC). Due to the lack of management from the governing organizations, the plastic waste goes in to the

dumping sites along with other wastes. In India, 60% of total plastic waste is recycled and rest goes for landfilling and incineration [6].

Plastics are non-biodegradable and the plastic waste generation leads to huge accumulation, instead of decay, in the landfills or in the various natural habitats like rivers and oceans. An estimated amount of 4.8 to 12.7 million MT of plastic waste debris can be found in all the oceans[8]. This situation getting worsen due to the global increase of plastic waste generation, which raise the concern regarding the adverse consequences to marine life and potentially to human health [13] . India generates 15342 tons of plastic waste per day (TDP) out of 0.14 million TDP of municipal solid waste which is responsible for many socio-environmental complications in recent times, likes of flash flood in cities, unavailability of MSW dumping sites, polluted cities and natural habitats etc. The thermal treatments such as combustion or incineration are able to eliminate the plastic waste permanently but such processes generate harmful emissions to the environment. Recycling (mechanical/chemical) is a possible alternative of plastic waste disposal. However, most of the recycling processes are costly, energy intensive and end up producing low-grade products. In the process of sustainable waste management, pyrolysis is one of the promising technique, which is very viable process in the treatment of municipal solid waste containing carbonaceous materials like plastics and biomass.

1.3 Plastic waste management and disposal technique

Plastic waste consists of around 10% of MSW and most of the plastic wastes are composed of packaging materials. Collection and segregation of the plastic waste from MSW is a challenging issue. The best way to segregate is at the source of generation by providing separate colour coded recycle bins (Fig. 1.2). However, a proper collection system varies from country to country based on the economic status of the country (Fig. 1.3). In low-income countries, like India the collection services make up the most of the municipality's solid waste management budget (as high as 80 to 90% in many cases), yet collection rates tend to be much lower, leading to lower collection frequency[14].

Plastic waste disposal and recycle can be carried out in various different ways and these methods are generally classified into three categories: primary, secondary and tertiary recycling.

Fig. 1. 2: Separate garbage containers, Singapore (Urban development series – knowledge papers)[4]

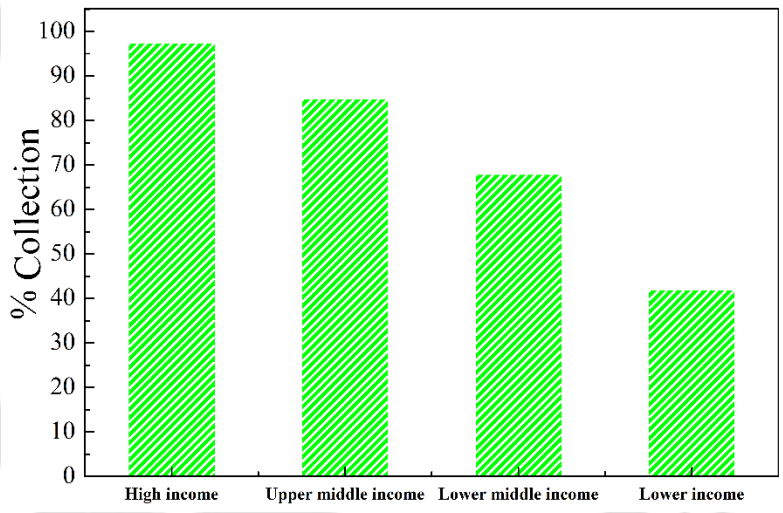

Fig. 1. 3: Waste collection (%) by income level of the countries (Urban development series –knowledge papers)[4]

1.3.1 *Primary and secondary (mechanical) recycling*

Primary and secondary recycling mainly concern the mechanical means of recycling of plastic waste such as grinding, washing, separating, drying, re-granulating, extrusion and compounding [15]. Mechanical processes are utilized to produce recyclates from plastic waste. Primary recycling is the process of producing the same

or similar products whereas secondary recycling produces products with substandard quality such as dustbins, furniture, plastic vases etc. Primary recycling needs pure and homogenous plastic wastes (in-plant scrap) while secondary recycling uses post-consumer plastic. High production costs are the concern in the implementation of primary and secondary recycling.

1.3.2 *Tertiary (chemical and thermal) recycling*

Tertiary or chemical recovery of plastic waste is a promising aspect in the recovery of valuable chemicals and fuels [16-18]. The principle of chemical recycling lies behind the alteration of chemical structure of the polymer by depolymerisation. The major advantages of chemical recycling over mechanical recycling is that it allows the processing of the heterogeneous and contaminated plastics with limited pre-treatment. Chemical recycling makes it possible to convert plastics like polyethylene terephthalate (PET) and nylon into their monomer units (feedstock recycling), while polyolefin type of plastics produce a mixture containing numerous components to be used as fuel. Processes such as dissolution, hydrogenation, gasification, pyrolysis, and catalytic cracking all comes under chemical recycling of plastics. Pyrolysis or thermolysis of plastic is a process of thermal decomposition of plastics under inert or oxygen starving condition. These processes are able to convert high molecular weight plastic into low molecular weight hydrocarbons and chemicals [19,20]. Process economy and technology up-gradation in the process of plastic pyrolysis is still improving for large-scale utilization [15].

The heat recovery processes like combustion, incineration and gasification areconsidered as tertiary recycling processes, however, they are also separately identified as quaternary recycling processes [15].

1.4 Thermal treatments of solid waste disposal

Combustion and incineration processes are the trivial thermal processes applied in the disposal of plastic wastes to produce energy. Contrarily, pyrolysis and gasification processes are used to recover value added chemicals and fuels from the plastic waste by thermal means. The advantages of combustion and incineration processes are that they consume less energy, require minor pre-treatment, and produce a significant amount of energy that can store and use in other purpose but also produce toxic gases and hazardous solid residue etc., which is not adequate for the sustainable environment.

1.4.1 *Combustion process*

Combustion is a fast chemical reaction between combustible material(s) and an oxidizing agent. Generally, combustion takes place in the presence of oxygen. Combustion of plastics under uncontrolled environment generates black plumes of smoke consists of toxic volatiles. In addition to that, large amount of greenhouse gases such as methane, carbon dioxides and particulate matters also emit to the atmosphere [21,22]. Therefore exit gases of combustion needs treatment to recover the harmful emission before releasing to the atmosphere.

1.4.2 *Incineration process*

Incineration is a high-temperature combustion process where organic matters from wastes were burnt and converted into ash, flue gas and heat. Heat generated from the incineration can be used in the production of electricity. Incineration process can able to reduce significant mass and volume of the waste stream. The ashes produced in the incineration process are the inorganic part of the waste that occupies lesser volume compared to the original waste and can be discarded safely. At a very high temperature, the ash produced in the incineration can be vitrified to produce high-density glassy material, which is a possible building material [23]. However, the incineration process is a highly contentious method because, incomplete incineration can produce carbon monoxide (CO), gaseous dioxins, polychlorinated dibenzo-p-dioxins (PCDP), polychlorinated dibenzofurans (PCBF) and other harmful substances [24].

1.4.3 ***Gasification process***

Gasification is one of the thermal disposal process used in the solid waste treatment and also used in the production of synthetic gas from carbonaceous material. In the gasification process the carbonaceous materials (plastics) are heated at high temperature (≈700 °C) to produce gaseous fuels such as syngas by supplying control amount of oxygen and steam. He, et al. [25] were able to produce syngas (H_2 + CO) from waste polyethylene in a bench scale downstream fixed bed reactor in the presence of NiO/Al_2O_3 catalyst in the temperature range of 700 – 900 °C. Coal

gasification [26] is a well-established technology to convert solid fossil fuel in to useful gaseous fuel. The gasification of waste like biomass [27], waste plastic[28], waste rubber/tire [29], low grade fuel[30] has been studied extensively in the recent years. Nevertheless, the process complexity and cost of steam, reactor design, intricacy in gas storage and transportation thwarted the large-scale utilization of gasification process as a technology in waste treatment.

1.4.4 ***Pyrolysis process***

Pyrolysis is a process of thermal decomposition of combustible/semi-combustible materials at elevated temperature under oxygen starving environments[31]. The process is irreversible and it involves changes in chemical composition of materials. Pyrolysis is carried out mostly for the thermal treatment of organic materials such as coal [32,33], biomass[14,34], waste plastic[19,35], heavy oil [36] and organic chemicals [9] and mineral composites. Pyrolysis of organic material produces volatile products like gas and liquid hydrocarbons and leaves a solid residue enriched in carbon, char. Product yield (gas, liquid and solid) and composition depend on feed composition, and the process conditions employed to perform the pyrolysis process. Addition of a suitable catalyst can significantly improve any particular product yield or quality. Pyrolysis of organic material carried out under very slow heating rate or at moderate to low temperature with long duration lead to the formation of carbon residue, this process is called carbonization [37,38]. Different types of reactors discussed in the literature utilized in the process of pyrolysis are autoclave reactor

[33], fixed bed reactor [39], fluidized bed reactor [40,41], catalyzed bed reactor [42], screw type spiral reactor [43] etc. Pyrolysis process is used extensively in industries to produce activated carbon, charcoal, methanol etc. In bio-fuel industry, pyrolysis process has been used to convert biomass into biofuel [44,45].

1.5 Classification of pyrolysis process

Different pyrolysis processes based on process conditions and reactor types are discussed below in details:

1.5.1 *Pyrolysis classification based on reactor design*

(a) Conventional thermal pyrolysis

Conventional thermal pyrolysis is carried out at an elevated temperature where degradation of matter takes place only due to heating. The batch, semi-batch, or autoclave type reactors are best-suited schemes for conventional thermal pyrolysis. The temperature range for thermal pyrolysis of plastic has been in the range of 400 – 700 °C [19,39]. F. Pinto et al. [46] carried out the pyrolysis of plastic waste at 440 °C in an autoclave reactor and achieved a maximum conversion of more than 90%. Demirbas et al. [31] used a stainless steel tubular reactor for the pyrolysis experiment of 1 g plastic sample in each run and products were collected externally after cooling.

(b) Conventional catalytic pyrolysis

In conventional catalytic pyrolysis, catalysts are used to enhance the production of specific components or to reduce the energy desired for the degradation. A wide

range of catalysts was mentioned in various literature, most of these catalysts are used extensively in the industries. The catalysts were categorised into homogeneous catalysts, acid mesoporous materials, non-acid mesoporous solids, zeolites, metallic oxides, smectite clays namely a saponite, a montmorillonite and beidellite as well as pillared derivatives, etc.[42,47,48]. Zeolites (ZSM5, HZSM etc.) are very effective in the degradation of plastics discussed in numerous past studies[49,50]. López, et al. [51] used red mud (Bauxite residue), a by-product waste from alumina industry, as a catalyst for waste plastic pyrolysis. The red mud as a catalyst mainly favours hydrogenation reaction, but the catalyst activity was found high at the higher temperatures (>500 °C). On the other hand catalyst like ZSM-5 was found to be active under lower temperature (440 °C) and also promotes production of lighter hydrocarbons (gas/liquid) with high aromaticity. De Stefanis, et al. [52] reported three alternative catalysts from restructured smectite clays, namely a saponite, montmorillonite, and beidellite. The catalysts were tested for their performance in the catalytic cracking of a medium-density polyethylene in a pyrolysis setup. The catalysts were able to reduce the cracking process temperature up to 300 °C, as compared to 650 °C or more for non-catalysed pyrolysis. In comparison to zeolites, the clay catalysts were found superior in producing liquid hydrocarbon from plastic waste. Clay catalysts favour the production of liquid hydrocarbons in the gasoline and diesel range liquid from the polyethylene plastics.

(c) Fluidized bed pyrolysis

Fluidized bed pyrolysis (FBP) favours the production of the gaseous product. A high heating rate is possible due to the uniform distribution of heat. FBP is very convenient for catalytic cracking. A schematic FBP pilot plant developed in the University of Hamburg [41] to recover feedstock from mixed plastic and elastomers is shown in Fig 1.4. The process utilized an indirectly heated fluidized bed and targeted the continuous production of range of chemicals like monomers of different polymers and hydrocarbons of various functional groups.

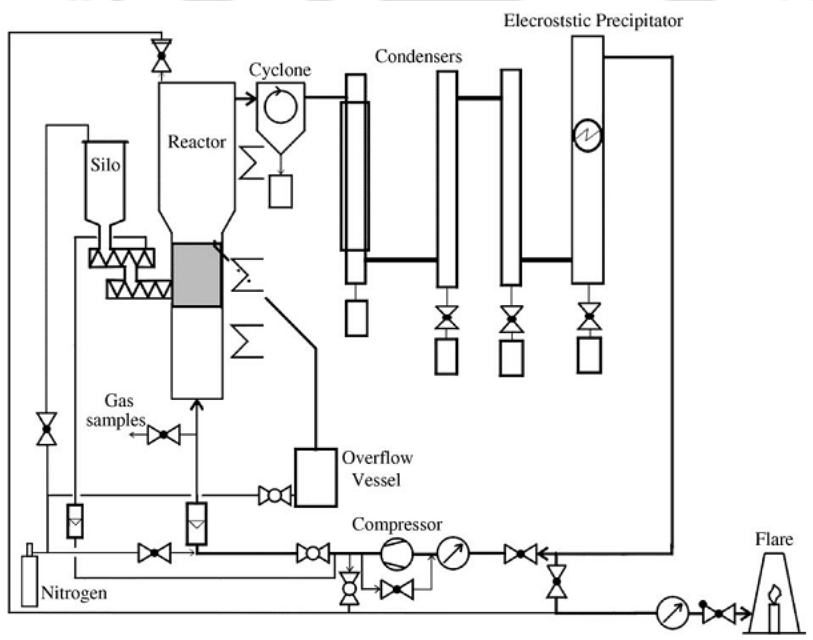

Fig. 1. 4: Flow scheme of fluidised bed pyrolysis plant (30 kg/h)[41]

Williams and Williams [53] carried out the pyrolysis of low-density polyethylene in a fluidized bed reactor to study the influence of temperature. It was observed that gas production increases (up to 71% at 700 °C) with the increase of pyrolysis temperature. Williams and Williams [54] were also performed pyrolysis of mixed plastics using a sand fluidized bed by supplying preheated (450 °C) nitrogen with

an externally heated ring furnace. It was found that FBP process have high installation and operating cost and slightly complex process mechanism in comparison to conventional thermal pyrolysis.

(d) Microwave pyrolysis

In microwave pyrolysis, the microwave is used as the energy source. The microwave is an electromagnetic wave spectrum having the wavelength ranging between 1 mm and 1 m [55]. Materials like water, biomass, metals and carbon particles are considered as good microwave absorber (dielectric materials). Polymer and plastics are transparent to microwave because they have low microwave absorption capacity [56]. However, these materials can undergo pyrolysis by mixing with carbon particles or metals in a microwave reactor. However, controlling the pyrolysis temperature in microwave heating is tricky due to the formation of hot spots during heating caused by localized microwave field that arises due to the difference in dielectric properties of the material and large wave length of the microwave [55].

(e) Screw kiln reactor type pyrolysis

Screw kiln reactors are generally utilized when high degree of mixing is required for efficient distribution of heat throughout the sample. It is highly recommended for slow pyrolysis at an industrial scale. Serrano et al. [57,58] performed both thermal and catalytic pyrolysis experiment in a continuous screw kiln reactor (Fig. 1.5). The reactor consists of three zones: feed zone (a hopper), reaction zone (a screw reactor) and product outlet zone. Screw kiln reactors provide continuous pyrolysis with a

continuous supply of feed. The other advantage of screw clean reactor is that a differential heating zone can be maintained throughout the reactor, which gives better control over conversion rate and flow of the reactant species. Operating and maintenance cost may be higher due to the complex mechanism.

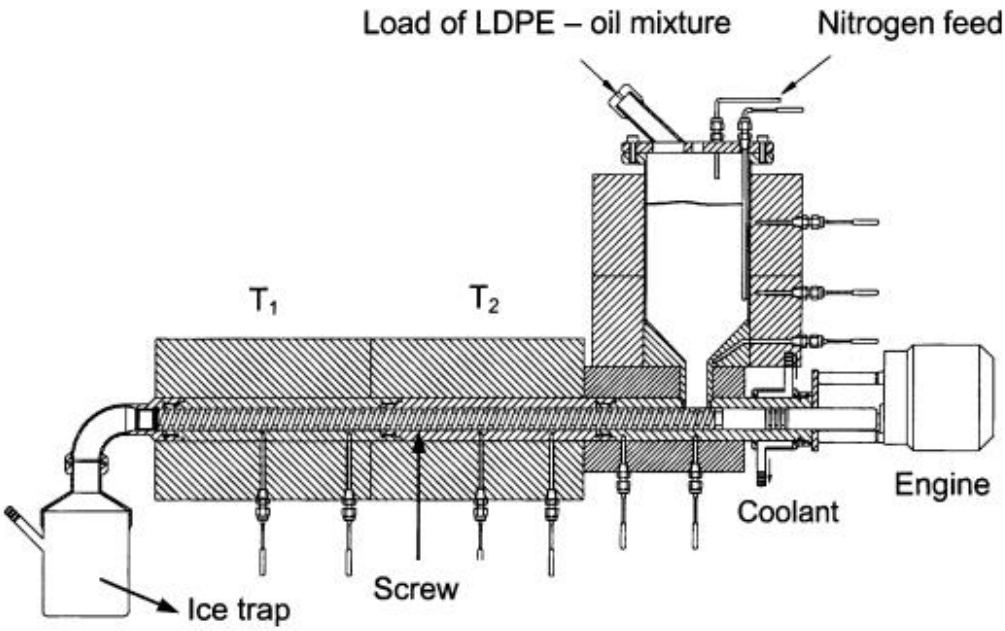

Fig. 1. 5: Schematic representation of screw kiln reactor [57]

1.5.2 *Types of pyrolysis depending on swiftness of the reaction*

Apart from reactor types and heating source pyrolysis processes can also be classified according to how fast or slow the heating of the material takes place. It was observed that the heating rate or time of exposer to heat significantly influence the product distribution of the pyrolysis process. Table 1.1 listed the classification of pyrolysis based on the swiftness of the reaction. The processes are explained in details in the subsequent section.

Table 1. 1: Pyrolysis classification based on swiftness of the reaction [32]

Process	Feed size	Moisture	Heating Rate	Residence Time	Temperature (^{0}C)	Pressure	Products
Slow Carbonisation	Large		Very Low	Days	450-600	Atmospheric	Charcoal
Slow Pyrolysis	<200 mm	<15 %	10-100 ℃ /min	10-60 min	450-600	Atmospheric/vacuum	Gas, oil, Char
Fast Pyrolysis	Small <1 mm	<10 %	Up to 1000 ℃/s	0.5-5 s	550-650	Atmospheric	Gas, oil, (Char)
Flash Pyrolysis	Small <1 mm	<10 %	Up to 10000 ℃ /s	<1 s	450-900	Atmospheric	Gas, oil, (Char)

(a) Carbonization of organic matters

Carbonization is a process of converting the organic substances into carbon or a carbon-containing residue through pyrolysis by removing water and volatile substances from the material [59]. Biomass, low-grade coals, and coal tars are generally considered for carbonization processes [38,60]. The reaction occurs at temperatures between 400 to 600 °C and sustain over a relatively long time (in days), which lead to the production of charcoal with a percentage of carbon equivalents to about 75% or more and a calorific value of 6000 – 7000 Kcal/kg (25 – 30 MJ/kg).

(b) Slow pyrolysis

Slow pyrolysis is the process of heating carbonaceous material at a very slow heating rate under the non-isothermal condition or at low degradation temperature with a long isothermal holding time. The choice of heating rate and the isothermal temperature completely depend on the degradation properties of the materials. The way to determine the degradation temperature and heating rate is thermogravimetry analysis (TGA). The range of heating rates for slow pyrolysis mentioned in various literature are in between 5 – 100 °C/min. [61]. Temperatures are generally depend on the material degradation temperature. Various types of reactors can be employed for slow pyrolysis having various sizes and shapes such as fixed bed reactor, rotary kiln reactor etc. [62,63]. Yang, et al. [62] studied the slow pyrolysis in a packed bed reactor to recover solid, liquid and gas from the three segregated wastes consist of waste wood, cardboard,

and waste textile. Investigation of the effect of final temperature has been done and char yield of more than 30 % of the feed has been reported.

(c) Fast pyrolysis

Fast pyrolysis have very small residence time (<5 s) and generally carried out in fluidized bed reactor at high temperature (~1000 °C).As the residence time is small, the heat transfer through the material has to be very high. Hence, small particle size is recommended. Demirbas [31] carried out a lab-scale pyrolysis experiment in a tubular reactor heated by an external heater. Mix plastic sample having small particle size was pyrolyzed in the reactor and product distribution was compared at different reaction temperatures. Fast pyrolysis results high yield of gaseous and liquid products.

(d) Flash pyrolysis:

Flash pyrolysis is performed in a very high-temperature zone and the residence time is maintained below 1 second [64]. This method is very flexible in the production of liquid and gaseous fuel. The high temperature corresponds to the high production of the gaseous product. When the temperature have a moderate value, the liquid product can also be expected. A comparison of all the four above-mentioned pyrolysis technology was classified based on the swiftness of the heating process are listed in Table 1.1.

1.6 Literature review

Pyrolysis is considered as one of the efficient ways to thermally degrade the plastic waste into useful products. The study of various pyrolysis (conventional and catalytic) techniques that includes waste plastics has been gaining attention in recent years. Many previous studies have discussed the degradation behaviour/degradation kinetics based on the mass loss data obtained in the thermogravimetric analysis (TGA). A few other studies focussed on the pyrolytic conversion of plastic waste into various products. Many researchers had discussed the effect of process condition, feed composition and reactor type on product distribution with varying quality. A brief discussion is given in the following sections regarding various past studies on plastic or polymer degradation kinetics, pyrolysis of plastics (waste) and subsequent discussion of lacunas and area of improvement in achieving the project goal that is the development of a pyrolysis process targeting value added production from plastic waste utilizing minimum energy.

1.6.1 *Degradation kinetics of plastics and polymers*

Most of the commercial plastics are non-biodegradable and are responsible for various environmental and ecological problems. Pyrolysis of waste plastics can transform solid waste into wide range of valuable chemicals and hydrocarbon compounds [31]. Designing and implementation of pyrolysis process for complex materials like plastics depend primarily on kinetic analysis. The precision of the pyrolysis kinetics heavily depends upon the reliable evaluation of the kinetic triplet,

such as activation energy (E_α), pre-exponential factor (A_α) and reaction model ($f(\alpha)$)[65].

Degradation of plastics includes all changes related to chemical structure and physical properties due to external stresses. The mechanism of thermal degradation of plastics is complex in nature. Thermal degradation involves the occurrence of molecular scission, which leads to the changes in molecular weight distribution of the plastics. This phenomenon is decisive for recycled plastics as they suffer continuous change with temperatures [66,67]. Heating any organic or inorganic solid results in many physico-chemical phenomena like melting, sublimation, polymorphic transformation, desolvation or degradation, etc.[68]. TGA provides the pathway to determine the macroscopic kinetics of these processes. The microscopic kinetic accounts for simultaneously occurring multistep phenomena and requires computational methods. Isoconversional methods recommended by International Confederation for Thermal Analysis and Calorimetry (ICTAC) are able to capture the complexity involved [69-73]. Isoconversional methods use the thermal degradation data at different temperature program and calculate the distribution of activation energy as reaction/process progresses. The variable activation energy [74] explains the complexity of thermal degradation process at various stages of conversion process. Friedman [75],Ozawa Flynn and Wall (OFW)[76,77], Kissinger Akahira Sunose (KAS) [78] and Starink [79] methods are popular choices of isoconversional techniques and have been practiced for the analysis of polymer degradation kinetics [80,81]. Vyazovkin et al.[82] modified the isoconversional

approach into more accurately acceptable advance isoconversional technique (AIC). Application of AIC method for kinetic analysis of thermally stimulated process in polymers for both oxygen initiated degradation and degradation under inert condition have been reported [82-84]. Peterson et al.[83] stated the increasing trend of activation energy with the extension of reaction for polyethylene (PE) and polypropylene (PP) whereas constant activation energy values were reported for polystyrene (PS) throughout the degradation. Saha et al. [85] determined the variable activation energy of waste PE degradation as around 200 kJ/mol (average) using multiple heating program (10, 15, 20 and 25 °C/min). Other studies also available where isoconversional methods were employed to evaluate the decomposition kinetics of materials such as HDPE [86], PS and PE [83], PP [87], tyre rubber[88], biomass [89,90], coal[91], cellulose[92] and polymer composites [93,94] etc. Most of the previous studies able to utilize the way of measuring distributed activation energy and their applications. However, only few of the past studies have captured the essence of kinetic triplets (E_α, A_α and $f(\alpha)$), that represent the complete understanding of reaction mechanism. The analysis techniques of degradation kinetics are explained in details in section 2.3 of chapter 2 (materials and methods).

1.6.2 *Conventional thermal pyrolysis of plastic waste*

P. T. Williams and his co-researchers [35,39,95] were carried out extensive study on the pyrolysis of thermoplastics in the recent past. Six thermoplastics such as high

density polyethylene (HDPE), low density polyethylene (LDPE), polystyrene (PS), polypropylene (PP), polyethylene terephthalate (PET) and polyvinyl chloride (PVC) were pyrolyzed in a static batch reactor heated externally to a temperature program between 25 °C and 700 °C under inert condition (by N_2 purging). The experiments were conducted with solo and mix samples. More than 80% yield of condensed product (in waxy state) was reported. The waxy products were highly aliphatic except those obtained from PS and PET, which contains a significant amount of aromatics due to the presence of the benzene ring in the polymer chain of PS and PET. Pyrolysis of PVC resulted in the production of hydrochloric acid (HCl). Hydrochloric acid was produced due to the presence of chlorine in the PVC, which underwent degradation at high temperature and hydrogenation reaction of chlorine in the presence of hydrogen radicals produced due to degradation. A small amount of char was seen in the product stream when PS, PET and PVC were in the feed. The gaseous product consists of hydrocarbons (C_1 - C_4) along with trace amount of H_2, CO and CO_2. Adrados, et al. [20] carried out pyrolysis experiment with real world packaging plastic waste and simulated plastic mixtures in a semibatch reactor in the presence of a waste catalyst (Red mud). Reaction temperature was maintained at 500 °C for half an hour. The liquid product obtained from simulated plastic mixture were highly viscous and semisolid state at room temperature, on the other hand oil obtained from real world waste samples were significantly less viscous due to low molecular weight. The aromatic components were found dominating in the liquid product composition (>70%). Presence of

catalyst in the pyrolysis process attributed to greater cracking, aromatization, and chances of hydrogenation of styrene to ethyl benzene. Similarities between the products from the real world plastic pyrolysis without catalyst and simulated plastic in catalytic pyrolysis were observed.

Sharma, et al. [96] carried out the pyrolysis experiments of high density polyethylene (HDPE) grocery bags in a batch reactor and a detailed characterization of produced plastic crude oil (PCO) was reported. PCO was then distilled into four fractions according to the boiling point range (<190 °C, 190-290 °C, 290-340 °C and >340 °C) and analysed extensively for various ASTM standard fuel tests. Fractions between 190 – 290 °C had maximum yield whereas fractions between 290 – 340 °C exhibited higher values of flash point, kinematic viscosity, density and lubricity etc. The diesel fractions obtained was compatible with the standard ultra-low sulphur (<15 ppm S) diesel (ULSD).

1.6.3 ***Effect of process conditions on the plastic waste pyrolysis***

Effect of feed composition

Pinto, et al. [97] studied the effect of plastic waste composition in the pyrolysis product distribution for three plastics namely PE (Polyethylene), PP (Polypropylene) and PS (polystyrene). The presence of PE increased the alkane content, whilst PS led to the formation of aromatics and PP was responsible for the production of olefins. The authors also highlighted the fact of increasing octane number of the liquid products due to the presence of PP and PS in the feed.

Siddiqui and Redhwi [98] conducted thermal and catalytic co-pyrolysis experiments at various mixing ratio of PS, LDPE, HDPE and PET in a 25 cm^3 stainless steel micro reactor at an optimum condition of 430 – 440 °C and 5.5 - 6.0 MPa of N_2 gas pressure. The presence of PS and PET increases the aromatic content in the feed. Hexane soluble liquid fractions of the different pyrolysis reactions were analysed using simulated distillation (SimDist). The low boiling fraction materials were not found because of vaporization and the cuts were obtained only after 96 °C boiling point.

Effect of temperature and heat exposer time/rate

Plastics are rigid polymers of organic substance that is actually millions of monomers connected and spread into linear, branched and network structure. The covalent bonds hold the atoms in the polymer molecules together and secondary bonds hold the cluster of polymer chains together to form a plastics. Plastics are made up of polymers with other additives to increase its functionality and applicability [99]. The bond energy of polymers vary according to the structure and elements involved in the monomer. During the degradation process, variation of temperature or heating time/rate influences the bond breaking process and subsequently effects the product distribution. Several past studies have been focussed on the influence of temperature programme on product distribution of plastic pyrolysis. The goal of doing pyrolysis is to convert the plastic waste into useful products like chemicals and fuels. Kaminsky, et al. [19] found out that below 700 °C temperature, pyrolysis of plastics such as HDPE can produce oil containing higher yield of aliphatic component,

whereas above 700 °C the produced oils were aromatic in nature. Sodero, et al. [30] estimated ~2% of aromatic compounds such as benzene and toluene along with other light hydrocarbons, while performing ultra-pyrolysis of LDPE at 800 and 900 °C in a Curie point micro-reactor. High temperature was recommended for gaseous production.

Williams and Williams [35] carried out high temperature fast pyrolysis of mix plastic feed (~60% PE) in a fluidized bed type reactor in the temperature range of 500 – 700 °C. They found out that the overall gas yield increased with temperature to give a maximum value (88.76 %) at 650 °C but further increase of temperature resulted in decrease of the gas yield. The gas yield was found to be increased from 9.79% at 500 °C to 88.76% at 650 °C. Conesa, et al. [26] reported an increase in gas yield in the range of 500 – 800 °C, for HDPE under fast pyrolysis in a fluidised bed reactor. Ballice, et al. [100] reported the maximum volatile product formation temperature at 425 and 430 °C for LDPE and HDPE respectively, in a fixed bed type reactor. Ramdoss and Tarrer [101] conducted liquefaction of postconsumer PE and virgin PE plastics, in a micro reactor with an operating temperature of ~500 °C (for 30 min) under a hydrogen atmosphere and reported a maximum liquid yield of 60 % liquid oil.

On the other hand, Shah, et al. [102] suggested two liquefaction process of post-consumer plastic, one was direct liquefaction using catalyst and the other one involved pyrolysis followed by hydro-processing of pyrolysis liquid product. In the later process heavy oil (70 – 80% yield) from pyrolysis of plastics at 600 – 650 °C,

were undergo hydro-processing at 450 °C and 200 Psig initial hydrogen pressure, with a 1% addition of HZSM-5. The hydro processing improve the liquid product quality with a significant increase of gasoline content.

Wong and Broadbelt [103] studied the effect of long-duration by maintaining two moderate temperatures, 350 and 420 °C for 180 min and 18 hours while performed the pyrolysis of polypropylene and polystyrene. They observed that the conversion of polypropylene increased with the reaction time at 350 °C while no significant change was observed at 420 °C beyond 90 min. Long reaction time could improve the product quality as heavier components decompose into lighter and low molecular weight products.

Marcilla, et al. [104] carried out the pyrolysis of commercial LDPE and HDPE (powder form) under dynamic condition of 5 °C/min from 30 to 550 °C in a quartz batch reactor under a N_2 flow rate of 150 ml/min. Gaseous and liquid samples were collected at 25 °C temperature difference to evaluate the effect of temperature in the product distribution. Under the dynamic heating condition, they were able to depict the evolution pattern of different product families that were formed during the progress of the pyrolysis reactions. They predicted n-paraffin as a major component in both gaseous and liquid product in the earlier stages of degradation, whereas 1-olefin had a maximum yield at the maximum reported degradation temperature reported.

Onwudili, et al. [105] investigated the effects of temperature and time duration in the composition of product obtained when pure LDPE, PS and their mixtures were pyrolyzed in a pressurized batch reactor under inert (N_2) atmosphere over a temperature range of 300 – 500 °C for 1 hour. The composition of gaseous products obtained from the pyrolysis of LDPE dominated by alkanes, followed by alkenes and traces of hydrogen. The fraction of alkane and hydrogen increased at higher pyrolysis temperature in the gaseous products. Maximum conversion of LDPE plastic to liquid oil occurred at 425 °C, beyond that the oil yield was decreased and gas/char yield was increased. On the other hand, PS degraded around 350 °C and produced dark colour oil, which is mostly composed of aromatic compounds such astoluene, ethylbenzene, and styrene. Effects of temperature and residence time in the oil composition and product distribution were observed in both individual plastic pyrolysis and in the co-pyrolysis of LDPE and PS. Highest calorific value (42.7 MJ/kg) was reported for the oil that was obtained from LDPE pyrolysis.

López, et al. [33] studied the influence of time and temperature on pyrolysis of simulated mix plastic waste consist of PE, PP, PS, PET and PVC in a semibatch reactor. Experiments were conducted with a heating rate of 20 °C/min to reach the final pyrolysis temperatures (460, 500 and 600 °C). The final temperatures were maintained for 0 - 120 min to investigate the effect of long duration. The PE and PP dominated the feed but high aromatic concentration was observed in the liquid produced at higher temperatures. High yield of aromatic compounds were resulted due to the presence of PS and PET, stabilization of free radical fragments and

secondary reaction at higher temperature. Light hydrocarbon gases (C_1 - C_3) were found more abundant in the gas produced at higher temperatures. Both liquid and gas yield was increased with time but after a certain time interval (>40 min) no significant difference was observed with respect to product yield and composition.

Singh and Ruj [106] studied the effect of time and temperature on the fuel gas generation in the pyrolysis of municipal plastic waste. Pyrolysis experiments were carried out in an electrically heated batch reactor. Heating rate of 30 °C/min was maintained to achieve final temperatures (450 – 600 °C). The gaseous products were mostly hydrocarbons (C_1 – C_4) along with a small amount of H_2, CO and CO_2. Low molecular weight gases were produced in the initial stages of the reaction (low temperature). However, H_2 and CO_2 gas yield increased with the increase of the temperature and the yield of heavier hydrocarbon gases like C_2H_6, C_3H_8 decreased at higher temperatures.

1.6.4 *Summary of the literature study*

To summarise the widespread literature in the field of waste plastic degradation and pyrolysis following points has been derived and discussed below:

a) By applying only heat under inert conditions, plastic wastes mostly PE, PP, PS, PET, PVC etc. undergoes degradation. The long chain polymer breaks down and produces low molecular weight gaseous and liquid products.

b) Isoconversional methods can be applied to study the kinetics of complex degradation mechanism of plastics. Vyazovkin's advance isoconversional

method (AIC) was reported as a reliable technique to calculate variable activation energy.

c) Temperature, heating rate and heating time significantly influence the product distribution in the plastic pyrolysis. High temperature (>700 °C) favours the production of gases whereas pyrolysis of plastic at intermediate temperatures (500 – 700 °C) produces a waxy liquid also known as plastic crude oil. Plastic crude oil requires significant post-processing before utilizing as fuel.

d) The feed composition influences on the product distribution as most plastics has different polymer backbone, which influences the product distribution and quality.

e) Very few studies have been found on pyrolysis of plastics at lower temperatures (<500 °C), including effects of long isothermal holding time and slow heating rate (<5 °C/min). It can be possible to manipulate the pyrolysis conditions like temperature and heating rate to target value added products like lighter hydrocarbon gases and liquids.

1.7 Scope and objective of the research

In view of the above discourse, it is clear that plastic waste is both social and environmental issue and requires sustainable technology for the disposal and recycling. Packaging plastics like low and high-density polyethylene (LDPE and HDPE) and polypropylene (PP) are a major constituent in any plastic waste stream. Most of the plastics are non-biodegradable and requires hundreds of years to degrade

naturally. Thermal degradation processes such as combustion and incineration of plastic should be avoided due to toxic emissions.

Pyrolysis is a plausible process that has been used to convert plastic waste into useful chemicals and fuels. The pyrolysis product distribution is largely influenced by the temperature program associated with the process. In the current study the pyrolysis, conditions like temperature, time and heating rates were manipulated to target value-added products like light hydrocarbons. The primary objective of this research is to develop an innovative, cost-effective, environmentally benign process and formulate the sustainable strategies to recover targeted value-added products.

Specific objectives:

The Ph.D. thesis with the title "Thermal degradation of packaging plastic waste and its conversion into fuel by slow pyrolysis" targets the fulfilment of the following objectives.

- Thermal degradation kinetic study of plastics using TGA based kinetic analysis.
- Calculation of degradation kinetics from the isothermal degradation data.
- Effect of temperature in the pyrolysis product distribution of individual and mixed plastic (virgin/real waste samples)
- Non-isothermal slow pyrolysis of plastics mixtures to study the variations in product distribution obtained at various temperatures for individual and mixed samples (virgin/real waste samples)

- Characterization of pyrolysis product to find out the effect of process conditions such as feed composition, temperature and heating rate.

1.8 Organisation of the thesis

Chapter 1 of the thesis gives a brief introduction of plastics, its history, and its socio-economic impact. Further, the chapter discusses the plastic waste generation, its effect and possible choices of disposal and recycling methods. The process of pyrolysis in the disposal of plastic waste and its advantages has been discussed with the state of the art literature. Finally, the scope, objectives and systematic organization of the thesis has been presented.

Chapter 2 summarises the material and methods adopted in the study, which include basic proximate analysis of the materials, the process adopted for TGA analysis and detailed method of lab-scale pyrolysis along with the analytical techniques used in the research. The theoretical aspects of the kinetic analysis based on non-isothermal and isothermal TGA data are discussed elaborately in this chapter.

The results of the detailed TGA analysis of all the materials are discussed in **chapter 3**. The variable activation energy (E_α) was calculated with the help of isoconversional techniques. The kinetic results are reported for multiple temperature programs and their significance in the degradation kinetics are explained. Other kinetic parameters such as pre-exponential factor (A_α) and reaction model ($f(\alpha)$) are determined from the TGA data and the simulated conversion and temperature

profiles are shown in comparison with the experimental plots. To understand the gas evolution pattern during the degradation process, thermogravimetric – Fourier transform infrared spectrometry (TG-FTIR) analysis were carried out and three-dimensional plots of IR spectra with respect to temperature and wavenumbers are reported.

Chapter 4 summarises the results from the lab scale pyrolysis study of the LDPE, HDPE and PP, which are collected as a virgin sample from the market and as real waste mix (RMIX) from the household solid waste under isothermal condition (holding a temperature in the range of 300 – 400 °C). The pyrolysis process was carried out at moderately low degradation temperature and the isothermal temperature was held for 8 hours. High heating rate (20 °C/min) was used to heat up the reactor to the isothermal temperature. The products, especially the plastic, derived oil (PDO) were analysed in details with the help of Fourier transform infrared spectrometry (FTIR), proton nuclear magnetic resonance spectroscopy (^{1}H NMR) and gas chromatography (GC). The carbon number (boiling point) distribution range was calculated with the help of simulated distillation in gas chromatography (GC-SimDist). The fuel properties of the PDOs suggest the resemblance to the conventional fossil fuels like diesel and gasoline. Gaseous products mostly dominated by hydrocarbon gases, which has significant fuel value.

In **Chapter 5**, the effect of very low heating rate (1 °C/min) on the product distribution at different stages of the non-isothermal pyrolysis process has been discussed. Products were collected at regular intervals and analysed for their

functionality and carbon number distribution. The temperature has a significant effect on the product distribution in both liquid and gaseous products. Gaseous products mostly composed of hydrocarbon gases (propylene is a major component) and can be used as a fuel gas since the gas possesses a high calorific value.

Chapter 6 summarises the overall conclusion of the research work and discusses the possible scope for the further research in this field.

Chapter 2

MATERIALS AND METHODS

Materials
Experimental procedure
Kinetic models and theory
Analytical techniques

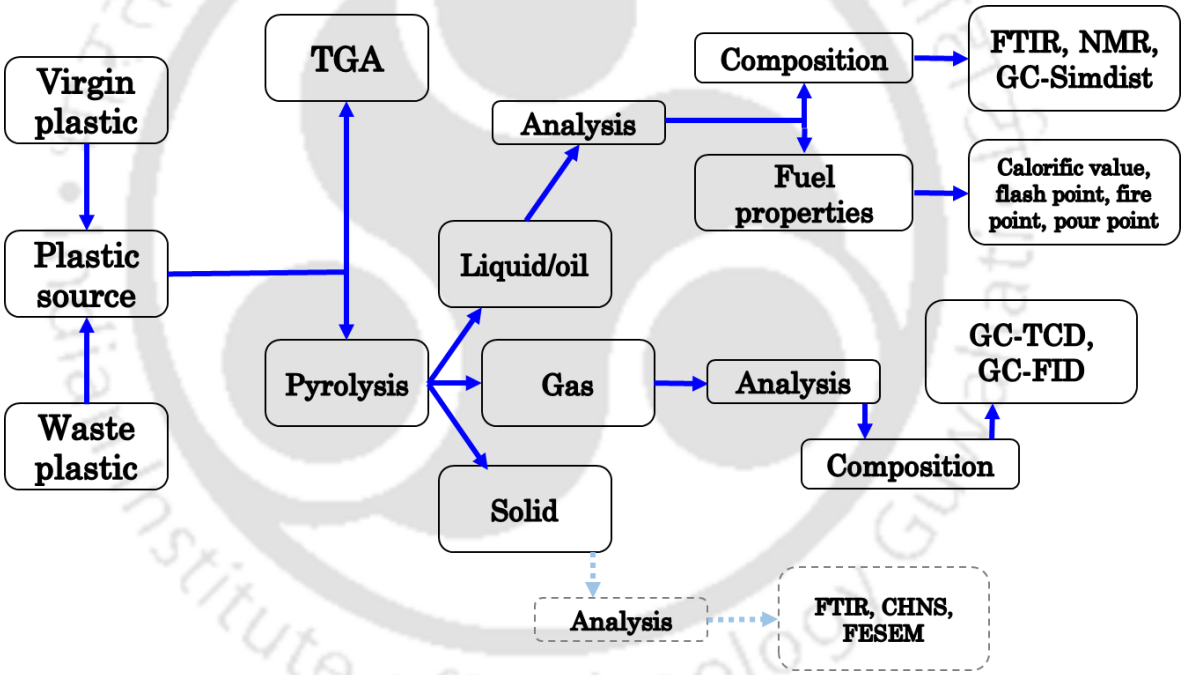

2 Materials and methods

In this chapter, the focus is given to explain the materials chosen for the study, experimental methods and theoretical methods applied for the research. The experimental and theoretical methods included thermogravimetric analysis (TGA), TGA based kinetic analysis, lab scale pyrolysis and the pyrolysis product characterization. Both isothermal and non-isothermal TGA was carried out at different temperatures and heating rates respectively. The kinetic study was carried out based on the isoconversional principle that includes both differential and integral approaches. The pyrolysis experiments were carried out in a semi-batch reactor. Both isothermal and non-isothermal pyrolysis experiments were conducted for packaging plastics (virgin as well as waste). Major pyrolysis products such as gas and liquid samples were analyzed using Fourier transform infrared spectroscopy (FTIR), nuclear magnetic resonance spectroscopy (NMR) and gas chromatography (GC).

2.1 Materials

Polyolefins like polyethylene and polypropylene are the most common form of polymers used in the production of packaging materials. Different grades (density, strength, flexibility etc.) of plastics can be manufactured from polyolefins by changing the polymerisation technique, polymer structure and adding suitable additives. In general, low density polyethylene (LDPE), linear low density polyethylene (LLDPE), high density polyethylene (HDPE), polypropylene (PP),

polystyrene (PS) and polyethylene terephthalate (PET) are the most common polymers in the manufacturing of packaging goods like carry bags, wrappers, food containers, water and soft drink bottles etc. These materials are abundantly found in the waste stream (9 - 11 % in municipal solid waste) [4]. In this study, three types of polyolefin plastics 1. LDPE, 2. HDPE and 3. PP were chosen. The samples were collected from two sources; Haldia petrochemicals Limited, India, provided the virgin LDPE, HDPE and PP in granulated form. The second source of material was the household plastic waste with same type of composition. Most plastic products such as bags, containers, toys etc. have their resin identification code embedded on the material for recycling purpose. The waste materials collected from the nearby household waste was segregated based on their resin identification code (Fig. 2.1). In addition, the degradation behaviour of two plastic materials viz. virgin polylactic acid (PLA) (Fig.2.2) and polyethylene terephthalate from waste soft-drink bottles (PET-SDB) (Fig. 2.2) were also studied using TGA (thermogravimetric analysis) based kinetic analysis. Virgin PLA granules were procured from Natures works (provider: CoE Suspol, Indian Institute of Technology Guwahati).

Important physical properties of the plastics are reported in Table 2.1 and the proximate analysis along with the heating values of the samples are shown in Table 2.2. The virgin plastics received from the market were in pellet form of size around 3 – 5 mm. The materials (virgin plastics) were manually sliced to make 1-2 mm average particle size before TGA. Granulated virgin samples were directly used for pyrolysis experiment.

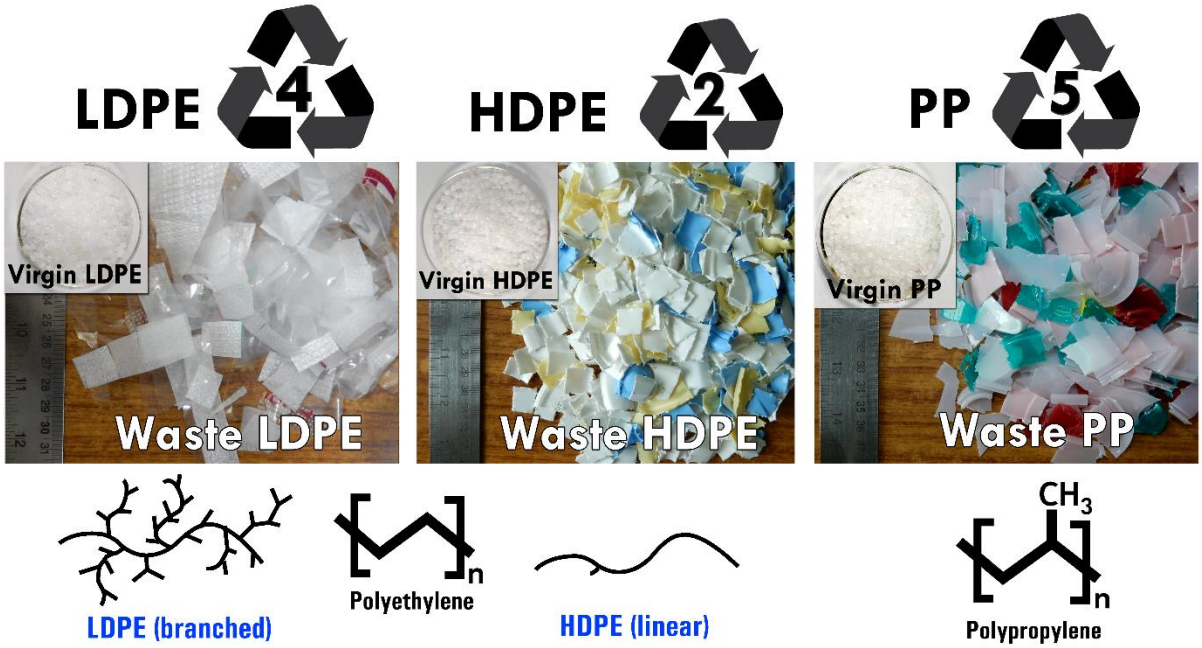

Fig. 2. 1: Materials used in the pyrolysis study collected from household waste as well as virgin samples from the market (with resin identification code and molecular structure)

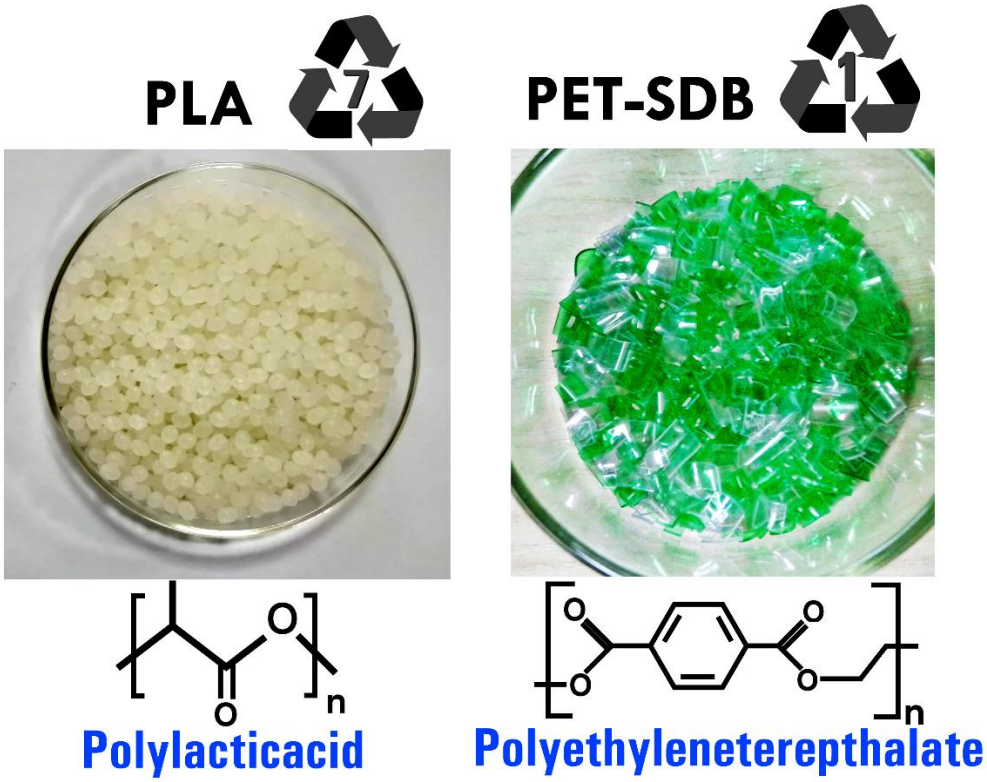

Fig. 2. 2: Granules of virgin PLA and PET from waste soft-drink bottles (PET-SDB) after cutting into small pieces (4 – 5 mm) with resin identification code and molecular structure

Table 2. 1: Physical properties of the plastic materials considered for pyrolysis and degradation studies [107]

Plastics	Density (g/cc) ASTM D1505	Glass transition temperature (°C)	Melting point (°C)	Average molecular weight ($gmol^{-1}$)
LDPE	0.934	-125.15	110.85	100,000-1,000,000
HDPE	0.950	-80.15	131.85	250,000-1,500,000
PP	0.9	-10.15	167.85	200,000-600,000
PLA	1.25	56.85	169.85	~200,000
PET	1.38	75.85	253.85	~30000

Table 2. 2: Volatile matter (VM), ash content (AC) fixed carbon (FC) and high heating value (HHV) of the individual samples

	VM (w/w %)	AC (w/w %)	FC (w/w %)	HHV (MJ/kg)
LDPE (virgin)	99.95	0	0.05	47.12 ± 0.8
HDPE (virgin)	99.97	0	0.03	46.95 ± 0.61
PP (virgin)	99.08	0	0.92	46.67 ± 0.5
PLA (virgin)	98.45	0	1.55	19.19± 0.22
LDPE (waste)	79.99	19.25	0.76	44.25 ± 0.35
HDPE (waste)	99.32	0.59	0.09	45.38 ± 0.66
PP (waste)	99.68	0.05	0.27	46.05 ± 0.49
PET-SDB (waste)	97.31	0.21	2.48	23.25± 0.35

Dry waste samples were manually cut into small pieces of size 1 – 2 cm for pyrolysis experiment (Fig. 2.1). Segregated samples were then mixed together in the proportion of 30% LDPE, 30% HDPE and 40% PP to prepare mixture sample (RMIX) for isothermal study and equal proportions were considered for non-isothermal pyrolysis study. Similar proportionate mixture with virgin plastics was coded as VMIX. Pre-process analysis of the collected waste samples were ignored

because of the complexity and non-homogeneity of the samples but the post processing products were analysed thoroughly and the results were compared with the products obtained from the virgin samples.

The hydrocarbon standards (ASTM D5307 internal standards) and gas sampling bags (Tedlar bags) were procured from Sigma Aldrich. Dichloromethane (HPLC grade) and Deuterated chloroform ($CdCl_3$ 99.8%) were used to dilute the liquid products for analysis were procured from Merck (India).

2.2 Methods

2.2.1 *Thermogravimetric analysis (TGA)*

Thermogravimetric analysis (TGA) is one of the very effective technique to study the degradation behaviour of any material under a simulated heating condition. Weight loss data obtained from TGA can be utilized to study the degradation kinetics[108].

Thermal degradation study was carried out using TGA (NETZSCH 209 F1 TG) equipment in the inert environment (N_2 gas) with a flow rate of 60 ml/min (40 ml/min as purge and 20 ml/min as protective gas). The samples (6 - 12 mg) were placed in an alumina crucible and both non-isothermal and isothermal degradation analysis was performed in the TGA. The non-isothermal TGA was carried out at the heating rates of 5, 10, 15, 20, 30, 40 and 50 °C/min. The temperature ranges for the non-isothermal TGA were maintained between 30 – 1000 °C. On the other hand, the isothermal experiments were conducted at the temperature ranging between 300

– 425 °C based on the material degradation data (non-isothermal). The heating rate maintained at 100 °C/min to increase the TGA temperature from ambient to the desired isothermal condition (Table 2.3). The isothermal temperature was then maintained for 8 – 10 hours. Except for PET-SDB, all the samples chosen for TGA study were virgin plastics.

TGA data were collected and processed in MATLAB software for the kinetic analysis. The different established methods used in the kinetic study are discussed in details in the following section.

Table 2. 3: Isothermal temperatures for individual plastics for isothermal TGA analysis

Material	Temperature (°C)	Isothermal holding time (hours)
LDPE (virgin)	350, 375, 400, 425	10 hours
HDPE (virgin)	350, 375, 400, 425	8 hours
PP (virgin)	300, 325, 350, 375, 400	10 hours
PLA (virgin)	250, 275, 300, 325	10 hours
PET-SDB	325, 350, 375, 400	8 hours

2.2.2 *Theory adopted for degradation kinetic study*

The study of the plastic degradation kinetics were carried out based on the Arrhenius rate equation in the pursuit of finding the three kinetic parameters of Arrhenius kinetic equation and their variation with the progress of the reaction. These kinetic parameters are activation energy (E_α), pre-exponential factor (A_α) and reaction model $f(\alpha)$. The suffix 'α' symbolizes the variation of kinetic parameters with the conversion or the progress of the reaction.

According to Arrhenius kinetic theory, the rate depends on temperature and reactant mass. The rate of degradation can be expressed as [109]:

$$\frac{d\alpha}{dt} = k(T) f(\alpha) \quad (1)$$

Where $k(T)$ is the temperature dependent term and *f(α)* is the mass dependent term (reaction model). The term α represents the extent of reaction or conversion. Mathematically α is defined as $\alpha = (W_0 - W)/(W_0 - W_\infty)$, where W_0 is the initial weight of the sample, W is the weight at any temperature T (or time t) and W_∞ is the residual/final weight (mass remain in the TGA crucible).

At any particular temperature, the distribution of energies in the molecules can be statistically described as Boltzmann distribution. To get involved in the reactions the portion of molecules have to pull through the energy barrier separating the minima of the potential energy relating to the initial and final thermodynamic state of the matter [110]. The activity of reactant molecules increases with the increase of temperature followed by the increase of the reaction rate. This increase of rate is exponential and this concept ultimately laid the foundation of Arrhenius equation, which defines the temperature dependence of rate constant[110].

$$k(T) = A_\alpha \exp\left(\frac{-E_\alpha}{RT}\right) \quad (2)$$

Eq. (2) relates the rate constant of a single-step reaction to the temperature through the apparent activation energy (E_α) and pre-exponential factor(A_α). Where, '*E*'

represents the energy of activation, and 'A' represents the frequency at which atoms and molecules collide so that reaction gets start. The reaction models ($f(\alpha)$) most commonly considered in the solid-state degradation reactions are listed in Table 2.4. The differential form of the Arrhenius rate equation is,

$$\left(\frac{d\alpha}{dt}\right)_{\alpha} = A_{\alpha} exp\left(\frac{-E_{\alpha}}{RT}\right) f(\alpha) \qquad (3)$$

For non-isothermal condition Eq. (3) can be rearranged by introducing heating rate $\beta = dT/dt$ in

$$\beta \frac{d\alpha}{dT} = A_{\alpha} exp\left(\frac{-E_{\alpha}}{RT}\right) f(\alpha) \qquad (4)$$

Integral form of Eq. (4) is,

$$g(\alpha) = \int_0^{\alpha} \frac{d\alpha}{f(\alpha)} = A_{\alpha} \int_0^{t} exp\left(\frac{-E_{\alpha}}{RT}\right) dt \qquad \mathbf{(5)}$$

Eq. (5) is the basic integral form of kinetic equation and can be used to calculate the kinetic parameters of degradation reactions under any temperature program ($T(t)$). For constant rate of temperature growth the integral with respect to time can be replaced by temperature by introducing heating rate β.

$$g(\alpha) = \frac{A_{\alpha}}{\beta} \int_0^{T} exp\left(\frac{-E_{\alpha}}{RT}\right) dT \qquad \mathbf{(6)}$$

Table 2. 4: Reaction models of most common reaction mechanism considered in solid-state reactions [108,111]

Reaction Model	Model Code	$f(\alpha)$	$g(\alpha)$
Power law	P2	$2\alpha^{1/2}$	$\alpha^{1/2}$
Power law	P3	$3\alpha^{2/4}$	$\alpha^{1/3}$
Power law	P4	$4\alpha^{3/4}$	$\alpha^{1/4}$
Avrami-Erofeev : Two-dimensional nucleation	A2	$2(1-\alpha)\left[-\ln(1-\alpha)\right]^{1/2}$	$\left[-\ln(1-\alpha)\right]^{1/2}$
Avrami-Erofeev : Three-dimensional nucleation	A3	$3(1-\alpha)\left[-\ln(1-\alpha)\right]^{2/3}$	$\left[-\ln(1-\alpha)\right]^{1/3}$
Avrami-Erofeev: Four-dimensional nucleation	A4	$4(1-\alpha)\left[-\ln(1-\alpha)\right]^{3/4}$	$\left[-\ln(1-\alpha)\right]^{1/4}$
Contracting cylinder : Two dimensional phase boundary reaction	R2	$2(1-\alpha)^{1/2}$	$1-(1-\alpha)^{1/2}$
Contracting sphere : Three dimensional phase boundary reaction	R3	$2(1-\alpha)^{2/3}$	$1-(1-\alpha)^{1/3}$
Two-dimensional diffusion	D2	$\left[-\ln(1-\alpha)\right]^{-1}$	$(1-\alpha)\ln(1-\alpha)+\alpha$
Three dimensional diffusion	D3	$3/2(1-\alpha)^{2/3}\left[1-(1-\alpha)^{1/3}\right]^{-1}$	$\left[1-(1-\alpha)^{1/3}\right]^{2}$
Mampel (first order)	F1	$1-\alpha$	$-\ln(1-\alpha)$
One-dimensional diffusion	D1	$1/2\alpha^{-1}$	α^{2}
Ginstling-Brounshtein	D4	$3/2\left[(1-\alpha)^{-1/3}-1\right]$	$1-(2\alpha/3)-(1-\alpha)^{2/3}$
Second order	F2	$(1-\alpha)^{2}$	$(1-\alpha)^{-1}-1$
Third order	F3	$(1-\alpha)^{3}$	$\left[(1-\alpha)^{-1}-1\right]/2$

In general, for most of the gas phase reactions, the kinetic parameters have constant values throughout the reaction [112]. However, in solid state kinetic study many researchers envisaged the possibility of variation of the kinetic parameters with the degree of conversion [109,113]. Solid-state reactions like plastic degradation is heterogeneous in nature and reactions involve many series parallel complex reactions

undergo simultaneously. The variable kinetic parameters (E_α and A_α) are argued to be the best way of explaining the mechanism of degradation [84,111]. To determine the variable kinetic parameters the most efficient and widely used methods are the isoconversional methods [73].

2.2.3 *Determination of kinetic parameter for non-isothermal process*

Isoconversional methods

The idea of isoconversional method is based on the foundation of the isoconversional principle, which describes that at constant conversion the reaction rate is a function of temperature. A mathematical demonstration can be written by taking the logarithmic derivative of the reaction rate at constant conversion.

$$\left[\frac{\partial ln(d\alpha/dt)}{\partial T^{-1}}\right]_\alpha = \left[\frac{\partial lnk(T)}{\partial T^{-1}}\right]_\alpha + \left[\frac{\partial lnf(\alpha)}{\partial T^{-1}}\right]_\alpha \quad (7)$$

The subscript α specifies the isoconversional values related only to a given extent of conversion regardless of any thermal history. If α is constant, $f(\alpha)$ is also constant, thus the second term of the right hand side of Eq. (7) is zero. Hence:

$$\left[\frac{\partial \ln(d\alpha/dt)}{\partial T^{-1}}\right] = -\frac{E_a}{R} \quad (8)$$

The isoconversional method is considered as "model free", if no reaction model is considered during calculations, however it assumes that reaction model is a function of conversion[73].

Friedman[75] isoconversional method is one of the most widely used differential isoconversional method. The mathematical expression for this model is

$$\ln\left(\frac{d\alpha}{dt}\right)_{\alpha,i} = \ln\left(\beta\frac{d\alpha}{dT}\right)_{\alpha,i} = \ln\left[A_\alpha f(\alpha)\right] - \frac{E_\alpha}{RT_i} \quad \textbf{(9)}$$

Eq. (9) can be derived from Eq. (3) based on isoconversional principle for multi-heating rate data. At any extent of conversion value α the activation energy value (E_α) can be deduced from the slope of the plot between $\ln(d\alpha/dt)_{\alpha,i}$ and $1/T_{\alpha,i}$. The index 'i' represents the temperature programs. $T_{\alpha,i}$ is the temperature corresponding to the conversion reached under any i^{th} temperature program or the heating rate. In the integral isoconversional method, the isoconversional principle is applied on the integral equation (Eq. (5)). Rearrangement of Eq. (5) can lead to:

$$\ln t_{\alpha,i} = \ln\left[\frac{g(\alpha)}{A_\alpha}\right] + \frac{E_\alpha}{RT_i} \quad \textbf{(10)}$$

Where $t_{\alpha,i}$ is the time required to reach a particular conversion at any temperature (T_i). Eq. (10) is the basis of many integral isoconversional methods. For constant heating rate data, Eq. (6) can be used but analytical solution of Eq. (6) does not exists, hence approximations can be made to derive integral isoconversional methods. A linear generalized equation mentioned in Vyazovkin, et al. [73] was derived from various such approximations. The equation is:

$$\ln\left(\frac{\beta_i}{T_{\alpha,i}^{\beta}}\right) = const - C\left(\frac{E_\alpha}{RT_\alpha}\right) \quad \textbf{(11)}$$

Where parameters B and C govern the approximations considered in the temperature integral. One of the most common approximation introduced by Doyle [114] uses B = 0 and C = 1.052. Considering Doyle approximation, the Eq.(11) can be modified to

$$\ln(\beta_i) = Const - 1.052\left(\frac{E_\alpha}{RT_\alpha}\right) \quad \textbf{(12)}$$

Eq.(12) which is known as *Ozawa and /or Flynn and Wall (OFW)* equation [76,77]:

Another approximation given by Murray and White suggests B = 2 and C = 1 which leads to another popular and widely used equation known as method of *Kissinger-Akahira-Sunnose (KAS)* [73,115].

$$\ln\left(\frac{\beta_i}{T_{\alpha,i}^2}\right) = Const - \frac{E_\alpha}{RT_\alpha} \quad \textbf{(13)}$$

Starink[79] approximation gives more accurate estimation of activation energy as compare to the KAS and OFW methods [111]. It takes the value of B = 1.92 and C = 1.0008 in the Eq. (11):

$$\ln\left(\frac{\beta_i}{T_{\alpha,i}^{1.92}}\right) = Const - 1.0008\left(\frac{E_\alpha}{RT_\alpha}\right) \quad \textbf{(14)}$$

Aforemention methods are equally easy to solve by applying linear regression analysis. However, numerical integration gives more accurate results compare to regression analysis. Vyazovkin and his team developed the advance isoconversional method (AIC), which considers the numerical integration of multi-heating data sets and calculate the activation energy at various conversions by optimization

[73,82,84,116]. Vyazovkin's AIC method can be derived from the integral form of Arrhenius equation (Eq. (6)). Eq. (6) can be rearranged for temperature integral.

$$\int_0^1 \frac{d\alpha}{f(\alpha)} = \frac{A_\alpha}{\beta}\int_0^T e^{-\frac{E_\alpha}{RT}} dT = g(\alpha) \quad \textbf{(15)}$$

Let $x = \frac{E_\alpha}{RT}$

Eq. (15) can be simplified to by considering the variable $x = \frac{E_\alpha}{RT}$.

$$g(\alpha) = \frac{AE_\alpha}{\beta R}\int_0^\infty \frac{e^{-x}}{x^2} dx \quad \textbf{(16)}$$

Further assuming $I(E_\alpha, T_{\alpha,i}) = \int_0^\infty \frac{e^{-x}}{x^2} dx$ one can rewrite the Eq. (16) into:

$$g(\alpha) = \frac{AE_\alpha}{\beta_i R} I(E_\alpha, T_{\alpha,i}) \quad \textbf{(17)}$$

Where, $I(E_\alpha, T_{\alpha,i})$ is an integral function with two variables E_α and $T_{\alpha,i}$.Eq. (17) can be written for any particular value of conversion α and for two different heating rates of β_1 and β_2:

$$g(\alpha) = \frac{A_\alpha E_\alpha}{\beta_1 R} I(E_\alpha, T_{\alpha 1}) = \frac{A_\alpha E_\alpha}{\beta_2 R} I(E_\alpha, T_{\alpha 2}) \quad \textbf{(18)}$$

For the experiments with "*n*" (number) heating rates, the relationship would be

$$\frac{A_\alpha E_\alpha}{\beta_1 R} I(E_\alpha, T_{\alpha 1}) = \frac{A_\alpha E_\alpha}{\beta_2 R} I(E_\alpha, T_{\alpha 2}) = \ldots = \frac{A_\alpha E_\alpha}{\beta_n R} I(E_\alpha, T_{\alpha n}) \quad \textbf{(19)}$$

Further, Eq. (19) can be simplified to:

$$\frac{I(E_\alpha, T_{\alpha 1})}{\beta_1} = \frac{I(E_\alpha, T_{\alpha 2})}{\beta_2} = \ldots = \frac{I(E_\alpha, T_{\alpha n})}{\beta_n} = \sigma \quad \textbf{(20)}$$

Where, σ is a constant. When only two heating rates were considered. Eq. (20) can be written as:

$$\frac{I(E_\alpha,T_{\alpha1})}{\beta_1}=\frac{I(E_\alpha,T_{\alpha2})}{\beta_2}=\sigma \qquad \textbf{(21)}$$

If both sides of Eq.(21) is divided by either right hand term or left hand term one can get,

$$\frac{\beta_2 I(E_\alpha,T_{\alpha1})}{\beta_1 I(E_\alpha,T_{\alpha2})}=\frac{\sigma}{\sigma}=1 \qquad \textbf{(22)}$$

Or

$$\frac{\beta_1 I(E_\alpha,T_{\alpha2})}{\beta_2 I(E_\alpha,T_{\alpha1})}=\frac{\sigma}{\sigma}=1 \qquad \textbf{(23)}$$

Adding Eq. (22) and (23) will give,

$$\frac{\beta_2 I(E_\alpha,T_{\alpha1})}{\beta_1 I(E_\alpha,T_{\alpha2})}+\frac{\beta_1 I(E_\alpha,T_{\alpha2})}{\beta_2 I(E_\alpha,T_{\alpha1})}=2 \qquad \textbf{(24)}$$

For three heating rates

$$\frac{\beta_2 I(E_\alpha,T_{\alpha1})}{\beta_1 I(E_\alpha,T_{\alpha2})}+\frac{\beta_3 I(E_\alpha,T_{\alpha1})}{\beta_1 I(E_\alpha,T_{\alpha3})}+\frac{\beta_2 I(E_\alpha,T_{\alpha2})}{\beta_1 I(E_\alpha,T_{\alpha1})}+\frac{\beta_3 I(E_\alpha,T_{\alpha2})}{\beta_2 I(E_\alpha,T_{\alpha3})}+\frac{\beta_1 I(E_\alpha,T_{\alpha2})}{\beta_2 I(E_\alpha,T_{\alpha1})}+\frac{\beta_2 I(E_\alpha,T_{\alpha3})}{\beta_3 I(E_\alpha,T_{\alpha2})}=6 \qquad \textbf{(25)}$$

For "n" number of heating rate we can summarize the equation as Eq. (25) to

$$\sum_{i=1}^{n}\sum_{j\neq i=1}^{n}\frac{\beta_j I(E_\alpha,T_{\alpha i})}{\beta_i I(E_\alpha,T_{\alpha j})}=n(n-1) \qquad \textbf{(26)}$$

Here i and j represents the number of experiments performed under different heating programs. Equating the Eq. (26) to zero,

$$n(n-1)-\sum_{i=1}^{n}\sum_{j\neq i=1}^{n}\frac{\beta_j I(E_{a\alpha},T_{\alpha i})}{\beta_i I(E_{a\alpha},T_{\alpha j})}=0 \quad \textbf{(27)}$$

Further simplification leads to

$$\Phi(E_{a\alpha})=\sum_{i=1}^{n}\sum_{j\neq i=1}^{n}\frac{\beta_j I(E_{\alpha},T_{\alpha i})}{\beta_i I(E_{\alpha},T_{\alpha j})}=0 \quad \textbf{(28)}$$

Eq. (28) represents the advance isoconversional (AIC) method proposed by Vyazovkin, et al. [73] for the estimation of variable activation energy (E_α) at different extent of conversion (α) The apparent activation energy E_a is determined by minimizing the function Φ at every extent of conversion α. Where, the temperature integral I is defined as:

$$I\left[E_\alpha,T_i(t_\alpha)\right]\equiv\int_{t_{\alpha-\Delta\alpha}}^{t_\alpha}\exp\left[\frac{-E_\alpha}{RT_i(t_i)}\right]dt \quad \textbf{(29)}$$

Eq. (29) can be solved numerically and the minimization of function Φ can be repeated for every conversion point to obtain a relative dependency between E_α and α. In this study fifty conversion points between 0.05 – 0.95 were simulated for the calculation. It was argued in the literature that the experimental errors are relatively higher at the lowest and the highest conversions [73]. Therefore, the conversion limit can be set in the range of 0.05 – 0.95. The isonconversional methods used in this study are summarised in Table 2.5.

Table 2. 5 : List of isoconversional models considered in the kinetic study

		Methods	Expressions	Comments
Isoconversional methods	Differential	Friedman	$\ln\left(\frac{d\alpha}{dt}\right)_{\alpha,i} = \ln\left(\beta\frac{d\alpha}{dT}\right)_{\alpha,i} = \ln\left[A_\alpha f(\alpha)\right] - \frac{E_\alpha}{RT_{\alpha,i}}$	Differential isoconversional method applicable for multiple heating rate data. Very sensitive to small changes in rate data.
	Integral	Ozawa Flynn Wall (OFW)	$\ln(\beta_i) = Const - 1.052\left(\frac{E_\alpha}{RT_\alpha}\right)$	Modified general isoconversional equation (Eq.(11)) by Doyle approximation of B = 0 and C = 1.052
		Kissinger Akahira Sunose (KAS)	$\ln\left(\frac{\beta_i}{T_{\alpha,i}^2}\right) = Const - \frac{E_\alpha}{RT_\alpha}$	Integral isoconversional method uses Murray and White approximation in Eq. 6 i.e. B = 2 and C = 1
		Starink	$\ln\left(\frac{\beta_i}{T_{\alpha,i}^{1.92}}\right) = Const - 1.0008\left(\frac{E_\alpha}{RT_\alpha}\right)$	Starink takes the value of B = 1.92 and C = 1.0008 in Eq. (11)
		Advanced Isoconversional Model (AIC)	$\Phi(E_\alpha) = \sum_{i=1}^{n}\sum_{j\neq i}^{n}\frac{J\left[E_\alpha, T_i(t_\alpha)\right]}{J\left[E_\alpha, T_j(t_\alpha)\right]} = 0$	Distributed activation energy with respect to degree of conversion is determined by minimizing the function Φ (E_α)

2.2.4 ***Determination of reaction model and pre-exponential factor***

The model free isoconversional method can be used to evaluate the distribution of activation energy values without considering any reaction model $\left(f(\alpha)\right)$. As a part of the kinetic triplet, the reaction model $f(\alpha)$ actually determines the possible reaction mechanism of thermal degradation process. The reaction models of thermal degradation of plastics can be determined by Criados' masterplot technique [117]. The Criados' method compares experimental TGA results with established frequently used reaction models as tabulated in Table 2.4. The method uses the following equation derived from Eq. (3) and (5).

$$\frac{z(\alpha)}{z(0.5)}=\frac{f(\alpha)g(\alpha)}{f(0.5)g(0.5)}=\left(\frac{T_\alpha}{T_{0.5}}\right)^2\frac{\left(d\alpha/dt\right)_\alpha}{\left(d\alpha/dt\right)_{0.5}} \qquad (30)$$

Where, $T_{0.5}$ and $(d\alpha/dt)_{0.5}$ represent temperature and rate at $\alpha = 0.5$. The purpose of dividing 50% condition is to normalize the $z(\alpha)$ function. The value of $z(\alpha)/z(0.5)$ is equal to 1 at 50% conversion for most of the theoretical plots. The left hand side expression of Eq. (30) $\left(f(\alpha)g(\alpha)/f(0.5)g(0.5)\right)$ is the theoretical masterplots, which indicates characteristics of each reaction mechanisms, which are listed in of Table 2.4. The right hand side of the Eq. (30) which is also known as reduced rate is calculated from the experimental data. Comparing the theoretical masterplots with the experimental reduced rate plot gives the most suitable reaction mechanism of degradation. For multi-heating rate data, the master plots are obtained for all the

heating rates and the most suitable model can be selected by comparing the linearity coefficient (R^2) between theoretical master plots and experimental reduce plots.

Finally, the pre-exponential factor (A_α) can be determined by making use of Constable plots (compensation method)[118]. Constable plots depicts the linear relationship between activation energy (E_α) and $\ln(A_\alpha)$. The logarithm form of rate expression can be derived from Eq. (4):

$$\ln\left(Af(\alpha)\right)_\alpha = \frac{E_\alpha}{RT_\alpha} + \ln\left(\left(\frac{d\alpha}{dt}\right)_\alpha\right) \quad \textbf{(31)}$$

In a more generalized form the equation Eq. (31) can be written as:

$$b = \ln\left(Af(\alpha)\right)_\alpha - aE_\alpha \quad \textbf{(32)}$$

Where, $a = 1/RT_\alpha$ and $b = \ln\left((d\alpha/dt)_\alpha\right)$

The calculated values of the activation energy (E_α) and $\left(Af(\alpha)\right)$ at various stages of conversion follows a logarithmic linear relationship and compensate each other in every stages of conversion. For a particular value of conversion α the a and b values can be calculated. Then the values of $\ln(Af(\alpha)_\alpha)$, can be determined from the intercept of a linear plot of b and aE_α. Using the known reaction model $f(\alpha)$ predicted by Criados' masterplots, the calculation of pre-exponential factor (A_α) values at various extent of conversion is possible by substituting the values of E_α, $f(\alpha)$ and experimental values of $(d\alpha/dt)_\alpha$ in Eq. (31).

2.2.5 *McCallum method (for isothermal data)*

The change in temperature influences the reaction rate. So, when the temperature is constant that is under isothermal process it is assumed that the rate is constant or rate of change is minuscule to influence the kinetics, provided all other conditions such as pressure, concentration, reaction order, catalyst activity etc. are fixed. Hence, it is unlikely to predict any kinetic parameters using a single isothermal degradation data at any temperature. However, kinetic parameters can be predicted utilizing multiple isothermal data obtained at multiple temperatures.

Hill et al. [119] carried out the thermal degradation kinetics of polymethacrylonitrile under several isothermal temperature by using the method recommended by McCallum [120]. The McCallum equation can be derived by manipulating the Eq. (2).

$$\frac{d\alpha}{dt} = A\exp\left(\frac{-E}{RT}\right) f(\alpha) \tag{33}$$

$$\int\left(\frac{d\alpha}{f(\alpha)}\right) = A\exp\left(\frac{-E}{RT}\right)\int dt \Rightarrow \Gamma(\alpha) = A\exp\left(\frac{-E}{RT}\right)t \tag{34}$$

$$\ln(t) = \ln\left[\Gamma(\alpha)\right] - \ln(A) + \frac{E}{RT} \tag{35}$$

Where, $\Gamma(\alpha)$ is the integral expression in Eq. (34). Based on Eq. (35), ln (t) vs. $1/T$ can be plotted against each other. Here the t represents the time taken to reach any conversion and T represents the isothermal temperature (in Kelvin scale). The slopes of the linear fit of ln(t) vs. $1/T$ will give the activation energy values at various conversion points. The McCallum method is applied based on the assumption that

over a range of isothermal temperatures $\Gamma(\alpha)$ has the same value for a given conversion.

2.2.6 *Thermogravimetric-Fourier transform infrared spectrometry (TG-FTIR)*

Perkin Elmer TGA 4000 coupled with a Perkin Elmer FTIR spectrometer frontier was used to investigate the composition of the evolved gas during the controlled thermal degradation of the plastic samples. TGA-FTIR analysis was carried out for all virgin samples such as LDPE, HDPE, PP and PLA along with the waste PET-SDB. Non-isothermal TGA was carried out at 10 °C/min under N_2 atmosphere with 60 ml/min (40 ml/min as purge and 20 ml/min as protective gas) flow rate. The final temperature (700 °C) was maintained for 10 min. The evolved gases from the TGA chamber were carried to the attached FTIR by N_2 gas through an insulated transfer line maintained a constant temperature of 250 °C. The data obtained from the FTIR then processed and the three dimensional (3D) infrared spectroscopy (IR) plots were generated. The 3D plots consist of changes in absorbance peaks with temperature and wavenumber. IR spectroscopy is a classical method, which relies on the interaction of infrared radiation with the vibrating dipole moments of gas molecules. It gives a characteristic wavelength spectrum for most gases except for homonuclear diatomics and noble gases.

2.2.7 ***Lab scale pyrolysis***

An experimental setup was design to carry out the lab scale pyrolysis under controlled temperature. The setup was fabricated and supplied by Das and Co., West Bengal, India. The pyrolysis experiments were carried out in the semibatch tubular reactor having capacity of 1000 ml (7 cm inner diameter and 6 mm wall thickness. The reactor vessel was made up of stainless steel (SS 316). A tubular uniformly mounted electrical furnace heated the reactor vessel externally. Reactor temperature of the pyrolyser was monitored at the outer surface of the reactor vessel (probe T_1) and inside the reactor (probe T_2) protected by a cylindrical sheath attached with the lid. The PID controller controlled the temperature of the reactor considering temperature of the probe T_1 as controlling parameter. The reactor has one inlet and one outlet. The inlet was used to supply nitrogen (N_2) from a nitrogen cylinder. A flow controller was used to maintain the N_2 flow rate. Nitrogen gas was purged continuously at a flow rate of 200 ml/min to maintain the inert environment inside the reactor and to sweep out the pyrolysis vapour products. The outlet tube was connected tightly with a glass condenser (borosil) the glass condenser was then connected with the sample collecting vessels (buncher/cylindrical separating funnel) through a glass bend adaptor. Two pyrolysis schemes were chosen for conducting the experiments:

i. Isothermal pyrolysis (rapid heating and holding the final temperature for long duration)

ii. Non-isothermal pyrolysis (throughout non-isothermal slow heating)

Three pyrolysis temperatures (350, 375 and 400 °C) were selected for all the isothermal experiments except for the pyrolysis of PP (325, 350 and 375 °C) as the degradation range of PP is lower than LDPE and HDPE. The following processing sequence was adopted: samples were heated at a rate of 20 °C/min and subsequently held at the final temperature for 8 h. In non-isothermal scheme a very low dynamic heating rate of 1 °C/min was maintain to increase the reactor temperature from ambient to 400 °C and the final temperature was held for ½ h to establish stability. The schematic representation of the experimental setups are shown in Fig. 2.3 and Fig. 2.4 for isothermal and non-isothermal schemes respectively. The image of the laboratory experimental setup is shown in Fig. 2.5. A sample amount of 50 g was taken for each pyrolysis run (in both isothermal and non-isothermal schemes).

During the reaction the gaseous products came out of the reactor outlet and passed through a long condenser maintained below 5 °C using water-circulating chiller. In isothermal experiments, the condensed liquid product was collected in the collecting vessel, which was submerged in an ice bath to confirm the complete condensation of the vapour effluent. In non-isothermal pyrolysis the condensed liquid products were collected first in a cylindrical separating funnel and then transferred to a 20 ml glass vials at regular interval of 10 min from the inception of condensation. The uncondensed gases were collected in Tedlar bags at regular intervals for analysis.

Incomplete conversion led to the wax and residue accumulation at the reactor bottom for low temperature pyrolysis. The amount (in g) of liquid (W_l) product was measured by weighing in an electronic balance. The amount of solid (W_s) was

calculated from the residue remained in the reactor at the end of the reaction. The gas yield (W_g) was measured by material balance $(W_g = 50 - W_l - W_s)$. Each experiment was duplicated for the data confirmation.

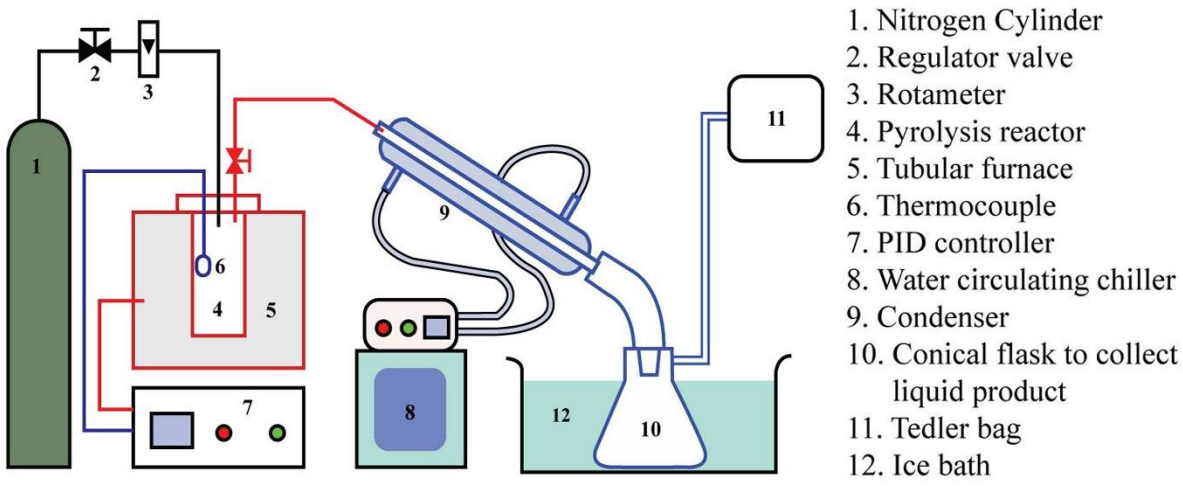

Fig. 2. 3: Schematic representation of semi-batch pyrolysis setup for isothermal pyrolysis

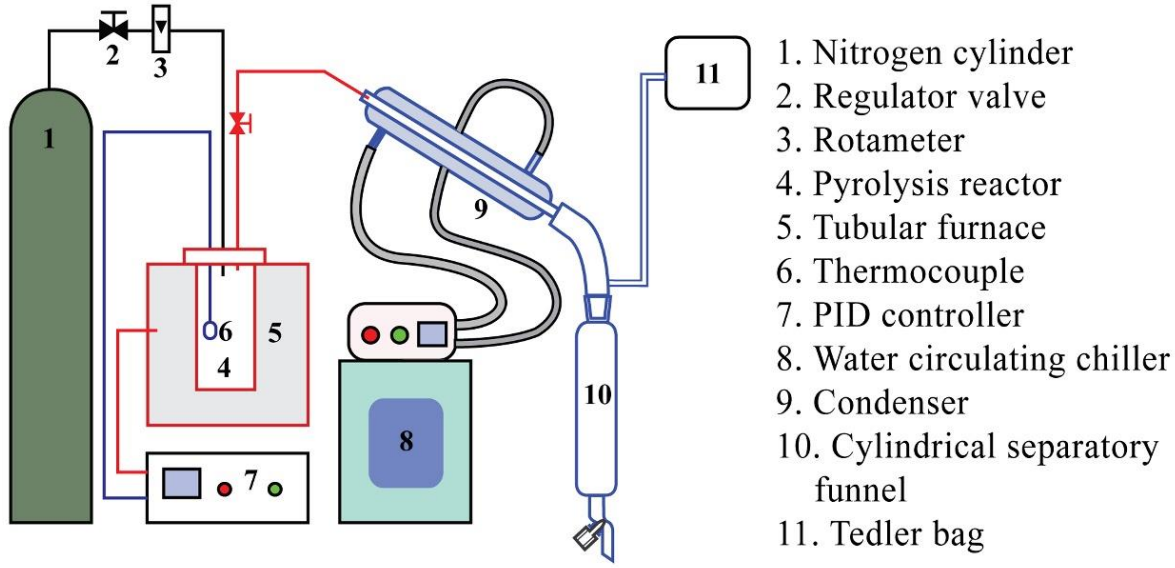

Fig. 2. 4: Schematic representation of semi-batch pyrolysis setup for non-isothermal pyrolysis

Fig. 2. 5: Semi-batch pyrolysis setup at energy conversion technology laboratory (ECTL) at Department of Chemical Engineering in Indian institute of technology Guwahati, Assam (India)

2.2.8 ***Analysis of pyrolysis products***

(a) Fourier transform infrared spectrometer (FTIR) analysis

Fourier transform infrared spectroscopy (make: Shimadzu; model: IR affinity 1) analysis of pyrolysis liquid products was carried out to identify the hydrocarbon functional groups. Attenuated total reflection (ATR) method was used to generate

the absorption spectra. The operation of FTIR-ATR governs by measuring the absorption of the internally reflected IR beam as the beam comes in contact with the sample [110]. The IR beam is directed on to an optically dense ZnSe (Zinc Selenium) crystal having a high reflective index at a particular angle. The internal reflection creates a transient wave (0.5 μ – 5 μ) that extend beyond the crystal surface to the sample that is held in contact with the crystal. The samples absorbed energy in the IR spectrum and the transient wave is attenuated and beam returned to the crystal and passed through the opposite end as shown in Fig. 2.6. The beam is then directed to the detector of the spectrometer, which recorded the interferogram signal that is used to generate IR spectrum. The wavelength range of IR spectra used in this study were in the range of 4000 – 600 cm^{-1} at a room temperature of 25 °C.

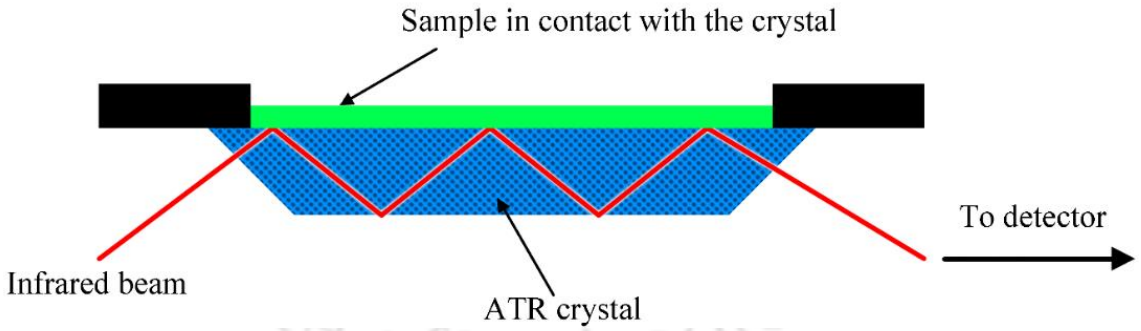

Fig. 2. 6: Schematic representation of the working principle of the FTIR-ATR analysis

(b) ^{1}H NMR analysis

Proton nuclear magnetic resonance (^{1}H NMR) spectroscopy (analysis) was performed in an Ascend™ 600 (make: Bruker) spectrometer operating at 600 MHz

(Fig 2.7). NMR spectroscopy is an analytical technique which exploits the magnetic properties of the atomic nuclei to study the physical, chemical, and biological properties of the matter [115]. Principle of NMR depends on the spinning of the nuclei of any atom under magnetic field. When atoms are placed between the poles of two powerful magnet, spinning nuclei will align with or against the field creating energy difference (ΔE) between the ground state to the excited state. When the spin reverse back to its ground state level, the absorbed radio frequency is emitted at the same level of frequency. The emitted radio frequency signal gives the NMR spectrum of the concerned nucleus. The schematic of the working principle is shown in Fig. 2.8.

Fig. 2. 7: 600 MHz NMR (Ascend™ 600 Bruker) at central instrumentation facility, IIT Guwahti

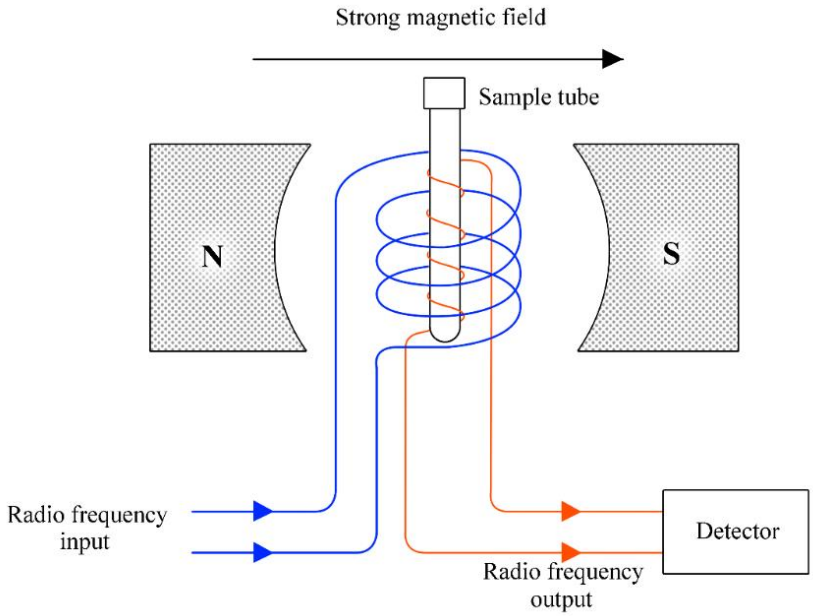

Fig. 2. 8: Schematic representation of the working principle of NMR

The oil samples were diluted in Chloroform-D1 or Deuterated chloroform ($CDCl_3$) up to ppm level before analysis and poured inside the NMR tube up to a height of 4.5 cm from the bottom. The analyses were performed at a controlled room temperature of 25 °C. Chemical shifts were reported as ppm from tetramethylsilane (TMS) based on the lock solvent (TMS is present in the $CDCl_3$ solution as a trace amount). Free induction decay files from the ^1H NMR was analyzed in ACD 1D NMR software for post processing. ^1H NMR analysis was carried out to identify the presence of various functional groups (paraffin, olefin and aromatic). It was also able to determine thevol% of aromatics, paraffins and olefins, along with isoparaffin index, H/C ratio and research octane number (RON) based on the correlations given by Meyers et al. [121,122]. Joo and Guin [123] and Sinag, et al. [124] utilized the correlations successfully in the characterization of reformed plastic pyrolysis oil and oil obtained from the co-pyrolysis of lignite and LDPE respectively. The correlations

entail several equations (Eq.(36) −(41)), consists of parameters A, B, C, D, E and F which represent the integrated area of the spectral regions, parts per million (ppm) from TMS reference peak as listed in Table 2.6 (Fig. A.1). These correlations have been established based on the known standard mixture (with an error margin of ±2%).

$$Aromatics,\ vol.\ \% = \frac{(A+C/3)0.97\times10^2}{(A+C/3)0.97+(D-2B+E/2+F/3)1.02+3.33B} \quad (36)$$

$$Paraffins, vol.\% = \frac{(D-2B+E/2+F/3)1.02\times10^2}{(A+C/3)0.97+(D-2B+E/2+F/3)1.02+3.33B} \quad (37)$$

$$Olefins, vol.\% = \frac{3.33B\times10^2}{(A+C/3)0.97+(D-2B+E/2+F/3)1.02+3.33B} \quad (38)$$

$$H/C = \frac{A+B+C+D+E+F}{(A+C/3)1.28+(D-2B+E/2+F/3)1.02+3.42B} \quad (39)$$

Table 2. 6: NMR spectral region [121,122]

	Proton type	Chemical shift region
A	ring aromatic	6.6 – 8.0
B	olefin	4.5 – 6.0
C	α - methyl	2.0 – 3.0
D	methane (paraffins)	1.5 – 2.0
E	methylene(paraffins)	1.0 – 1.5
F	methyl(paraffins)	0.6 – 1.0

It was established in petroleum studies that there is a close correlation exists between the amount of branching in the structure of a paraffinic hydrocarbon and its octane number [125]. A measure of the amount of branching is known as '*iso-paraffin index*' [122], which is the ratio of CH_3:CH_2 in the paraffin. The CH_3:CH_2 ratio for an unknown paraffin or a mixture of paraffins can be determined experimentally by nuclear magnetic resonance (NMR) spectrometry.

$$\textit{Iso-paraffin index} = CH_3/CH_2 = (F/3) \,/\, (E/2) \tag{40}$$

$$\textit{RON} = 80.2 + 8.9\ \textit{iso-paraffin index} + 0.107\ \textit{aromatics (vol. \%)} \tag{41}$$

The RON values predict the behaviour of the liquid fuel if it is used as a fuel for engines that runs at low temperatures and speed. It is the measure of knock resistance of gasoline in the engine [126].

(c) Simulated distillation (SimDist) analysis of PDO

Simulated distillation (SimDist) analysis is a well-known technique to characterise petroleum fractions for rapid determination of the carbon number distribution (boiling range) using gas chromatography. The GC (model: GC Trace 1110, make: ThermoFisher scientific) operating conditions are summarised in Table 2.7. Two internal hydrocarbon paraffin standards (ASTM D5307 from Supelco) with serial numbers 48182 (C_3 – C_9) and 48179 (C_{10} – C_{44}) were used to determine the retention time of n-paraffins which helps establishing the carbon number (boiling point) distribution of PDOs. All the liquid samples were filtered with a syringe filter (45 µm) and subsequently diluted with HPLC grade dichloromethane (DCM) up to

concentration of 1 ppm before analysis. The chromatographic spectra of the paraffin standards are shown in Fig. 2.10. The composition (% w/w) of the PDOs were calculated by taking the ratio of the individual peak area to the total peak area of the full spectra over a baseline.

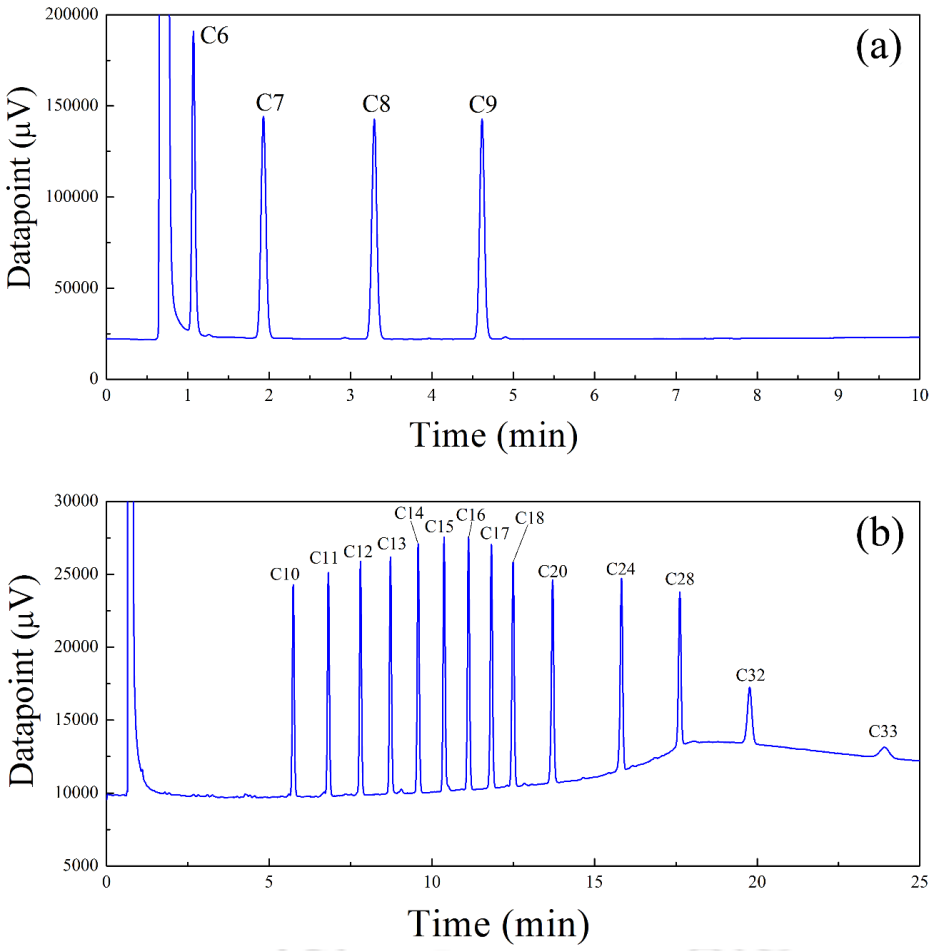

Fig. 2. 9: GC chromatographic FID spectra of the n-paraffin standards (a) Supelco 48182 (Sigma-Aldrich), (b) Supelco 48179 (Sigma-Aldrich)

(d) Gas chromatography (TCD and FID) for gases

The analysis of non-condensable gases was carried out with the help of gas chromatography (Thermo Fisher Scientific: GC Trace 1110). The concentrations of

hydrogen (H_2), carbon monoxide (CO) and carbon dioxide (CO_2) were identified by using thermal conductivity detector (TCD). Flame ionization detector (FID) was used to determine the hydrocarbons (saturated and unsaturated) components. GC configuration for TCD and FID analysis is summarised in Table 2.7. Gas standards (Chemtron science laboratories Pvt. Ltd., Mumbai, India) with known concentrations were used to identify and quantify the components. The chromatographic spectra's of the gas standards are shown in Fig. 2.11 (Fig. A. 12). The gross and net calorific values of dry gaseous product were calculated using the mixing rules [21].

Table 2. 7: GC configuration for both FID-Simdist, TCD and FID and detection for the analysis of hydrocarbon gases

Parameters	GC method		
	GC-Simdist (liquid)	TCD (gas)	FID (Gas)
Column (make)	TR-Simdist (Thermo scientific)	60/80 Carboxen-1000 (Supelco)	TG-BOND Alumina (Thermo scientific)
Length	10 m	4.57 m	30 m
Int. Diameter	0.53 mm	2.1 mm	0.53 mm
Carrier gas	N_2 (high pure)	Helium	Helium
Flow rate (Carrier gas)	8 ml min^{-1}	30 ml min^{-1}	4 ml min^{-1}
Oven temperature program	60 °C (2 min) to 350 °C at 5 °C min^{-1} and 5 min hold	40 °C (5 min) 200 °C at 5 °C min^{-1}	130 °C isothermal (15 min)
Injector temperature	350 °C	150 °C	200 °C
Detector temperature	350 °C	150 °C	200 °C
Sample injection	2 µµl	1 ml	1 ml

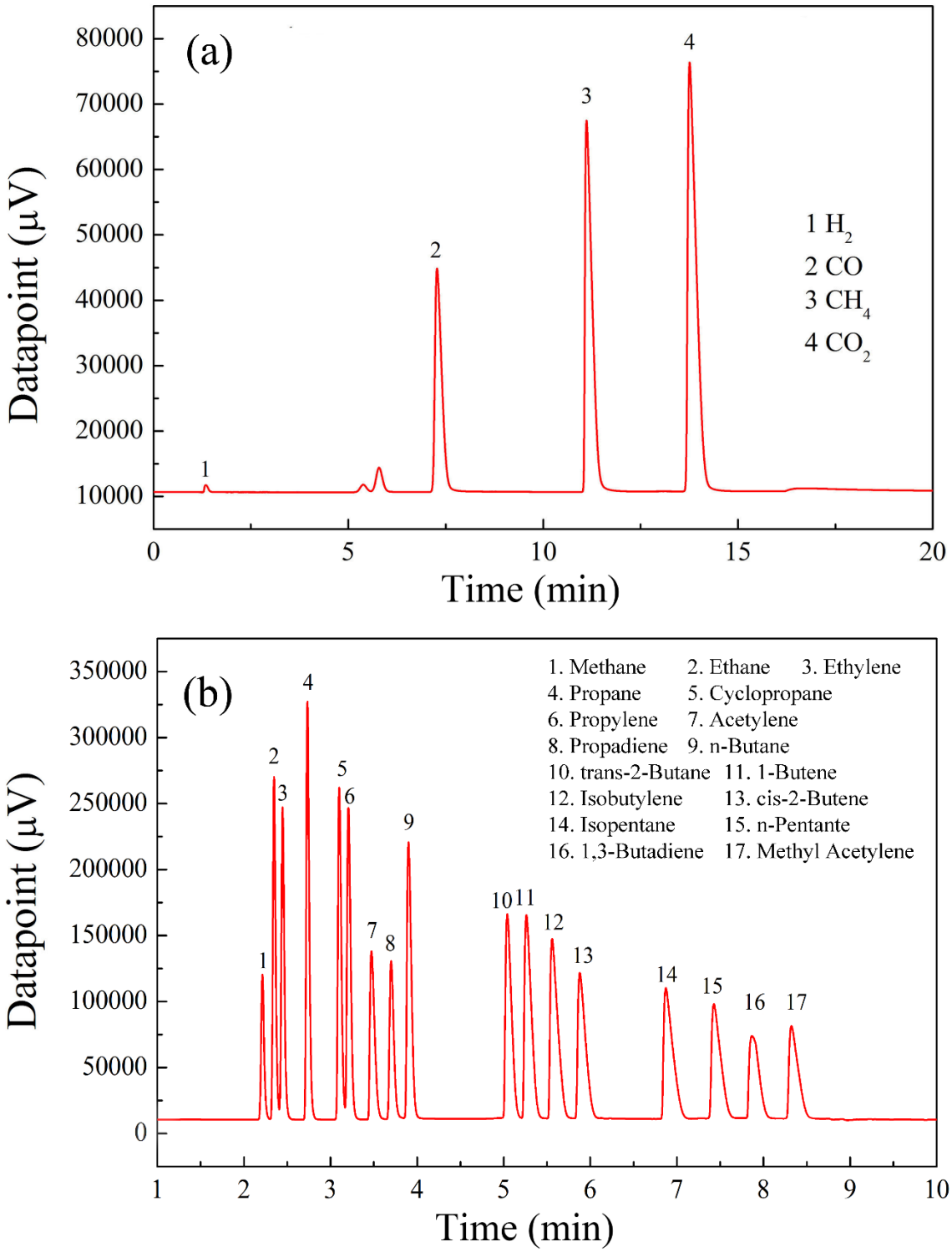

Fig. 2. 10: GC spectra for the standard gases (a) non-hydrocarbon gases (TCD) and (b) hydrocarbon gases (FID)

2.2.9 ***Analysis of fuel properties***

(a) Calorific (heating) value (CV)

The calorific value (heat of combustion) of any sample is broadly defined as the number of heat units or heat liberated by a unit mass of the sample when burned with access amount of oxygen in an enclosure of constant volume. The calorific value (or heat of combustion) that was measured using bomb calorimeter denotes the heat liberated by the combustion of all the carbon and hydrogen with oxygen to form carbon dioxide and water, including the heat liberated by the oxidation of other elements such as sulphur.

Oxygen Bomb calorimeter (Parr 1341 plain Jacket Bomb Calorimeter) was used to determine the calorific value of the liquid products. The schematic representation of the bomb calorimeter is shown in Fig. 2.12. The known amount of sample (0.5 – 1g) placed in a crucible (sample holder), was burnt inside a sealed container/bomb pressurized by pure oxygen gas. During burning, the bomb was submerged in a bath containing a known amount of demineralized water in a metal bucket, which was kept inside an insulated chamber. The energy equivalent or heat capacity of the calorimeter was determined before a material with an unknown calorific value was tested in the bomb calorimeter. This value represents the sum of the heat capacities of the components in the calorimeter, notably the metal bomb, the bucket, and the water in the bucket. The exact amount of the heat capacities for each of the particulars used in the bomb and bucket is difficult to determine and the values are

continually changing with use. Hence, energy equivalents are determined empirically at regular intervals by burning a sample of a standard material (Benzoic acid) with a known heat of combustion under controlled and reproducible operating conditions. The energy released due to the burning of the sample inside the bomb increased the temperature of the water in the bucket. This rise in temperature was recorded and the energy equivalent or the calorific value (CV) was calculated based on the ASTM D 4809 standard method.

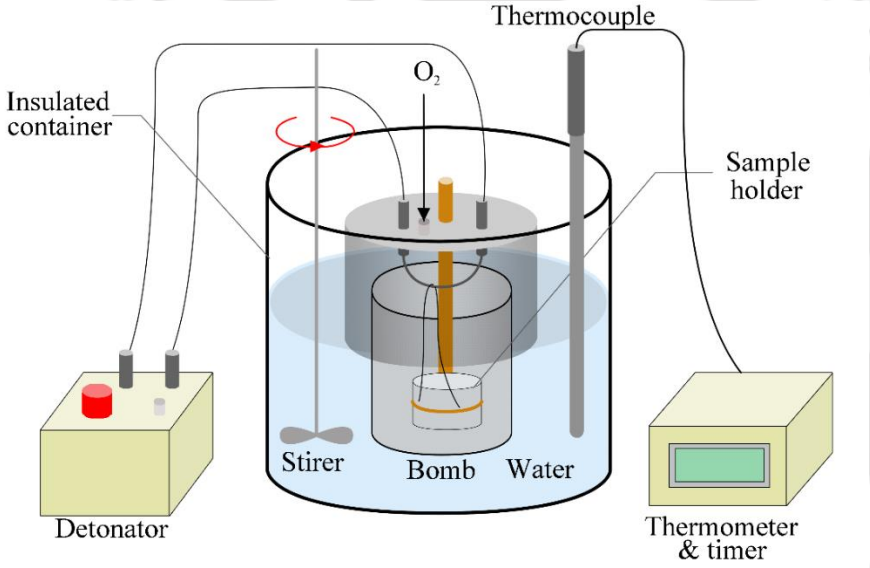

Fig. 2. 11: Schematic representation of the working principle of Bomb calorimeter

(b) Viscosity

Viscosity of the PDOs was measured in an Anton Parr MCR 301 Rheometer using a parallel plate setup at room temperature (25 °C). Viscosity was measured at variable share rate ranging between 100 to 1000 (1/s). The average value of the viscosity was reported since all the liquid products are Newtonian fluids.

(c) Flash and fire points

The flash point is the temperature at which the liquid fuel produce enough vapor that ignites as a flash while the test flame is passed over it. The fire point is the temperature at which the oil sample started burning continuously for 5 s. The flash and fire points of the PDOs were measured using the Cleveland open cup apparatus (manual). The tests were conducted based on the procedure suggested in the standard ASTM D92 test method [127]. Approximately 50 – 70 ml of the test specimen was filled into the test cup. The temperature of the test specimen was increased rapidly in a controlled manner in the beginning and then the heating rate was constantly slowed down before the temperature of the fuel reached the fire point temperature. A test flame was passed over the cup at regular intervals. The temperature of the sample in the cup was measured continuously using a thermometer.

(d) Cloud and pour point

Cloud point (CP) and pour point (PP) of the oil samples were measured utilizing ASTM D97 standard test method [127]. The apparatus use is shown in Fig. 2.12(a), which consist of a chiller, two-test jars (cylindrical, clear glass, flat bottom), and thermometers etc. The cloud point refers to the temperature below which the liquid hydrocarbons like diesel undergoes crystallization and forms wax, which has a cloudy appearance (Fig. 2.12 (b)). On the other hand, pour point refers to the lowest temperature at which the liquid fuel cease to flow as a fluid due to increase of viscosity (Fig. 2.12 (c)).

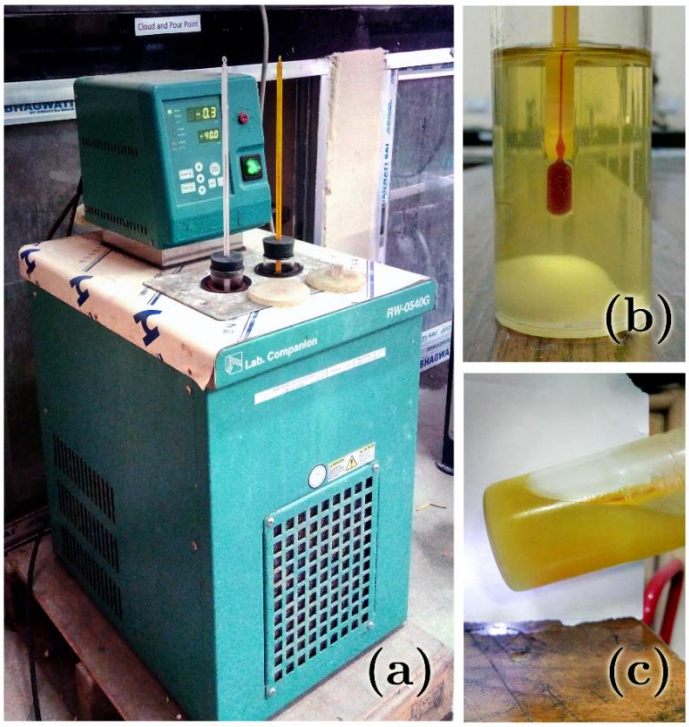

Fig. 2. 12 (a) Pour point and cloud point measuring apparatus, (b) PDO at cloud point and (c) PDO at pour point (PDO collected from the pyrolysis of RMIX sample at 350 °C)

Summary

Firstly, the chapter presented the details of the types of materials considered in the pyrolysis as well as TGA based kinetic study. The theoretical aspects of kinetic analysis were covered in details. The methods used in the analysis of degradation kinetics of plastics were explained. The experimental procedure of the pyrolysis (isothermal and non-isothermal) was explained elaborately and brief explanation was given for individual analytical techniques used to characterize the pyrolysis products. The chapter laid the foundation in the understanding of the remaining chapters with appropriate methodology.

Chapter 3

THERMAL DEGRADATION KINETICS OF PLASTICS AND MODEL SELECTION

Plastics

Thermal degradation kinetics

Isoconversional methods

Kinetic model selection

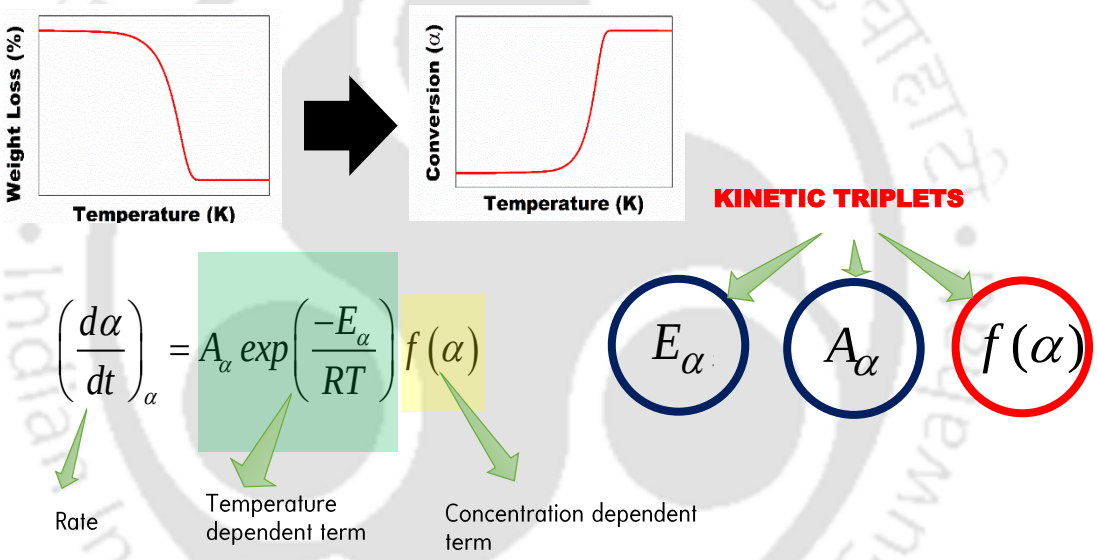

Work published at:

- Pallab Das and Pankaj Tiwari, 'Thermal degradation kinetics of plastics and model selection', Thermochimica Acta, Vol. 654, pp. 191-202 (2017). IF = 2.251
- Pallab Das and Pankaj Tiwari, 'Thermal degradation study of polyethylene terephthalate from waste soft drink bottles, under inert and oxidative environments', Thermochimica Acta, pp. 178340. IF = 2.251

3 TGA based kinetic analysis

This chapter focuses on the investigation of thermal decomposition behaviour of high and low-density polyethylene (LDPE and HDPE), polypropylene (PP), poly(lactic acid) (PLA) and polyethylene terephthalate form waste soft drink bottles (PET-SDB) under inert condition by dynamic and static thermogravimetric analysis (TGA). Determination of distributed activation energy values at various stages of degradation process and their implication in the degradation mechanism was investigated with the help of the isoconversional methods. The reaction models (f(α)) were predicted using Criados' masterplot technique. The corresponding values of the pre-exponential factors were calculated using the compensation effect. A comparative study of various isoconversional models like Friedman, Kissinger-Akahira-Sunnose (KAS), Ozawa- Flynn and Wall (OFW), Starink and Advance isoconversional method (AIC) were discussed and their reliability was examined. The α-T plots were reconstructed with the calculated kinetic data. The experimental and simulated data (α -T) were compared to select the appropriate models for kinetic analysis. Under isothermal temperature, the variable kinetics were determined using multiple data at different temperatures. TG-FTIR analysis was performed to identify the evolved components and their evolution behaviour during thermal degradation.

3.1 Non-isothermal TGA kinetics

3.1.1 *Non-isothermal thermogravimetric analysis (TGA)*

Thermogravimetric analysis (TGA) or weight loss with temperature and derivative thermogravimetric (DTG) curves obtained at seven heating rates for LDPE, HDPE

and PP are shown in Fig. 3.1 and for PLA and PET-SDB are shown in Fig 3.2. From the TGA curves, it was observed that the shape of the weight loss curve did not change with the variation of heating rates. Complete (100%) degradation was observed for polyolefin plastics (LDPE, HDPE and PP) with negligible residue accumulation. On the other hand, 0.5 – 1 % and 15 – 20% residue (char) accumulation was observed for PLA and PET-SDB respectively at different non-isothermal TGA. Oxygen present in the PLA and PET molecules may responsible for the formation of the stable char [119]. A slow degradation of char was observed when the sample was heated further under inert atmosphere [128]. Derivative thermogravimetry (DTG) is the rate of mass change with the change of time or temperature [129]. It is commonly used to establish the kinetic parameters, degradation steps, degradation range and peak degradation temperature etc. Single degradation peak was appeared in all the DTG curves irrespective of materials and heating rates, which confirmed a single step degradation of the organic matter present in the plastics under inert condition. However, the thermal degradation of plastics consists of numerous parallel and series scission reactions that undergo simultaneously[130]. The lone peak actually combines all the reactions together (overlapped) and demonstrates the overall rate of degradation.

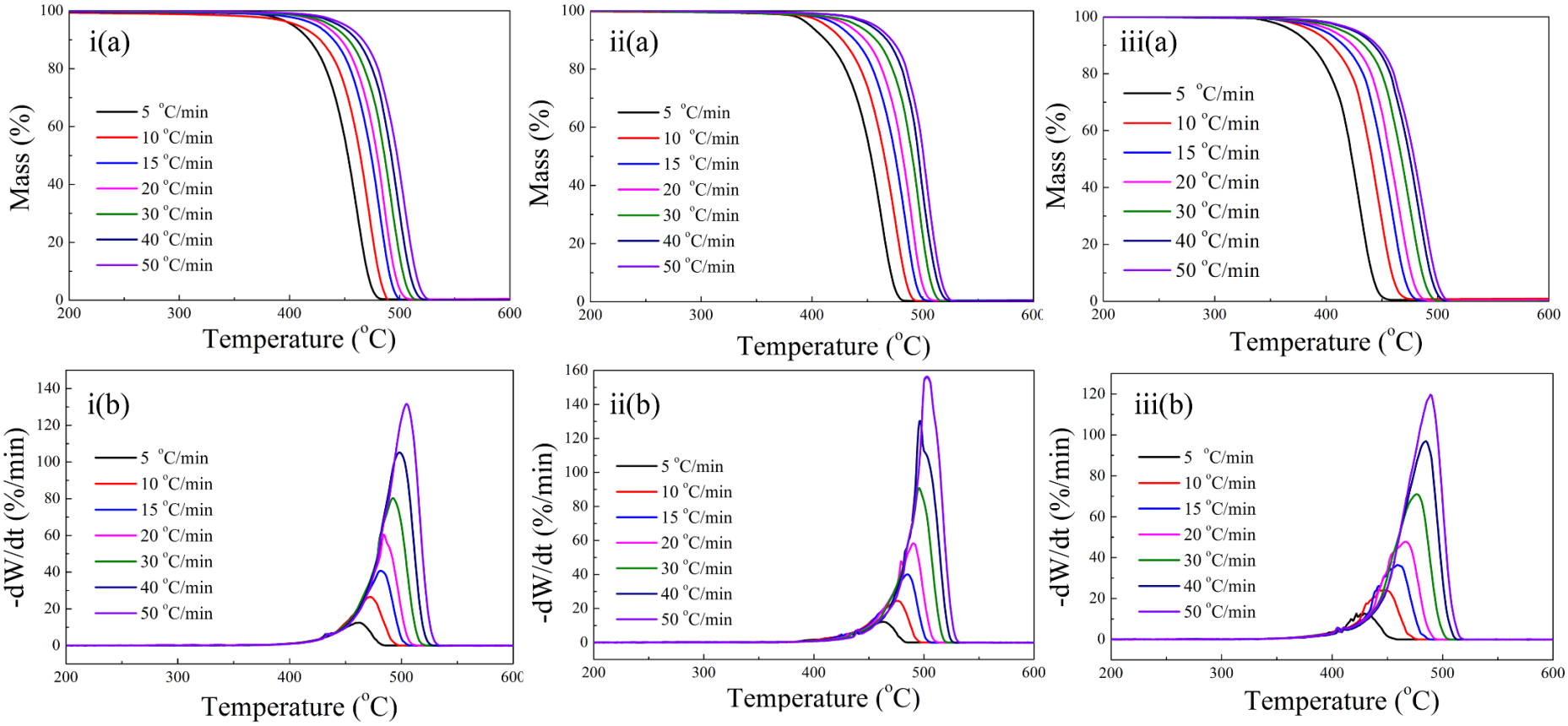

Fig. 3. 1: Thermogravimetric profiles (a) TGA and (b) DTG of (i) LDPE, (ii) HDPE and (iii) PP at seven heating rates (5, 10, 15, 20, 30, 40, 50 °C/min)

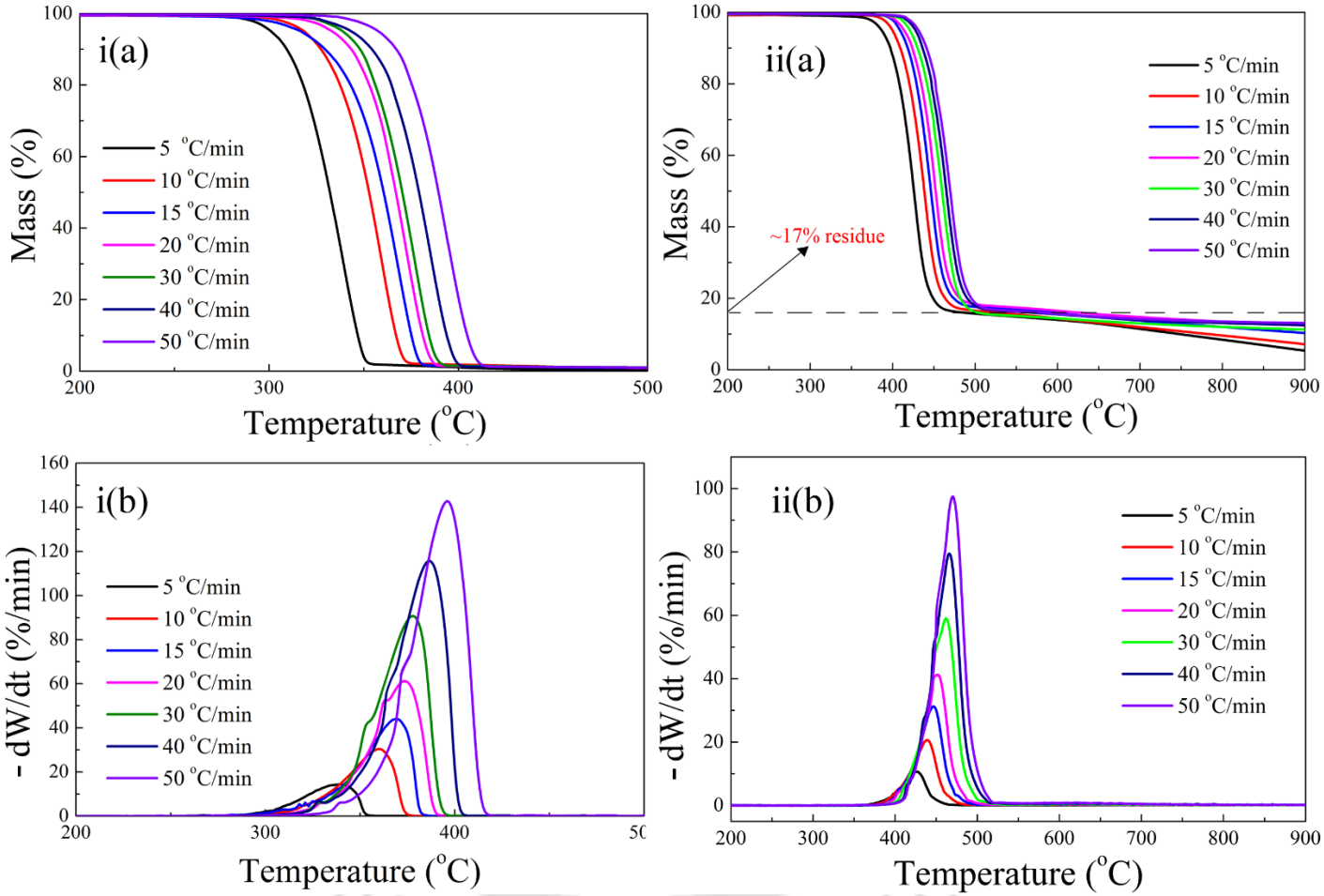

Fig. 3. 2: Thermogravimetric profiles (a) TGA and (b) DTG of (i) PLA and (ii) PET-SDB at seven heating rates (5, 10, 15, 20, 30, 40, 50 °C/min)

Fig 3.3 demonstrates the scheme used to estimate the values of onset temperature (T_o), end temperature (T_e) and temperature at maximum degradation rate (T_m) from the DTG curve. Table 3.1 shows the TGA degradation data at different heating rates, which includes initial weight of the sample, T_o, T_e, and T_m for the materials considered. With the increase of the heating rates, the degradation temperatures (T_o, T_e, and T_m) shifted to higher values, which is due to the different time and temperature history subjected to the material. Previous studies reported similar degradation profiles for LDPE [61], HDPE[83,131], PP[132], PLA[81] and PET-SDB[133]

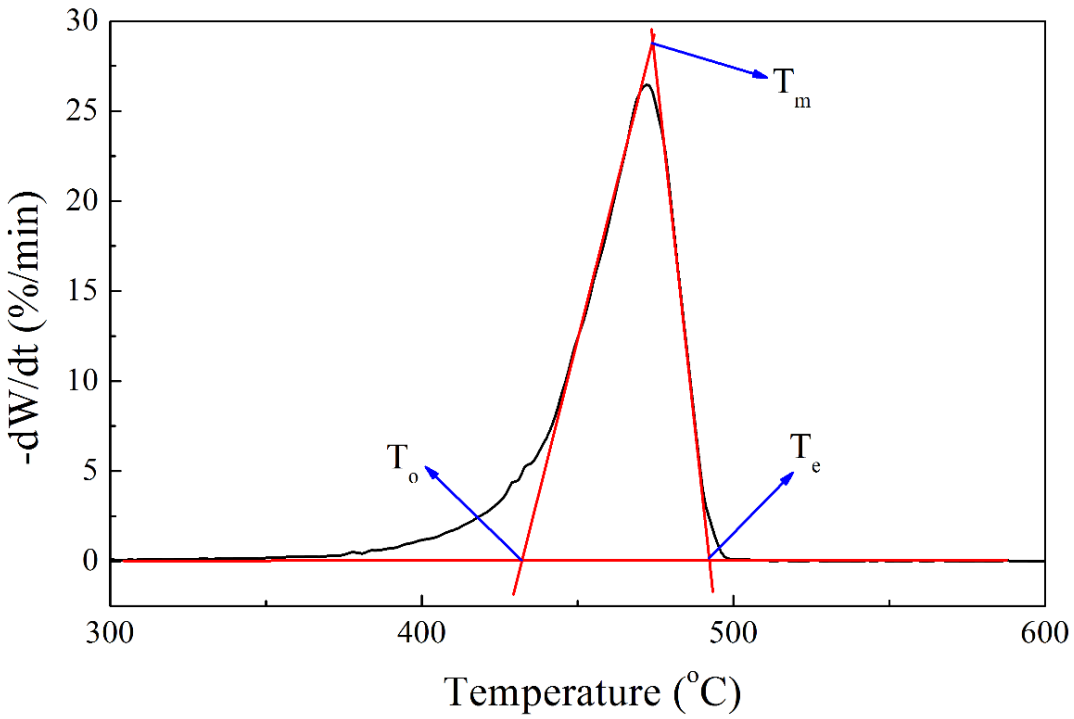

Fig. 3. 3: Scheme adopted for the estimation of onset temperature (T_o), end temperature (T_e) and maximum degradation temperature (T_m) from DTG curve (i.e. DTG curve of LDPE at 10 °C/min)

Table 3. 1: TGA analysis data

Materials	Initial weight, (mg)	Heating rate, (°C/min)	Onset temperature, T_o, (°C)	End temperature T_e, (°C)	Maximum degradation temperature T_m, (°C)
LDPE	6.29	5	418.45	481.55	462.05
	6.46	10	433.35	492.75	472.95
	6.56	15	448.95	501.05	481.05
	6.51	20	454.05	505.35	484.05
	6.06	30	454.05	513.45	491.95
	6.03	40	468.65	519.75	498.05
	6.02	50	466.65	526.45	505.05
HDPE	6.89	5	273.15	480.15	463.05
	6.94	10	426.45	493.25	475.25
	6.88	15	439.05	501.15	485.05
	6.67	20	450.65	505.95	490.25
	6.55	30	456.95	515.95	495.95
	7.09	40	468.15	522.65	500.25
	6.46	50	473.05	526.25	504.95
PP	8.03	5	397.45	451.45	432.35
	7.49	10	408.15	469.05	447.95
	7.34	15	413.95	480.35	459.05
	7.54	20	423.15	487.65	466.45
	7.33	30	434.05	497.95	476.55
	7.87	40	437.35	504.75	484.75
	7.29	50	438.95	509.85	489.25
PLA	6.65	5	300.15	352.45	339.95
	6.51	10	322.65	373.35	359.95
	6.26	15	331.55	381.45	368.95
	6.83	20	335.95	388.85	373.95
	6.57	30	339.35	391.95	378.05
	6.63	40	346.85	401.85	386.95
	6.73	50	359.15	414.25	395.95
PET-SDB	8.94	5	388.95	427.45	448.25
	6.56	10	396.35	438.95	463.45
	6.73	15	404.85	445.85	471.55
	8.68	20	411.15	453.35	475.35
	7.42	30	414.15	460.85	485.75
	7.84	40	423.65	465.95	487.85
	6.69	50	425.75	470.25	495.15

3.1.2 ***Kinetic analysis***

(a) Determination of activation energy

The values of activation energy (E_α) with respect to conversion (α) were obtained by the isoconversional methods (explained in section 2.2) are shown for LDPE, HDPE and PP in Fig. 3.4 and for PLA and PET-SDB in Fig. 3.5. The activation energy values of the plastics were determined for 50 conversion points (equal interval) in the conversion range of 0.05 – 0.95 for LDPE, HPDE, PP and PLA. On the other hand, The rate of weight loss (DTG) of PET-SDB decreased to negligible value after ~80% weight loss as the temperature reached T_e (Fig. 3.2 ii(b)), beyond that the change was trivial. Hence, the kinetic study was carried out between the conversion range of 0.05 – 0.8 (at 50 intervals) for PET-SDB. The range of activation energy values obtained for all five isoconversional methods are listed in Table 3.2. Diversity among the values of the activation energy obtained with the different isoconversional methods were the results of various approximations and mathematical formulations chosen during the model building. Certainly, in all the methods the gradual change of E_α with the extent of conversion (α) was observed. An abrupt increase of activation energy was observed between the conversions 0.7 - 0.8 in case of PET-SDB (Fig. 3.5(b)). The increasing values of the activation energy may related to the slow degradation rate at the end. The evolution of volatile matter from PET-SDB sample ceases near the end temperature (T_e) and the rate of degradation slows down to negligible value due to the formation of stable char.

Examining the activation energy profiles in Fig. 3.4 and Fig. 3.5, it was found that Friedman method lead to the largest spread of activation energy and the distributed profile was found discontinuous compared to the profiles obtained from other

methods considered in the current study. Differential isoconversional method such as Friedman method does not consider any approximations like integral methods, hence it is expected that this method should give more accurate results [73]. However, to apply differential method to integral data (e.g. TGA) requires numerical differentiation. Numerical differentiation brings noise in the data estimation and smoothing the same brings inaccuracy, which ultimately leads to the discontinuous activation energy profile [111]. The trend of activation energy obtained from other methods were found consistent.

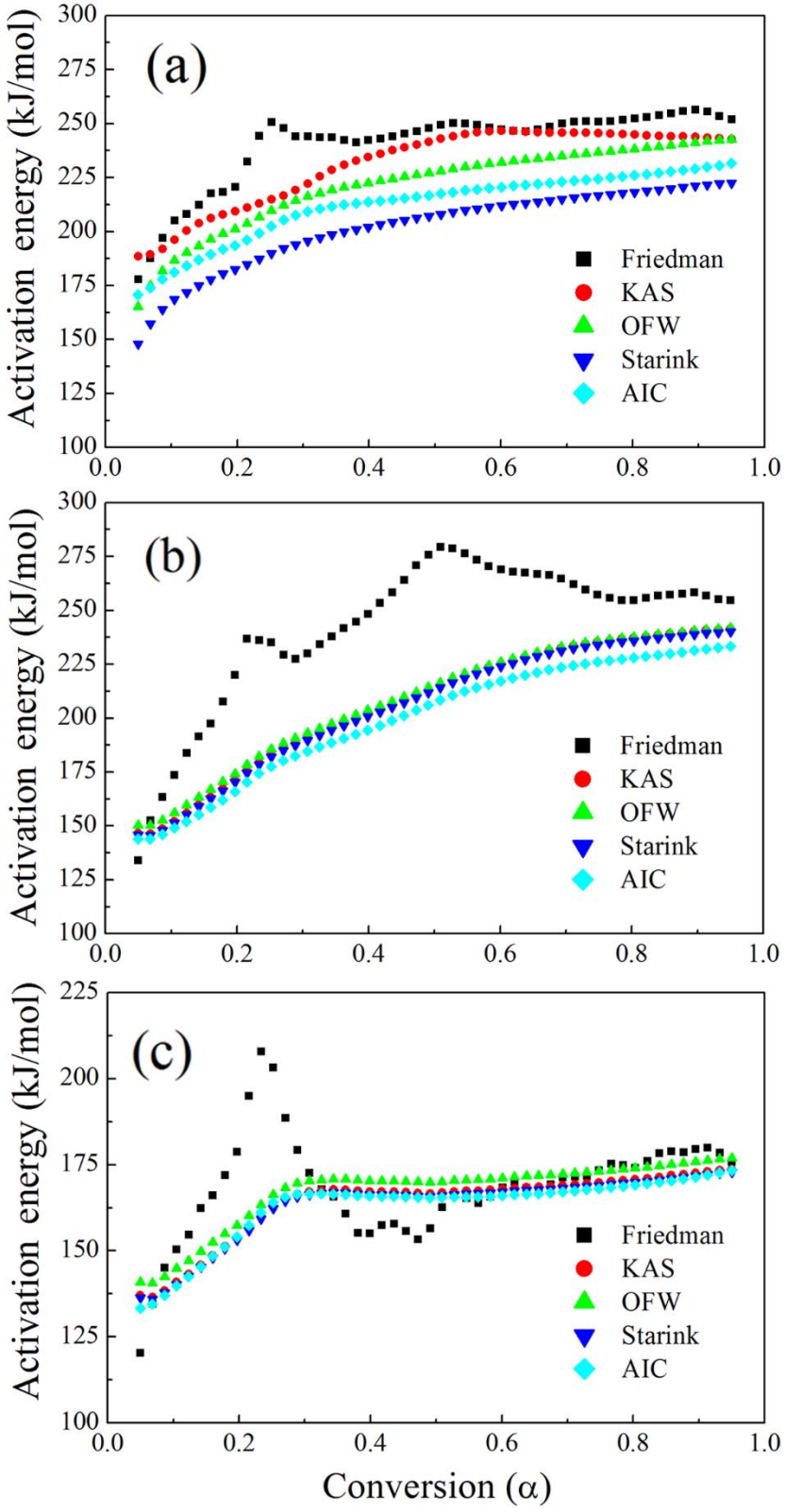

Fig. 3. 4: Distribution of activation energy (E_α) obtained by using various isoconversional methods for (a) LDPE, (b) HDPE and (c) PP

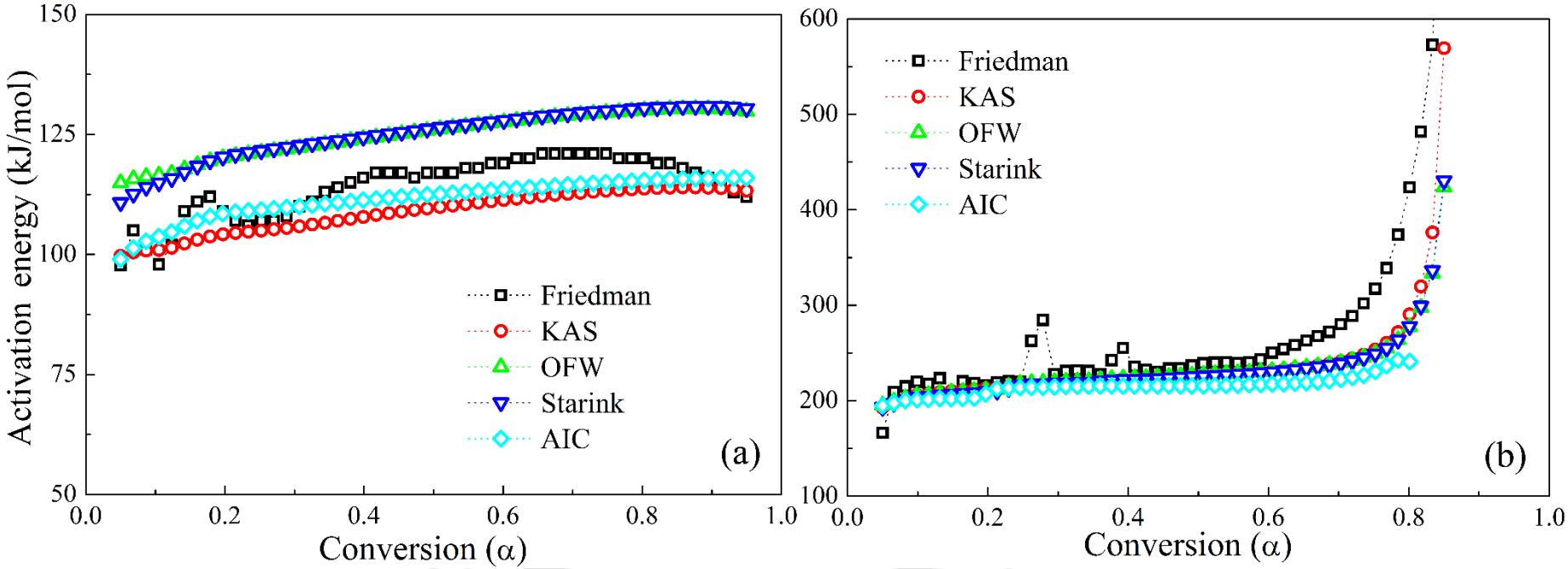

Fig. 3. 5: Distribution of activation energy (E_α) obtained by using various isoconversional methods for (a) PLA and (b) PET-SDB

The distributed activation energy values E_α obtained from isoconversional methods were the first dataset of the three kinetic triplets. The AIC method was prioritize in the further calculation due to the better precision in kinetic calculations as suggested by ICTAC committee [69-72,111]. Reconstruction of degradation profile with the estimated kinetic parameters was carried out in the subsequent section to establish the best-suited isoconversional methods for the kinetic analysis. The $Af(\alpha)$ values were obtained by substituting estimated values of E_α and the experimental values of $(d\alpha/dt)_\alpha$ in Eq. 31. The $Af(\alpha)$ values were used further to calculate the values of A_α. The values of distributed activation energy (E_α) calculated by AIC method with the associated uncertainties and the values of $Af(\alpha)$ as a function of conversion is shown in Fig 3.6 for LDPE, HDPE, and PP and in Fig 3.7 for PLA and PET-SDB. The distribution of activation energy obtained from AIC method were in the range of 170 – 232 kJ/mol for LDPE, 143 – 231 kJ/mol for HDPE, 133 – 173 kJ/mol for PP, 99 – 116 kJ/mol for PLA and 198 – 226 kJ/mol for PET-SDB (between α = 0.05 – 0.8). The polyolefins such as LDPE, HDPE and PP decompose into smaller hydrocarbons of various kinds under thermal treatment [83]. The range of activation energy values varies with the type of plastics due to different molecular (polymer) structure. The degradation of plastics actually involves the breaking of the bonds between individual atoms forming the polymer chains. The breaking of C – C bond (~350 kJ/mol) requires higher activation energy and the degradation occurs above 400 °C temperature [83].

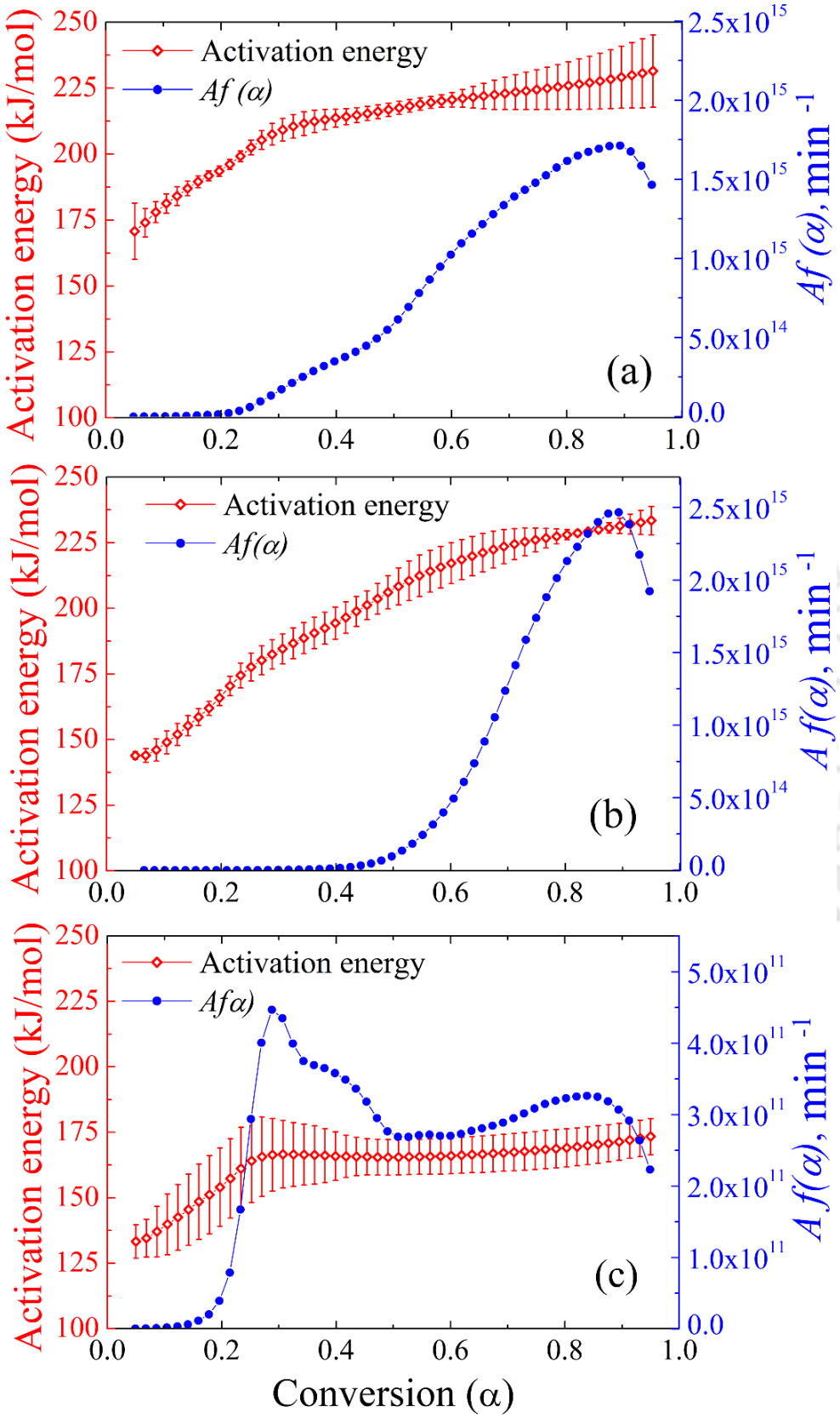

Fig. 3. 6: Distribution of activation energy (E_α) (with uncertainty) and $\left(Af\left(\alpha\right)\right)_\alpha$ values for (a) LDPE (b) HDPE and (c) PP using AIC method

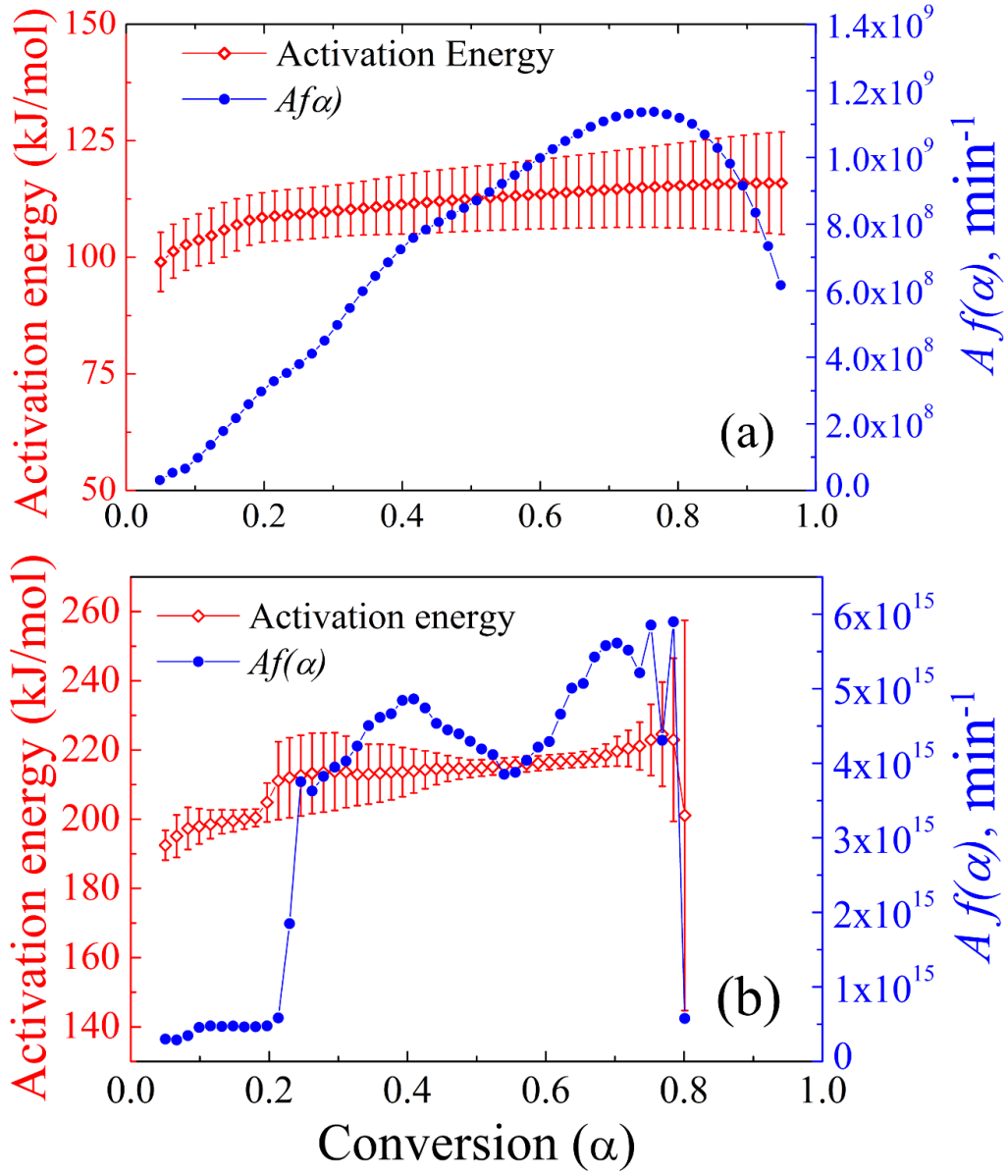

Fig. 3. 7: Distribution of activation energy (E_α) (with uncertainty) and $(Af(\alpha))_\alpha$ values for (a) PLA (b) PET-SDB using AIC method

The degradation of plastics at the onset temperature initiate due to the breaking of thermally labile bonds (weak links like branching and head-to-head links) inherent with the polymer chain. Low activation energy at the beginning of the degradation process indicates the bond breaking of weaker links of the polymer chains [84]. The thermal stability of polyolefins is also affected by the presence of branching in the

polymer. In the PP polymer chain, the presence of one tertiary carbon atom (methyl group) attached with every alternate carbon atom provides more weak links for the initiation of the degradation reactions. Hence, low activation energy was observed in the initial degradation period of PP. However, in the literature it was argued that the degradation of PE and PP occur via random scission followed by radical transfer process [83,108,111,130,131]. An increase in effective activation energy with the progress of reaction for PE (LDPE and HDPE) and PP is caused by the shift of the rate-limiting step from initiation to the degradation initiated by the random scission. On the other hand, PLA is a linear aliphatic hydrocarbon polymer, which is produced from renewable resources. The kinetic analysis of virgin PLA based on non-isothermal TGA (inert condition) revealed that the activation energy has lower values compared to polyolefins (Fig 3.5 (c)). The variation of activation energy throughout the degradation process was also found minimum. In thermal degradation process, PLA undergoes end chain scission involving OH group and random scission at the main polymer chain involving alkyl-oxygen homolysis or acyl-oxygen homolysis. Low activation energy of PLA degradation may speculate the low energy of non-radical backbiting ester interchange reactions involving OH chain ends [134,135]. Structure of PLA with the presence of alkyl or acyl-oxygen group makes it thermally less stable than polyolefins. The reported studies [128,136] suggested that thermal degradation of PET (polymer) follows a random scission of the in-chain ester linkage by forming vinyl ester and carboxyl end groups. The vinyl ester then undergoes transesterification reaction to produce vinyl alcohol, which immediately

transformed into acetaldehyde. The thermal degradation may also responsible for hydrogen atom abstraction when impurities in the polymer generate macro-radical sites [28,128].

(b) Determination of reaction model $\left(f(\alpha)\right)$ *and pre-exponential factor*$\left(A_\alpha\right)$

The reaction model *f(α)* was determined with the help of Criados' masterplot technique [117]. Section 2.4 discusses the calculation method of *f(α)* and A_α. All the models and associated functions, *f(α)* and *g(α)* used in Criados' masterplot technique are listed in Table 2.4.

The theoretical masterplots $z(\alpha)/z(0.5)$ vs. α for different mechanisms along with the experimental reduced plots for LDPE, HDPE, PP and PLA are illustrated in Fig. 3.8 (a) at a heating rate of 5 °C/min. The selection of the reaction model $f(\alpha)$ was done by calculating the regression coefficient (R^2) between experimental and theoretical masterplots considering all the heating rates. Fig 3.8 (b) shows the regression coefficient (R^2) at seven heating rates for LDPE. Similar charts were also prepared for HDPE, PP & PLA and provided in the Appendix A (Fig. A.2). The degradation reaction models for LDPE, HDPE, PP, PLA were found to be R2, R2, R3, and R2 respectively. Both R2 and R3 are geometrical contraction models, and assume that the rate of degradation reaction starts at the surface and rate is controlled by the resulting interface reaction progress toward the centre. R2 and R3 models consider changes in geometry of different particle shapes. R2 generally considers contracting cylinder or contracting area and R3 represents contracting

sphere or contracting volume [137]. Knowing the values of the reaction model $f(\alpha)$ the values of pre-exponential factor (A_α) can be estimated for each conversion point from the values of the $Af(\alpha)$. The change in the pre-exponential (A_α)values as a function of the conversion (α) is shown in Fig. 3.9 for LDPE, HDPE, PP and PLA degradation reaction. The logarithmic values of the pre-exponential factors $\ln(A_\alpha)$ should compensate the values of the activation energy (E_α) linearly (Eq. 32). These linear plots are known as constable plots. The constable plots of LDPE, HDPE, PP and PLA are shown in Fig. 3.10. Linearity coefficient close to 1 $(R^2 \approx 1)$ indicates that for all heating rates the values of A_α accord with the distributed activation energy for all the stages of degradation process.

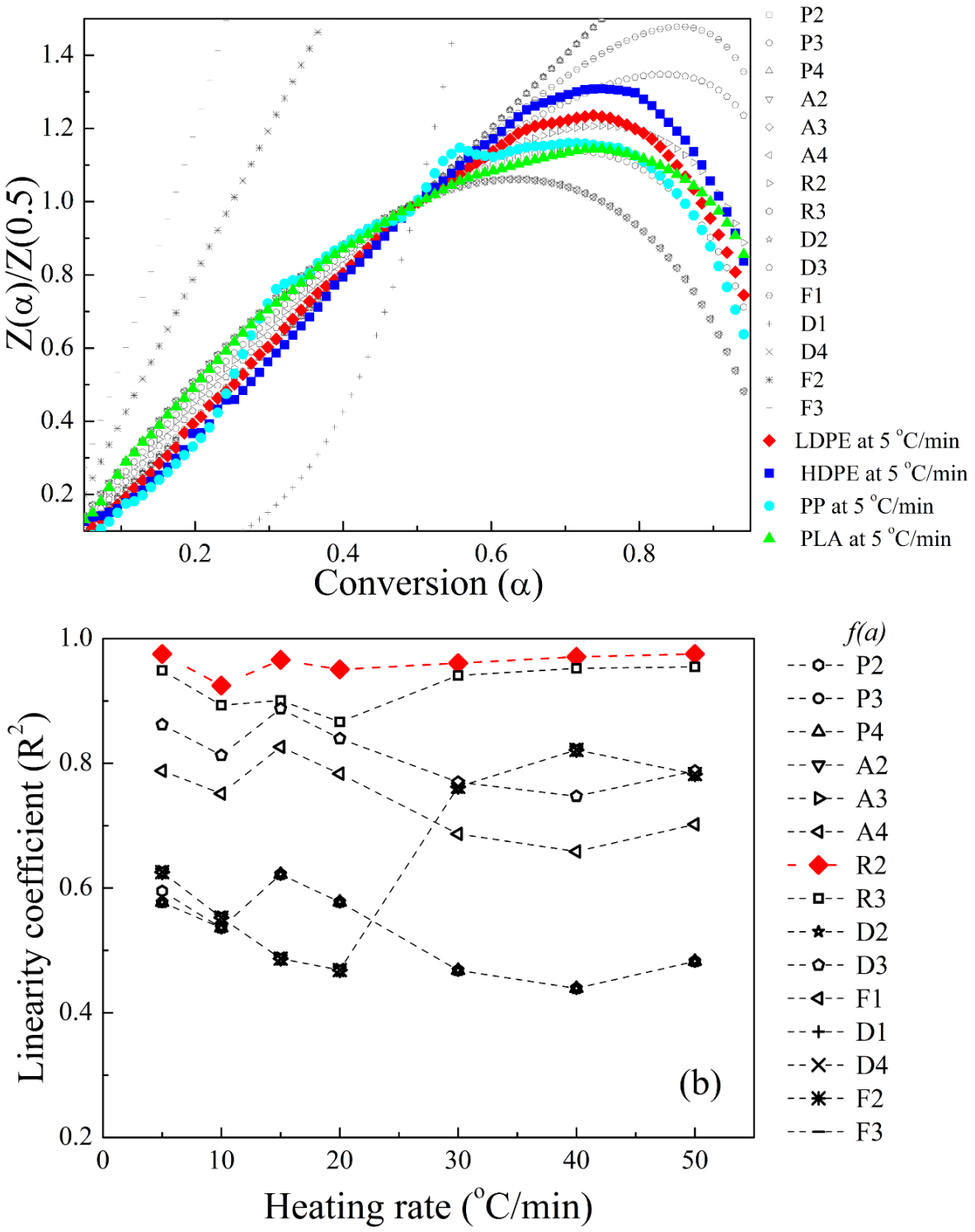

Fig. 3. 8: (a) Theoretical masterplots of different reaction models and experimental reduced rate plots at 5 °C/min for LDPE, HDPE, PP and PLA samples and (b) Selection of the reaction model based on linearity coefficient ($R^2 \approx 1$) considering all seven heating rates (shown for LDPE as an example)

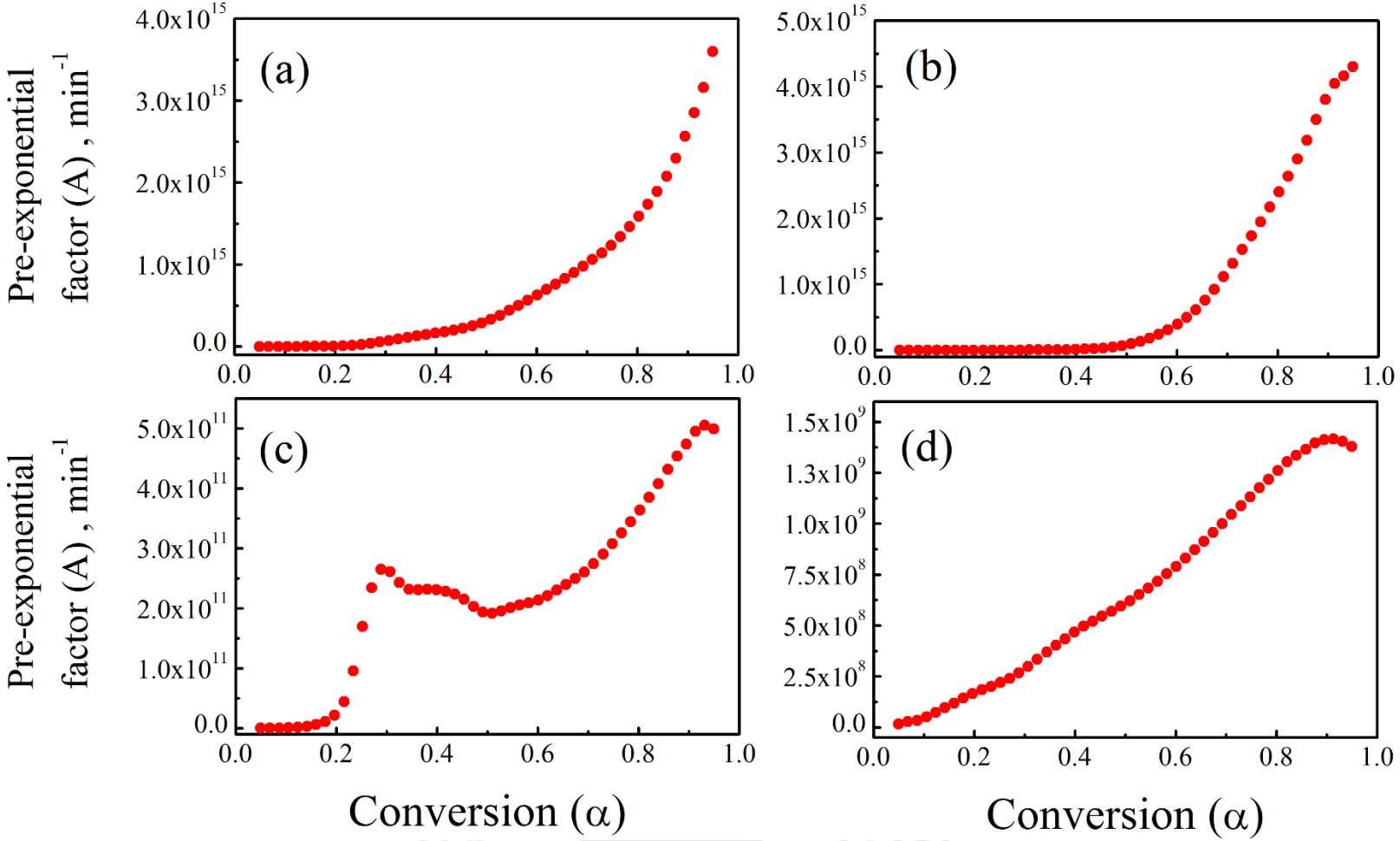

Fig. 3. 9: Distributed pre-exponential factor (A_α) with the extent of conversion for (a) LDPE, (b) HDPE, (c) PP and (d) PLA (Following AIC method for activation energy(E_α) determination)

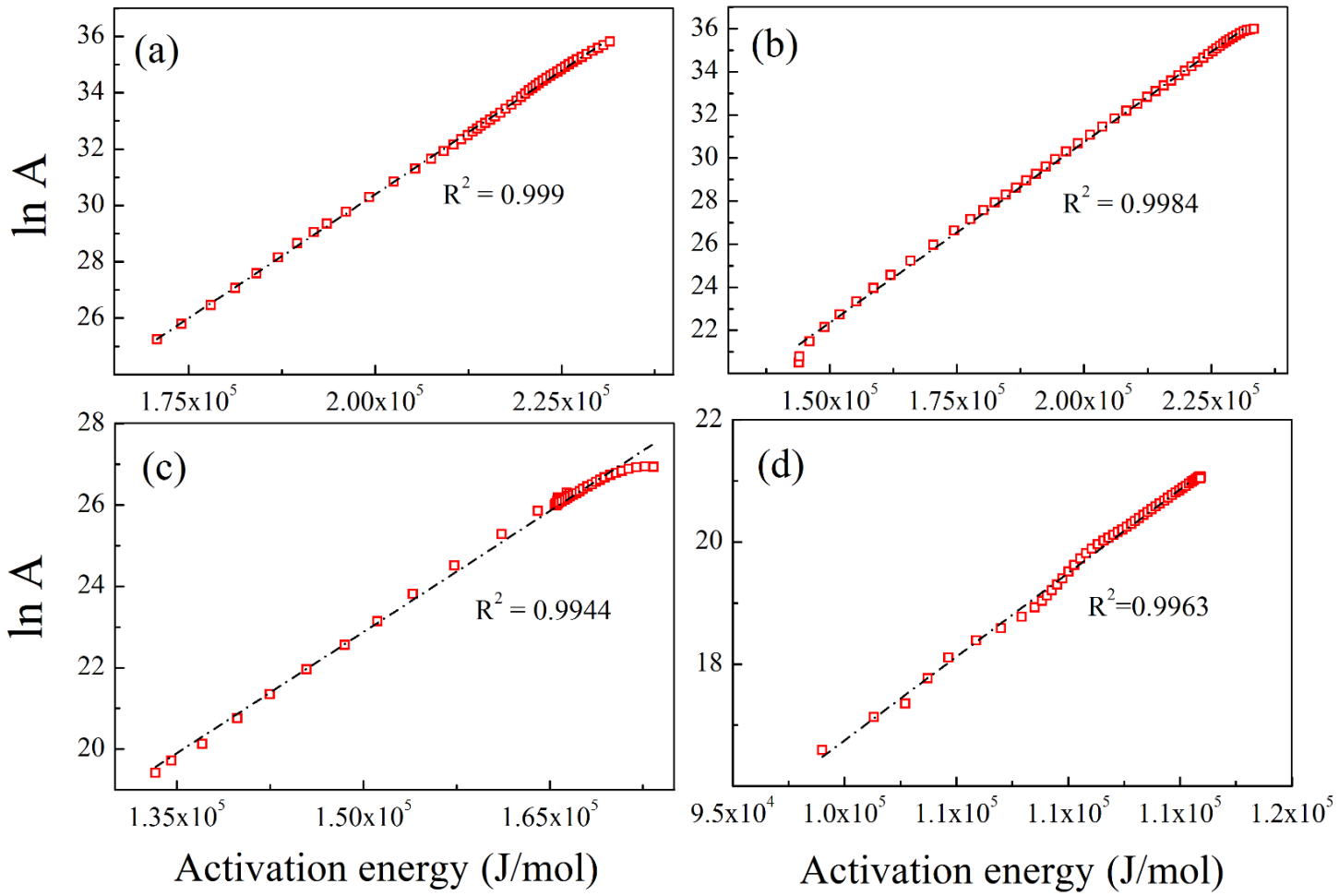

Fig. 3. 10: Constable plot between logarithmic pre-exponential factor and activation energy calculated for (a) LDPE, (b) HDPE, (c) PP and (d) PLA

The Criados' masterplots (theoretical and experimental) for PET-SDB sample is shown in Fig. 3.11 (a) and the regression coefficients (R^2) between experimental and theoretical masterplots with the considered heating rates is shown in Fig. 3.11(b). The masterplots deduce four reaction models (A2, A3, A4 and F1) for non-isothermal thermal degradation of PET-SDB. To choose one of the best-fitted reaction model, all four models were substituted in the $Af(\alpha)$ values to evaluate the values of pre-exponential factor (A_α). The relationship between E_α vs. $ln(A_\alpha)$ was plotted in Fig. 3.12 and the linear regression coefficient (R^2) was calculated (based on compensation effect). The corresponding values of pre-exponential factors of PET-SDB for all four cases is shown in Fig. 3.11. It was observed that for the reaction model F1, the linear fitting between E_α and $\ln(A_\alpha)$ has the highest value of R^2 (0.96). Hence, the thermal degradation reaction of PET-SDB under inert atmosphere follows first order model (F1).

A qualitative prediction of the reaction model was achieved by using Criados' masterplot technique. Plastic degradation reactions are complex. Therefore, more rigorous experimental and theoretical calculations are needed to establish correct reaction models. Obtained reaction models in this study also resemble with the reaction models reported by Aboulkas, et al. [108], Gutiérrez and Palza [138] and Saha and Ghoshal [136]. The range of the values of all three kinetic triplets are listed in Table 3.2. The application of various kinetic methods, temperature programs and materials used in previous studies produced variations in kinetic values obtained,

although most of the results are as per with the findings in the current study (Table 3.3).

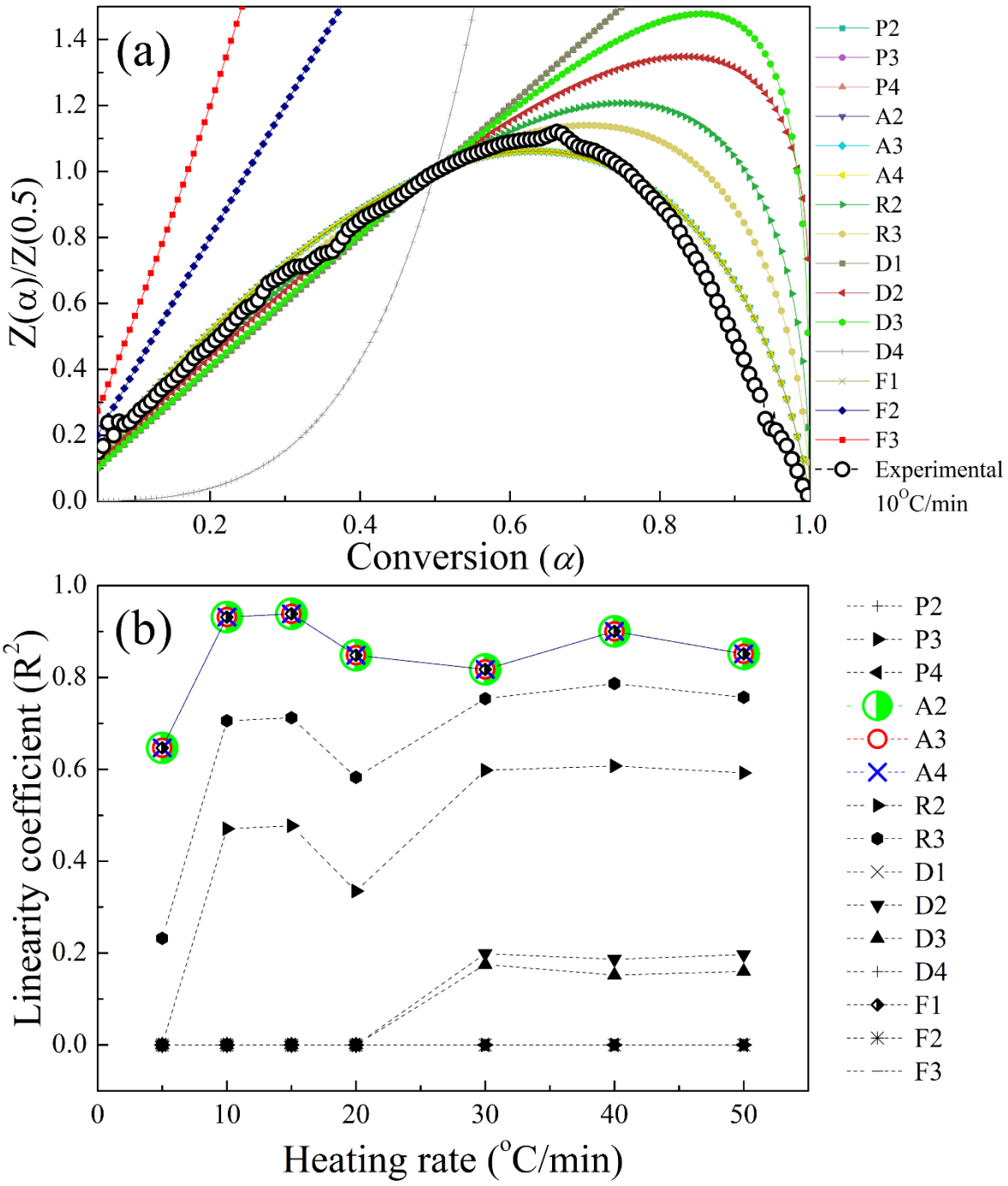

Fig. 3. 11: (a) Criados' masterplots for non-isothermal TGA in N_2 environment of PET-SDB (b) Linearity coefficient (R^2) values between theoretical and experimental masterplots at different heating rates (of PET-SDB)

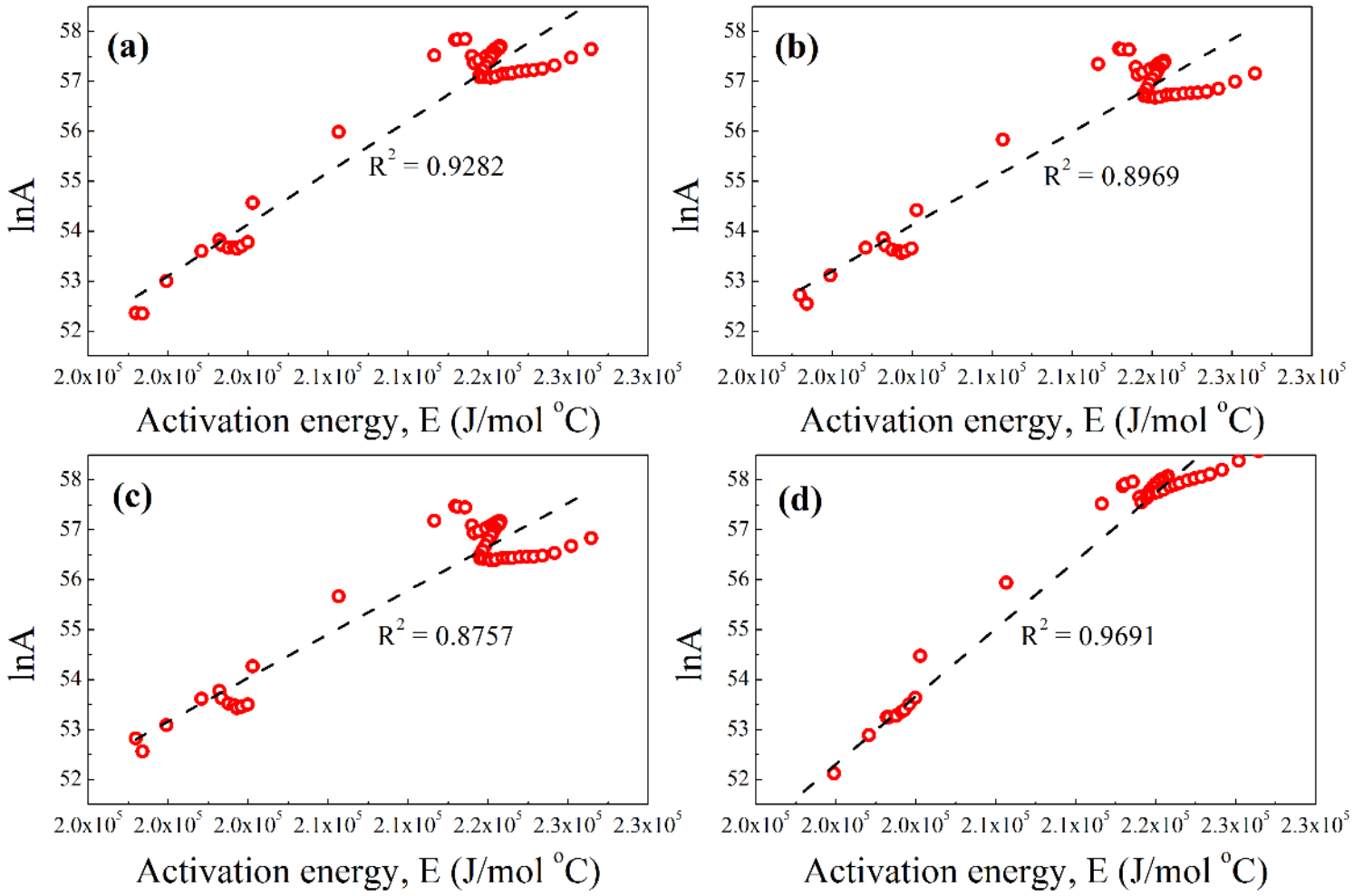

Fig. 3. 12: Constable plot for PET-SDB between logarithmic pre-exponential factor and activation energy obtained for four reaction models (a) A2, (b) A3, (c) A4 and (d) F1 with linearity coefficient R^2

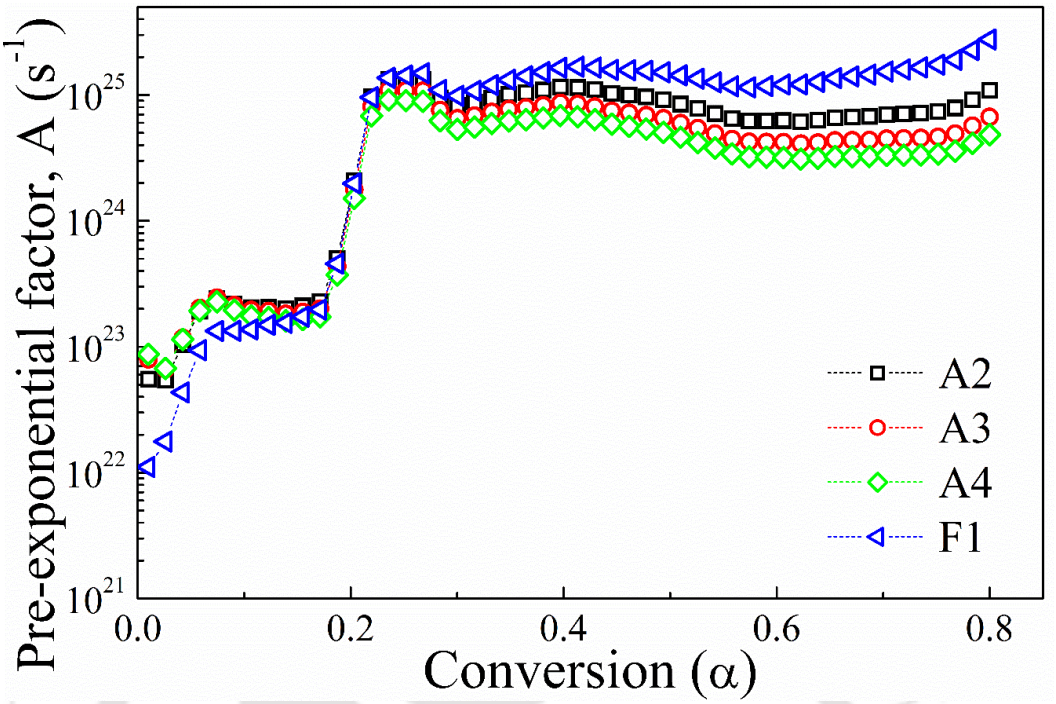

Fig. 3. 13: Variation of pre-exponential factor (A) with conversion considering four reaction models for waste PET-SDB degradation under N_2 environment

3.1.3 *Kinetic method selection*

The choice of a particular model can be done by examining the deviation (regression coefficient, R^2) of simulated degradation profile from the experimental data. The kinetic parameters (E_α and $Af(\alpha)$) obtained from different models were subjected to reconstruct the conversion and temperature ($\alpha - T$) profiles. MATLAB 2015 software was used to solve the differential form of equation (Eq. 4) numerically considering temperature as independent variables with initial value taken from onset point of TGA curve. Similar methodology was used for constructing the $\alpha - T$ data for all the materials at the experimental heating rates. The comparison of simulated results (AIC method only) with experimental data for all five materials (Fig. 3.14 and Fig. 3.15) were found in good agreement. To ensure the similarity between

experimental results with simulated profiles the regression analysis for all the heating rates was performed.

Table 3. 2: The values of the kinetic parameters (range) obtained using various isoconversional techniques

Material	Isoconversional methods	E_α (kJ/mol)	A_α (s^{-1})	$f(\alpha)$†
LDPE	Friedman	178-256	2.79×10^{11}-1.64×10^{17}	R2
	OFW	165-242	5.77×10^{10}-1.78×10^{16}	
	KAS	162-242	3.67×10^{10}-1.72×10^{16}	
	Starink	148-222	4.07×10^{09}-8.44×10^{14}	
	AIC	170-231	9.19×10^{10}-3.59×10^{15}	
HDPE	Friedman	134-258	1.89×10^{08}-2.34×10^{17}	R2
	OFW	146-242	1.26×10^{09}-1.57×10^{16}	
	KAS	146-241	1.18×10^{09}-1.52×10^{16}	
	Starink	146-240	1.06×10^{09}-1.23×10^{16}	
	AIC	143-233	8.06×10^{08}-4.29×10^{15}	
PP	Friedman	124-187	4.74×10^{07}-4.98×10^{12}	R3
	OFW	140-176	5.77×10^{08}-9.65×10^{11}	
	KAS	136-173	3.22×10^{08}-5.91×10^{11}	
	Starink	136-173	2.92×10^{08}-5.16×10^{11}	
	AIC	133-173	1.82×10^{08}-5.48×10^{11}	
PLA	Friedman	97-120	1.28×10^{07}-3.25×10^{09}	R2
	OFW	113-129	1.92×10^{07}-1.58×10^{10}	
	KAS	99-113	1.80×10^{07}-1.01×10^{09}	
	Starink	108-124	8.62×10^{07}-6.95×10^{09}	
	AIC	99-116	1.60×10^{07}-1.41×10^{09}	
PET-SDB ($\alpha = 0.05 - 0.8$)	Friedman	166 - 423	$4.6\times10^{14} - 1.94\times10^{33}$	F1
	OFW	195 - 277	$5.27\times10^{13} - 1.92\times10^{21}$	
	KAS	192 - 290	$1.73\times10^{13} - 2.7\times10^{22}$	
	Starink	193 - 277	$3.63\times10^{13} - 2.23\times10^{21}$	
	AIC	198 - 226	$3\times10^{14} - 5.9\times10^{25}$	

† The reaction model $f(\alpha)$ was predicted by Criados masterplot technique

Table 3. 3: Kinetic parameters reported in literature using various methods

Material	E (kJ/mol)	A×1/60(1/s)	$f(\alpha)$	Method	References
LDPE	222	-	nth order; n=0.7	DTG curve fitting	[130]
	221 ± 3	-	R2	FR	[108]
	215 ± 8	-	R2	KAS	[108]
	218 ± 7	-	R2	OFW	[108]
	150-240	-	-	AIC	[83]
	100-220	-	-	Direct integration	[85]
	176-245	-	-	AIC	[130]
	178-190	-	-	AIC	[87]
HDPE	240	3.4×1016	nth order; n=0.56	DTG curve fitting	[139]
	247 ± 5	-	R2	FR	[108]
	238± 11	-	R2	KAS	[108]
	243±11	-	R2	OFW	[108]
PP	126	-	nth order; n=0.5	DTG curve fitting	[139]
	53-194	-	-	FR	[132]
	188±6	-	R3	FR	[108]
	179±8	-	R3	KAS	[108]
	183±8	-	R3	OFW	[108]
	150-250	-	-	AIC	[83]
	106-134	-	-	AIC	[130]
	215±9	-	-	FR	[138]
	203±6	-	-	Starink	[138]
	204±6	-	-	OFW	[138]
	203±	-	-	KAS	[138]
	52-145	9.58-4846	-	AIC	[83]
PLA	161-177.5	-	-	OFW	[140]
	172-183.6	-	-	FR	[140]
	174.7±16.5	3.97×104 - 5.68×105	-	IKP method	[141]
	215	5.32×107	nth order; n=0.5	Coats-Redfern	[142]
	170	-	-	OFW	[81]
PET-SDB	173.6 – 205.85	3.1×1012 – 7.8×1014	F1	Isoconversional method	[143]
	162.15 – 210.64	2.34×1026 – 6.45 ×1034	F1	ASTM 698	[136]

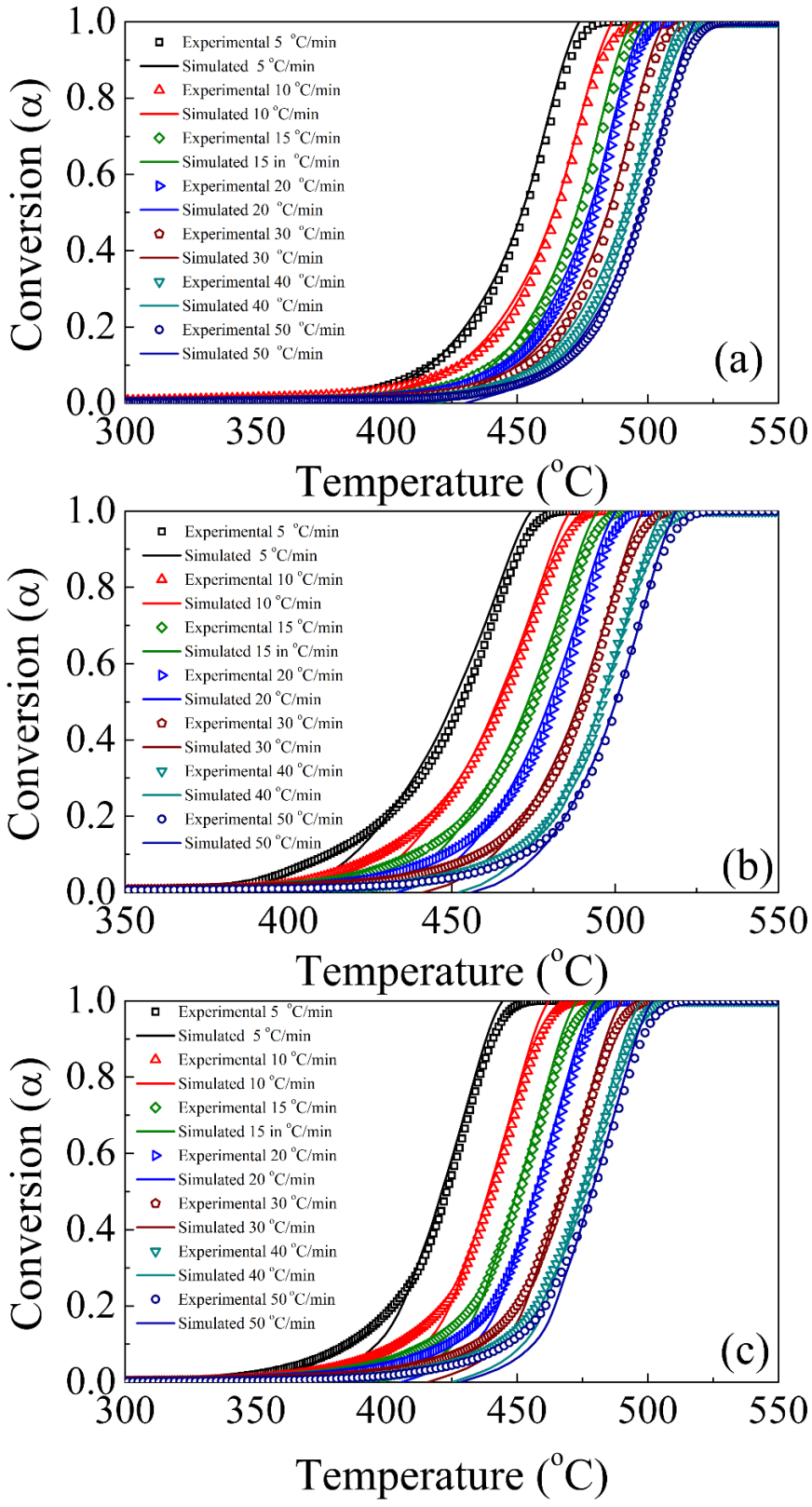

Fig. 3. 14: Experimental and simulated (using AIC method) conversion profiles at various heating rates for (a) LDPE, (b) HDPE and (c) PP

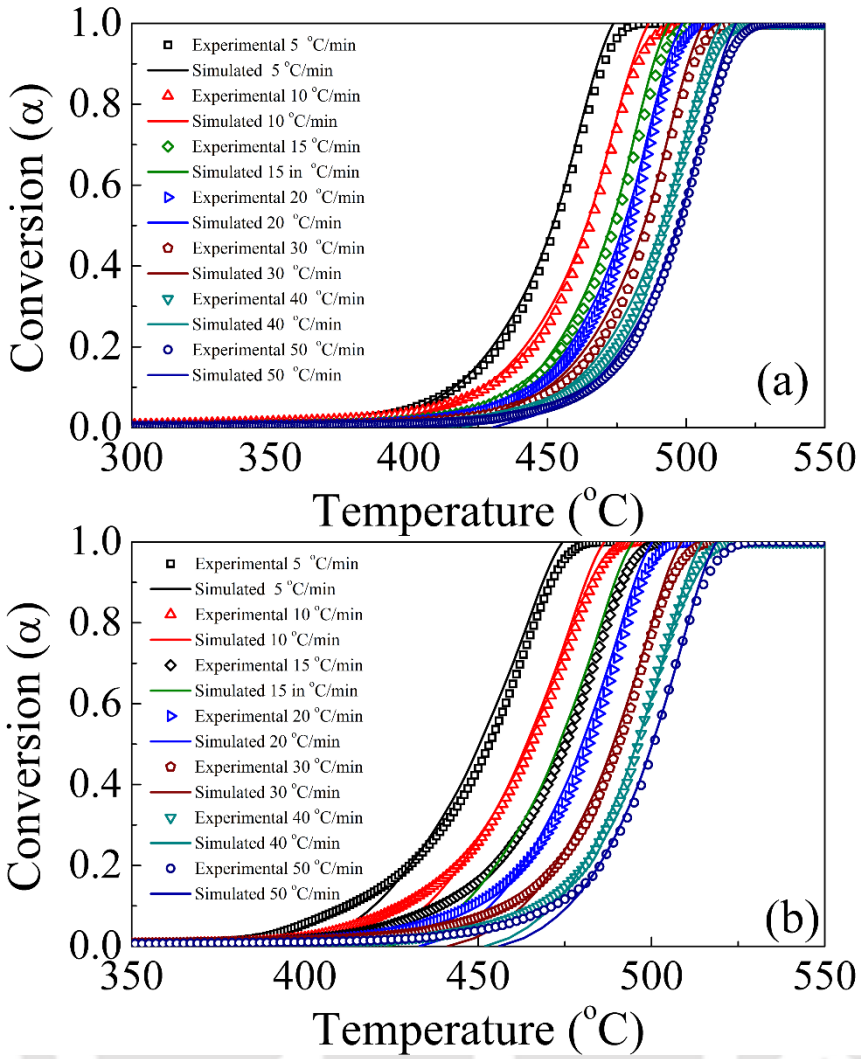

Fig. 3. 15: Experimental and simulated (using AIC method) conversion profiles at various heating rates for (a) PLA and (b) PET-SDB

The linearity was determined by calculating the regression coefficient (R^2) for each heating rate considered and for all the isoconversional methods. Fig. 3.16 shows the comparison of average regression coefficients (R^2) for seven heating rates for all the methods considered. A model selected for kinetic analysis should be able to reproduce the data and extrapolate the profile to the conditions and experiments not performed. Overall, the R^2 average analysis suggested that the AIC method is more appropriate to capture the complexity of the thermal degradation process of materials such as plastics having better R^2 value. This may be due to the regress

data sampling for small temperature interval adopted in the analysis for each heating rate considered. Due to the optimization by minimization of the function Φ (Eq. (28)), AIC model is more accurate for a large pool of data collected at wide range and as well as more number of heating rates. To further validate the obtained kinetic parameters beyond the range of the temperature profiles used in kinetic analysis, two extrapolated degradation profiles at a very low (of 1 °C/min) and high (100 °C/min) heating rates were simulated. The simulated kinetic profiles then compared with the experimental profiles obtained at the same heating rates for LDPE (Fig. 3.17). The linear regression coefficient (R^2) between experimental and simulated profiles of LDPE were found to be 0.98 and 0.99 for the heating rates of 1 °C /min and 100 °C /min respectively. The degradation step ($\alpha - T$) varies with varying heating rates lead to low onset and end degradation temperatures at lower heating rates (slow pyrolysis) whereas the degradation temperatures are shifted to higher temperatures at high heating rates.

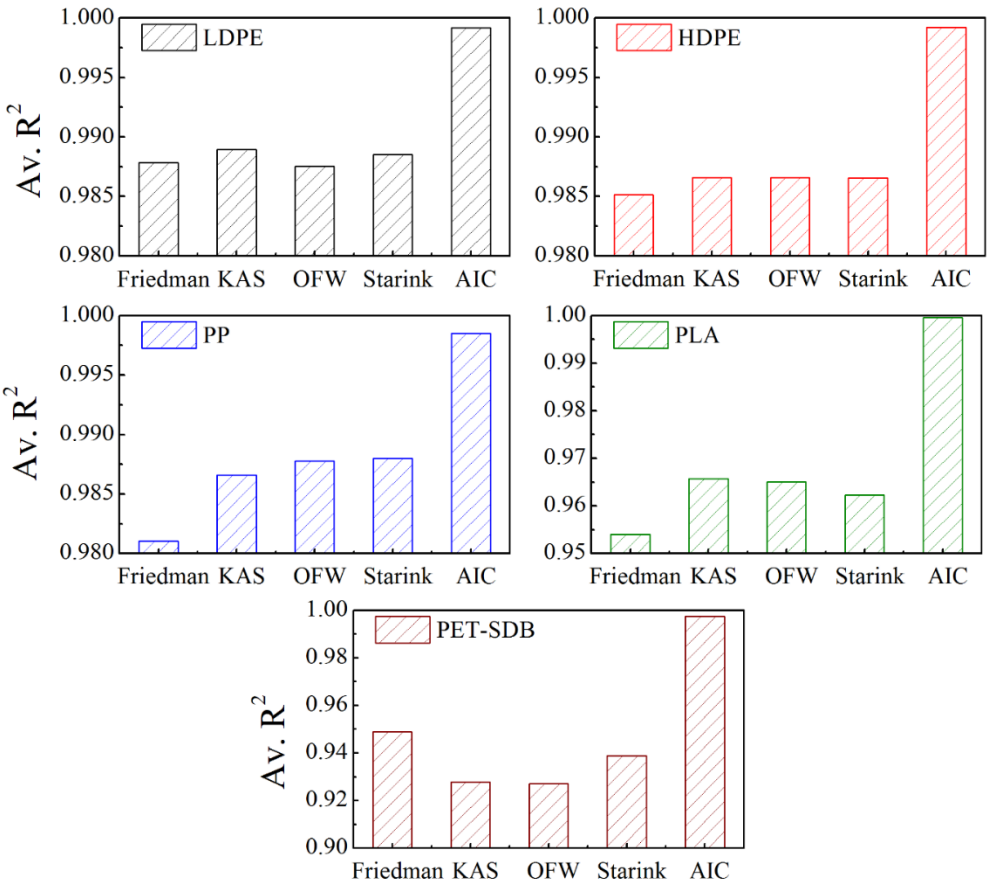

Fig. 3. 16: Comparison of different isoconversional methods based on average linearity coefficient (R^2) between experimental reconstructed $\alpha - T$ data

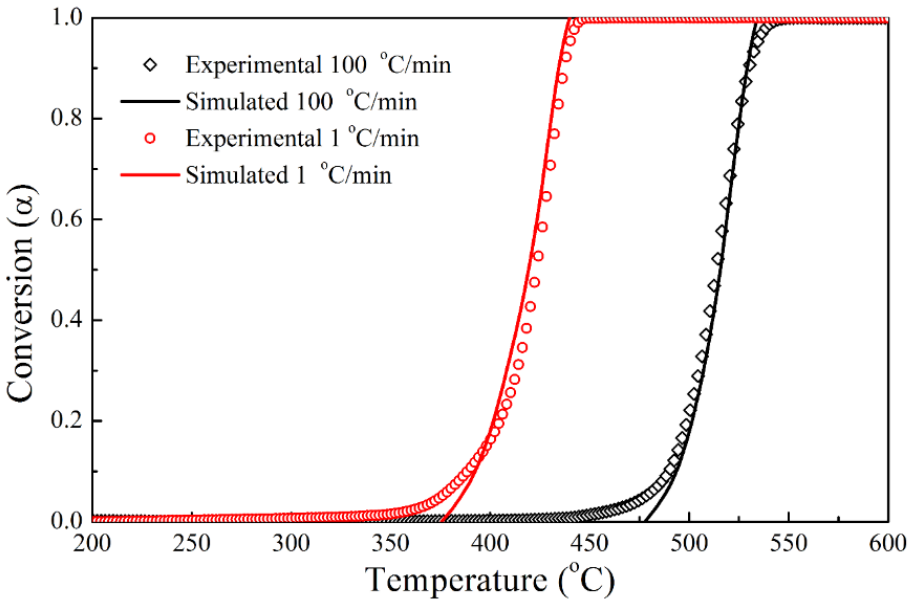

Fig. 3. 17: Fitness of the extrapolated simulated profiles (α-T) at 1 °C/min and 100 °C/min for LDPE using the kinetic values obtained from AIC method

3.2 Isothermal TGA kinetics

In the previous section (section 3.1), the non-isothermal TGA based kinetic analysis was discussed. In practice, many of the degradation reactions performed at isothermal temperatures. Hence, the degradation behaviour of the plastics under the isothermal condition is the subject of focus in the current section. The degradation of plastics start only if the temperature reaches to a certain value, known as onset temperature. Four to five temperatures (at regular intervals) were selected for the isothermal degradation study. The temperatures were chosen from the degradation temperature range (between onset and end temperature), that is reported in the non-isothermal study (Table 3.1). Temperature programme was set in such a way that the non-isothermal heating rate was maintained at 100 °C/min between ambient to isothermal temperature. A high (allowable) heating rate was maintained to reduce the time to reach the final isothermal temperature. The TGA data regarding isothermal experiments are reported in Table 3.4. The initial weight of the sample (in gm) was chosen almost constant in each isothermal experiment to maintain the consistency in the TGA analysis and avoid any effect of mass in the heat diffusion. The plot of weight loss with respect to time is shown in Fig. 3.18. The residual weight of each run is the final weight of the sample left after completion of isothermal holding time. The residual weight varies with temperature because of the incomplete conversion under low temperatures. At low temperature, more time is needed for the complete degradation. At higher temperatures (375, 400 °C) complete degradation was observed in the case of LDPE, HDPE, PP, and PLA. On

the other hand, for PET-SDB, the degradation reaction stopped with the formation of stable char. The yield of residue (Fig 3.18 (e)) was found higher at 375 °C compared to 400 °C. The possible explanation would be the cyclization with the formation of stable ring structure without the weight loss [119].

The rate of reaction depends on the temperature and mass. In isothermal TGA the temperature is constant and only the mass change with time was recorded. Since the temperature is constant, the temperature dependent term in the rate equation can be avoided. However, with the multiple data obtained at different isothermal temperatures, the activation energy of the degradation kinetics can be predicted. The method of McCallum (section 2.5) was used to predict the activation energy values with multiple isothermal data. The calculation of activation energy was not possible for the entire range of conversion (0 – 1) as partial degradation took place when low isothermal temperature was subjected. Hence, calculations were done from an initial conversion value to a value it reached in the isothermal heating period at lowest isothermal temperature. Minimum number of isothermal profiles for McCallum method was not less than three. The activation energy values were calculated from up to the degradation conversion reached at lowest isothermal temperature possible. Applying the degradation data to Eq. (34), the $ln(t)$ vs $1/T$ was plotted and the graphs are shown in Fig. A3 (appendix) for all the plastics. The slope of the regression will give the activation energy at each degree of conversion. The variation of activation energy with conversion are shown in Fig. 3.19. The ranges of activation energy of each material is listed in Table 3.4. The values of the

activation energy obtained from the isothermal TGA is lower than the values obtained from non-isothermal TGA. For example the PP degradation under non-isothermal TGA have the activation energy values (AIC method) in the range of 133 – 173 kJ/mol which was much higher than the values obtained under isothermal TGA, that was 58.4 – 109 kJ/mol in the same conversion range i.e. 0.05 – 0.95. Similar conclusion can be made for the other plastics. The kinetics obtained from the isothermal TGA is useful considering most of the industrial processes are running isothermally. In the following chapter of the thesis lab scale isothermal slow pyrolysis of the polyolefin plastics was carried out, to produce value added fuels and chemicals. Low activation energy obtained for isothermal TGA suggests that the isothermal degradation (pyrolysis) requires less energy to carry out the degradation reaction under inert condition than compared to the non-isothermal fast pyrolysis.

Table 3. 4: Isothermal TGA data and the range of activation energy obtained using McCallum method

Material	Final temperature (T_∞) °C	Isothermal holding time (t_h) *min*	Initial weight (W_o) *mg*	Residual weight (W_∞) *mg*	Range of activation energy (kJ/mol)
LDPE	350	600	10.19	7.44	81.6 – 176.7 *(α = 0.05 – 0.85)*
	375		10.68	1.16	
	400		9.04	0	
	425		11.68	0	
HDPE	350	600	9.13	6.05	66.4 – 195.4 *(α = 0.05 – 0.85)*
	375		12.58	0.08	
	400		10.03	0	
	425		10.8	0	
PP	300	600	11.89	7.09	58.4 – 109 *(α = 0.05 – 0.95)*
	325		9.36	0.12	
	350		11.89	0.078	
	375		11.35	0.036	
	400		10.44	0.04	
PLA	250	600	10.86	6.39	101.6 - 132.78 *(α = 0.05 – 0.85)*
	275		10.34	0.32	
	300		8.85	0.17	
	325		12.6	0.09	
PET-SDB	325	480	13.88	8.65	97.7 – 185.4 *(α = 0.05 – 0.65)*
	350		11.42	3.45	
	375		11.52	2.03	
	400		12.65	1.43	

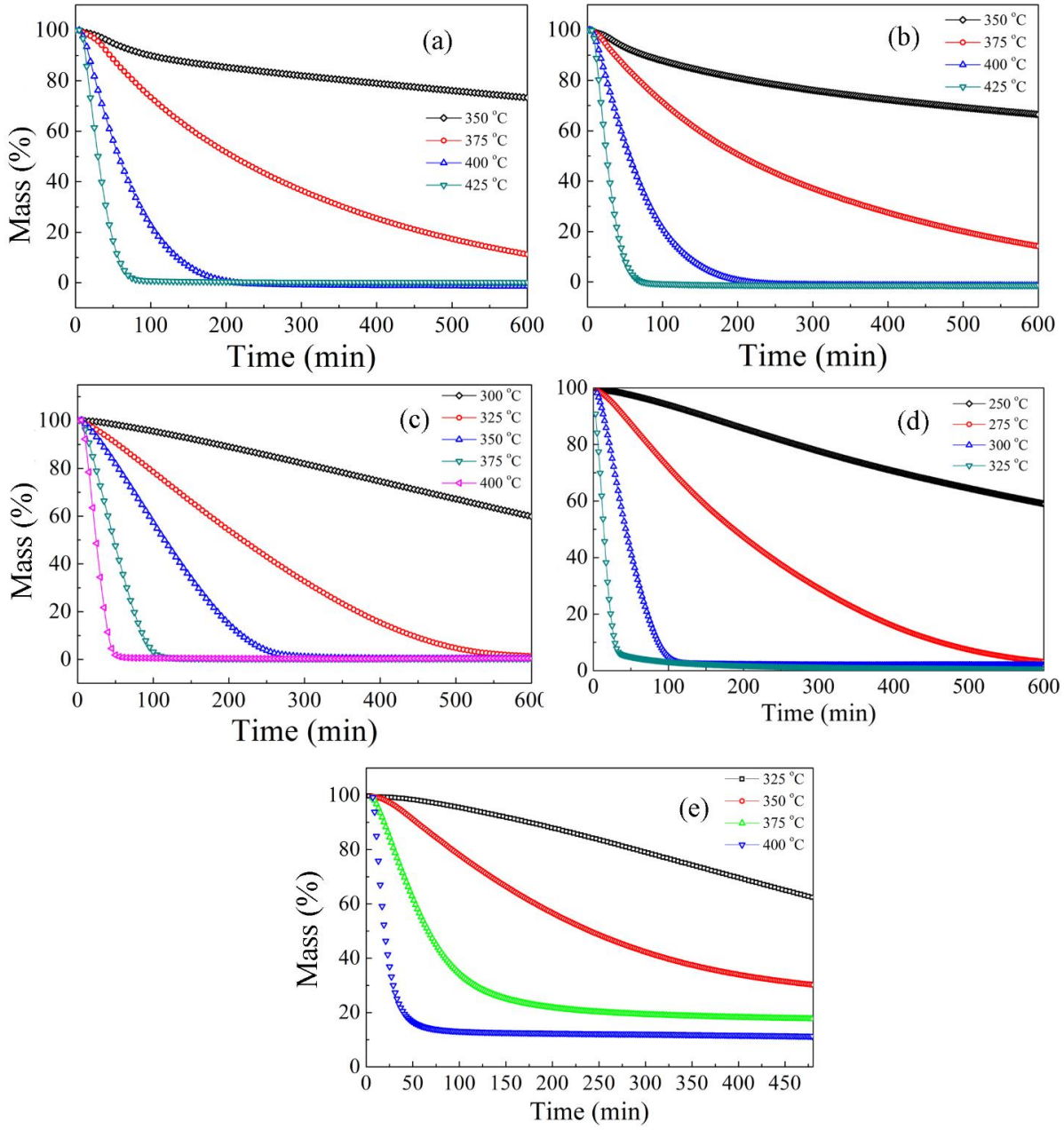

Fig. 3. 18: Weight loss with time at different isothermal temperature plots (isothermal TGA) for (a) LDPE, (b) HDPE, (c) PP and (d) PLA and (e) PET-SDB

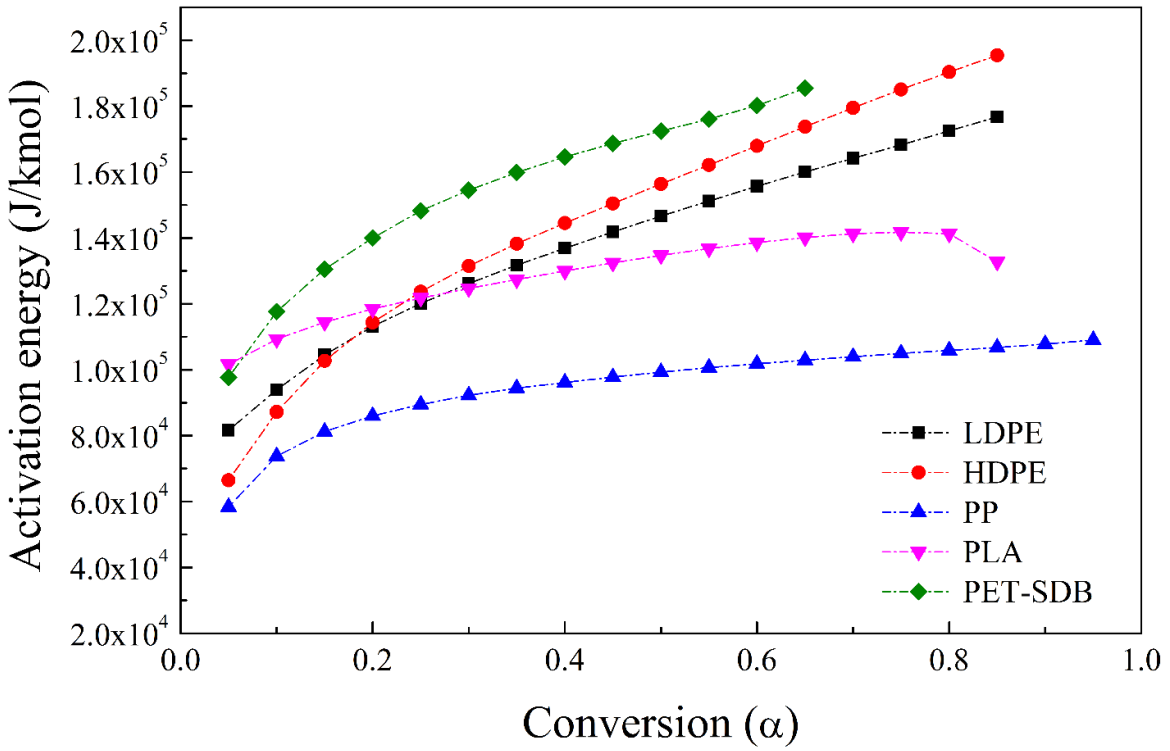

Fig. 3. 19: Distribution of activation energy with the degree of conversion obtained from isothermal degradation profiles

3.3 TG-FTIR analysis

Thermogravimetric coupled with Fourier transform infrared spectroscopy (TG-FTIR) provides a real time gas evolution pattern under thermal degradation. The IR signatures provide the information regarding the functional groups as absorbance with respect to temperature and the functional groups. TG-FTIR data is important to understand the evolve gas formation pattern during pyrolysis reaction and ascertain the possibility of doing pyrolysis in the disposal of plastics in terms of toxic emission. Experiments were performed at 10 °C/min and the 3D surface plots of the FTIR absorbance values with respect to time and wave number are shown in Fig. 3.20(a) for LDPE, HDPE and PP and in Fig. 3.21(a) for PLA and PET-SDB samples. The functionality of the peaks are shown in Fig. 3.20(b) and Fig. 3.21 (b)

respectively. It was clearly observed that the gas-phase produced from the degradation of LDPE, HDPE and PP have shown only the functional groups of hydrocarbon components like alkane and alkene. A strong sharp absorption at around 2950 cm^{-1} corresponds to C – H stretch recommends the presence of alkane groups and a moderately sharp peak around 1750 cm^{-1} signals the presence of alkene/olefins components in the product stream. Exceptions can be seen for the PLA and PET-SDB degradation. The FTIR peaks of evolve gases from PLA and PET-SDB clearly indicate the presence of oxygenated components in the product stream including the existence of CO and CO_2 components. The reason behind the production of oxygenated component from PLA and PET-SDB is the presence of oxygen in the polymer molecule [81,134,135,143]. Due to this reason, further lab scale study of this two plastic sample was not carried out as both CO and CO_2 is unwanted product of any pyrolysis, further presence of any oxygenated component in the liquid product may decrease the fuel value and cause corrosion problem in the downstream process.

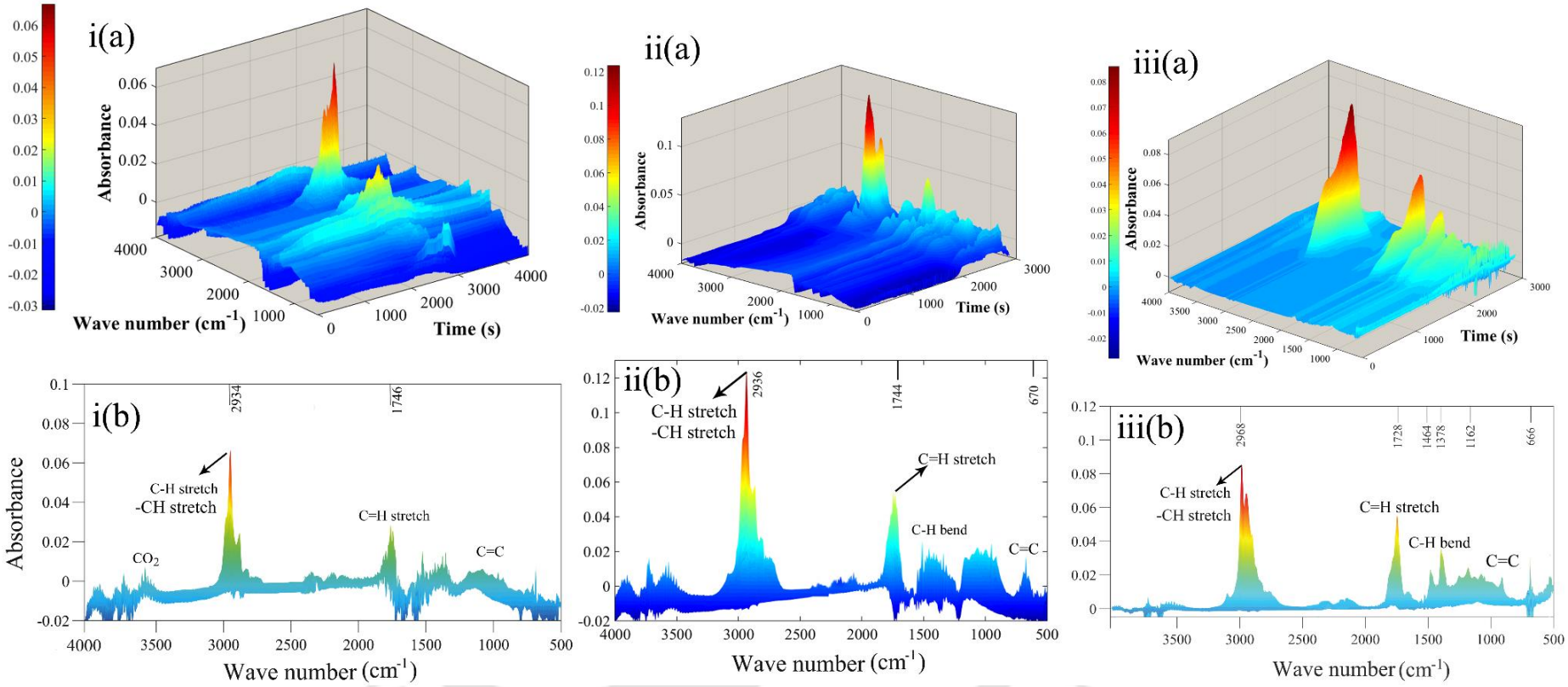

Fig. 3. 20: (a) 3D display of IR spectra and (b) 2D overlay display of IR spectra with functionality for i. LDPE, ii. HDPE and iii. PP

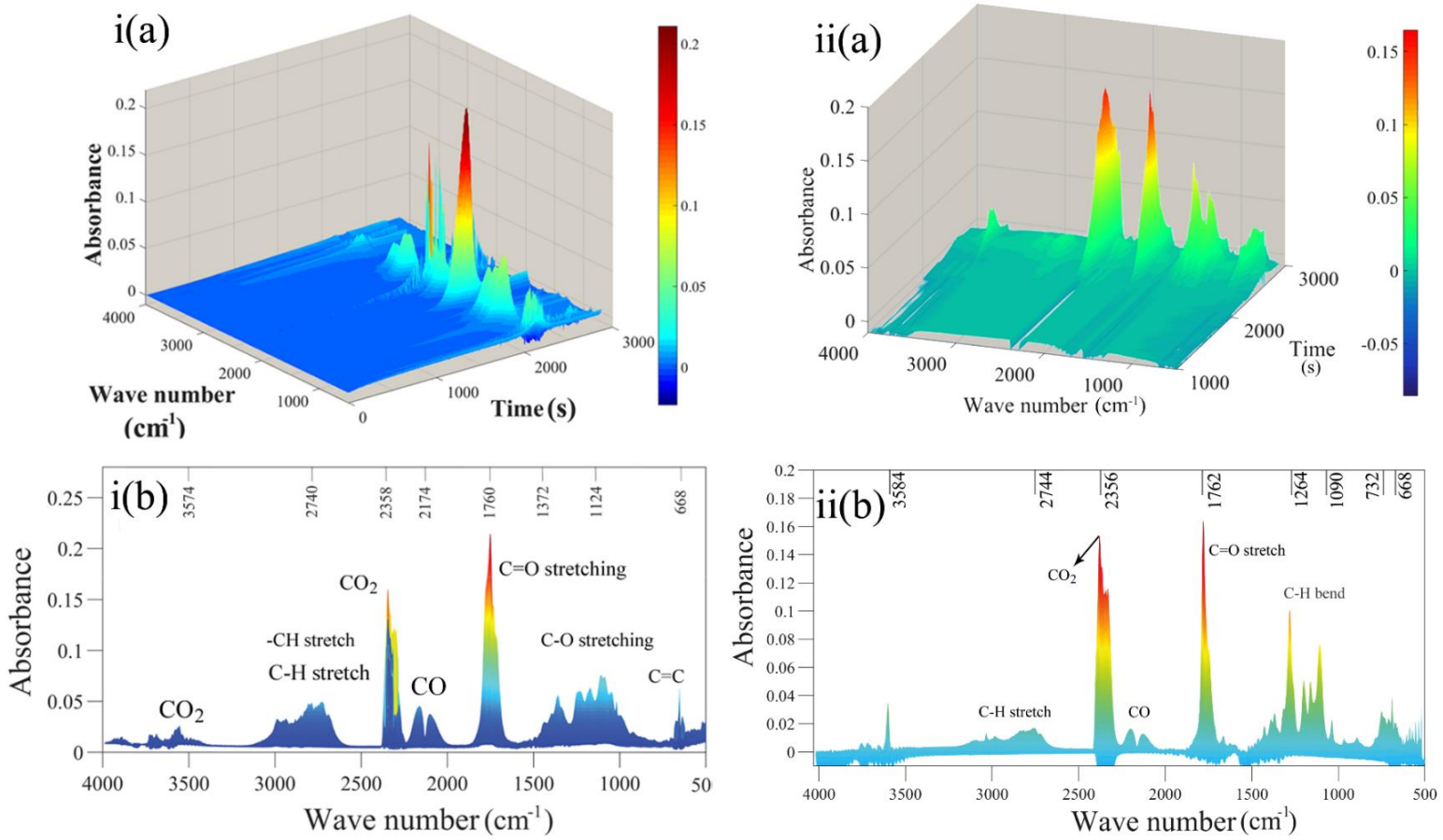

Fig. 3. 21 (a) 3D display of IR spectra and (b) 2D overlay display of IR spectra with functionality for i. PLA and ii. PET-SDB

3.4 Summary

TGA based thermal degradation kinetics of five plastic materials were studied using isoconversional principle. The kinetic study concludes that PLA requires less activation energy than PE, PP and PET-SDB while degrade thermally. Within a variety of kinetic models available for thermal degradation, it is difficult to choose one model, which can extract appropriate kinetic parameters from complex reaction mechanisms occurring. The continuous change in E_α values with α explains the change in mechanism of degradation and it was found to be important in the early and end stages of the degradation process. Isoconversional models are able to capture the reaction mechanism as kinetics follow the reaction progress. The advanced isoconversional method (AIC) uses an optimization function to calculate the kinetic parameters and produces fewer errors (better R^2) for multiple heating rate data. Lower activation energy at the beginning of the degradation process refers that the initiation of degradation starts at weaker links of the polymer chain mostly follows side chain scission. In later stages, the degradation follows random chain scission, where the polymer chain breaks at any random position and forming various monomers and oligomers. The exact mechanism can be determined by any model fitting method using different reaction models *f(α)* or *g(α)*. However, the kinetic analysis is also very subjective to the reaction configuration, data sampling and careful analysis of onset points. McCallum method can be utilized to calculate variable activation energy from isothermal TGA data. The TG-FTIR ascertain the composition of evolve gas during various stages of the degradation process.

Chapter 4

VALORISATION OF PACKAGING PLASTIC WASTE BY SLOW PYROLYSIS

Isothermal slow pyrolysis

Carbon number distribution

Fuel properties

Effect of temperature

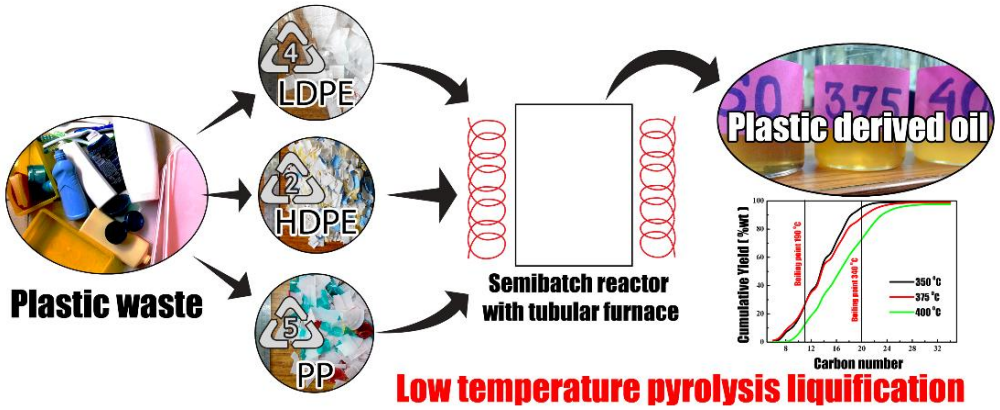

Work published at:

Pallab Das and Pankaj Tiwari, 'Valorisation of packaging plastic waste by slow pyrolysis,' *Resources, Conservation and Recycling*, vol. 128, pp. 69-77 (2018). IF = 7.044

4 Valorisation of packaging plastic waste by slow pyrolysis

In this chapter, the process of slow pyrolysis at low degradation temperature and long isothermal holding time is discussed. The lab scale pyrolysis process was carried out to produce liquid/gaseous hydrocarbons from low and high-density polyethylene (LDPE and HDPE) and polypropylene (PP). These are common polyolefin profusely used as packaging materials and abundantly found in the plastic waste stream. The plastic waste samples were collected from household waste along with virgin samples acquired from Haldia petrochemicals, India were considered for the study. The plastic derived oil (PDO) samples have shown variation in their compositions and fuel properties based on the pyrolysis temperature. The degradation mechanism follows end chain scission, which produces monomer units whereas random scission results most of the hydrocarbon products. Subsequent reactions like radical recombination and inter or intra molecular hydrogen transfer results in the formation of most of the olefinic components.

4.1 Thermogravimetric analysis (TGA) and semi-batch pyrolysis yield

Thermal degradation and kinetic analysis of considered plastics are covered in Chapter 2. For a comparative assessment, TGA analysis of the real-world plastic waste sample (RMIX) was performed at 10 °C/min. The RMIX composition was maintained at 40% PP, 30% LDPE, and 30% HDPE for the isothermal pyrolysis. Plastic types were identified based on their resin identification code. The TGA weight loss curves along with DTG curves of three virgin samples (LDPE, HDPE,

PP) and RMIX are shown in Fig. 4.1 for 10 °C/min. Degradation pattern of all three plastics was found similar, as it was perceived from the shape of the weight loss curve. Degradation temperatures have different values for different plastics. Such as the onset temperature (T_o) values of LDPE, HDPE and PP were found at 335, 370 and 300 °C respectively. Similarly, the values of peak degradation temperature (T_m) were found at 472, 475 and 440 °C for LDPE, HDPE and PP respectively. TGA of PP exhibited low degradation temperature than polyethylene (LDPE and HDPE). The molecular structure of PP has more branching than LDPE and HDPE as it carries one extra methyl group in every other carbon in the polymer chain. Branching makes the polymer weaker and thermally less stable than polyethylene. In case RMIX sample, three peaks (DTG curves) were observed (Fig. 4.1(d)), which indicated the maximum degradation points of individual plastics in the mixture. In case RMIX sample, three peaks (DTG curves) were observed (Fig. 4.1(d)), which indicated the maximum degradation points of individual plastics in the mixture. The first peak appeared at 460 °C indicated the peak degradation point of polypropylene in the mixture (RMIX). The peak temperature was 20 °C higher than the original peak temperature of PP (440 °C). The decrease in temperature might be due to the synergistic effect.[103]. Diversity in the degradation temperatures can be incorporate to the molecular structure of the plastics [144].

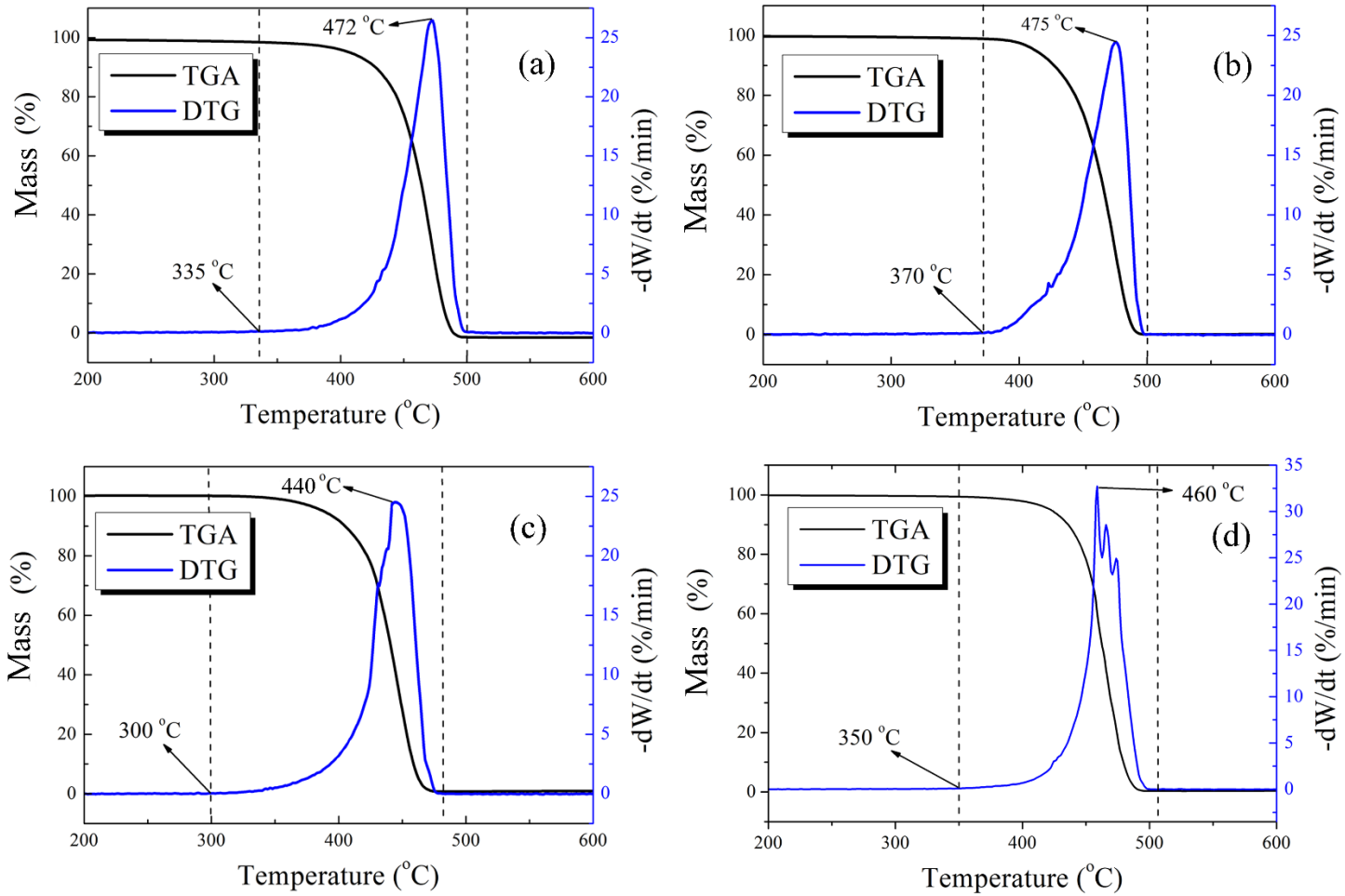

Fig. 4. 1: Non-isothermal TGA and DTG curves of (a) LDPE, (b) HDPE, (c) PP and (d) RMIX at heating rate 10 °C/min

Pyrolysis experiments were carried out in a lab-scale semi-batch reactor. Details of the experimental setup and conditions were explained in section 2.2.7. The pyrolysis experiments were performed to see the effect of different isothermal temperature and long duration of holding time in the product distribution. Pyrolysis experiments were performed for three virgin plastics (LDPE, HDPE and PP) individually and real-world waste mix (RMIX). The process of pyrolysis converts the plastics into the products of three phases (gas, liquid and solid residue). Uncondensed gases were collected at regular intervals (approximately 10 min). The liquid product also referred to as plastic derived oil (PDO) collected in the collecting bottle after the vapour outlet passed through a long water-cooled (chiller) condenser. The solid residue or the unconverted wax (appeared at low-temperature pyrolysis) was collected from the reactor at the end of the experiment after cooling. Liquid and solid samples were weighed and a gas yield was analysed by mass balance. A minimum of three numbers of experiments were performed and average values (%wt) were reported with standard deviation <5%. Pyrolysis product yields under different temperature condition is listed in Table 4.1. In all the pyrolysis experiment, the yields of both plastics derived oil (PDO) and gaseous products were found significant compared to the solid residue. Oil yield was found maximum at higher reaction temperature and a reverse trend was observed for gaseous products. The pyrolysis of PP produced the highest amount of PDO compared to other individual plastics. At low temperature, the solid residue (or wax) yield was higher due to incomplete conversion. The residue yield was higher in case of LDPE and HDPE than PP as

the required energy for degradation or activation energy of LDPE and HDPE was higher compared to PP[108,144]. At high temperature, the plastic undergoes thermal cracking furthermore the large polymer molecules degrade into smaller molecules of gaseous and liquid products. Thus, the PDO obtained at different temperatures may vary from light hydrocarbon oil (at low temperature) to moderately heavy hydrocarbon oil (at high temperature). The waxy residue found in the reactor bottom in low-temperature pyrolysis resembled the high boiling heavy oil from vacuum distillation of petroleum. The waxy residue can be used as source material for the production of lubricant base-stock. Further refining (dewaxing/ wax isomerization) may result in API (American petroleum institute) group II/III lubricant base oils [96]. The % yield compared with the literature studies in the Table 4.4

Table 4. 1 Pyrolysis product yield from individual virgin plastics and mix plastic feed

Feed material	**Pyrolysis temperature (°C)**	**Product distribution (%wt)**		
		PDO	**Gas**	**Solid residue/ wax**
LDPE (Virgin) (LDPE = 50 g)	350 °C	48.75±2.55	21.27±2.61	29.98±0.6
	375 °C	71.56±3.28	22.53±2.09	5.91±1.9
	400 °C	81.4±2.57	16.58±2.81	2.02±0.33
HDPE (Virgin) (HDPE = 50 g)	350 °C	49.28±3.66	27.52±2.71	23.2±1.35
	375 °C	76.73±2.55	22.14±1.85	1.13±0.77
	400 °C	81.48±3.05	17.8±2.11	0.72±0.51
PP (Virgin) (PP = 50 g)	325 °C	54.02±4.36	29.79±3.5	16.19±1.86
	350 °C	81.31±1.81	16.8±0.89	1.89±0.36
	375 °C	81.97±2.47	17.26±2.36	0.77±0.11
RMIX (from waste) (LDPE = 15 g ; HDPE = 15 g; PP = 20 g)	350 °C	57.3±3.65	26.98±2.68	15.72±2.3
	375°C	71.44±1.7	28.21±2.99	0.35±0.2
	400°C	76.38±2.12	23.22±1.49	0.4±0.15

4.1.1 ***Liquid product analysis***

The composition of the liquid samples were analysed with the help of Fourier transform infrared spectroscopy (FTIR) with attenuated total reflection method (ATR), nuclear magnetic resonance spectroscopy with respect to hydrogen 1 nuclei (^{1}H NMR) and gas chromatography with simulated distillation setup (GC-SimDist). The fuel properties of the PDOs were calculated using bomb calorimeter, rheometer, Cleveland apparatus, pycnometer (density bottle), and various ASTM standard techniques. Details of the analytical methods, operating procedure and conditions were discussed in details in section 2.9. The liquid product analysis revealed the application of low temperature slow pyrolysis in the production of high quality liquid fuel.

FTIR and ^{1}HNMR analyses

The FTIR spectra are shown in Fig. 4.2. The %yield of aliphatic (paraffins and olefins) and aromatic hydrocarbons present in the PDO samples obtained at different pyrolysis temperature from ^{1}H NMR is shown in Fig 4.3. PDOs were composed of mostly of aliphatic hydrocarbons. Presence of aromatics were found negligible. In Fig. 4.2, the peak area of the IR spectra between 3000 cm^{-1} and 2850 cm^{-1} demonstrated the presence of $–CH_3$, $–CH_2$ and C–H groups of highly paraffinic components in the PDO. In addition, sp^3 C – H bending appeared in the range of 1470 to 1350 cm^{-1} as a set of two or more peaks. The peak near 3000 cm^{-1} (3075 cm^{-1}) was observed in the PDOs from PP indicated a sp^2 C – H stretch, which implies

that PDOs from PP is highly unsaturated. Peaks in the vicinity of 1575 and 1675 cm^{-1} as well as those between 875 and 950 cm^{-1} indicated C=C stretches. A *mono* substituted double bond ($RCH=CH_2$) was responsible for two peaks in all the spectra: one approximately at 990 cm^{-1} and the other 910 cm^{-1}. Peak near 720 cm^{-1} pointed to the *cis* di-substituted double bond.

At different pyrolysis temperatures, the functionality of the PDOs remained consistent. Practically identical elucidations have also been reported in literature [35,39,96]. Williams and Williams [35] described the stretches around 1650 cm^{-1} at higher temperature due to the presence of dienes and broadening of olefin peaks at 2850 and 2950 cm^{-1} with increasing temperature. The signatures of FTIR (Fig. 4.2) spectra were found consistent with the ^1H NMR findings.

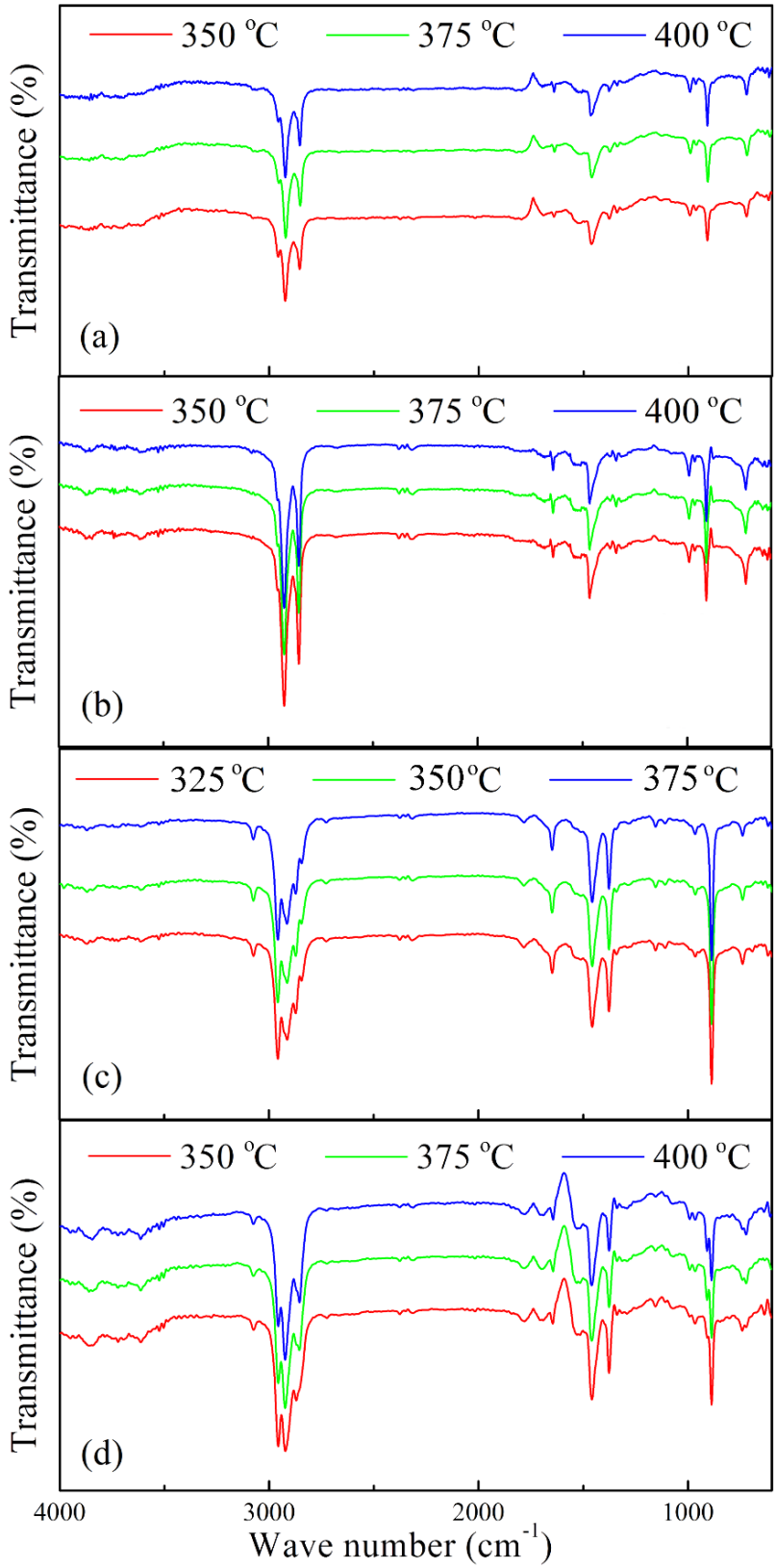

Fig. 4. 2: FTIR-ATR spectra of PDO obtain from a) LDPE, b) HDPE, c) PP and d) RMIX at three-pyrolysis temperature considered

Quantification of hydrocarbon compositions of PDOs with respect to functionality was carried out by ^{1}H NMR analysis and using the correlations provided by Myers, et al. [121]. Paraffin and olefin concentrations of PDOs were found in the range of 60 – 70% and 30 – 40% respectively (Fig. 4.3) in all the runs. The ^{1}H NMR analysis revealed that (Fig. 4.3) the oil derived from PP was relatively more olefinic. However, the paraffin concentration reduced and olefins concentration increased as the pyrolysis temperatures increased to higher values. The Similar trend was also observed by Marcila et al. [104] under identical but dynamic temperature conditions. High olefin content in the PDOs from PP pyrolysis was due to presence of one extra methyl group in every other carbon atom in the PP polymer chain, which according to Pinto et al. [97] stabilized the intermediate radicals by forming double bond between two carbon atoms. At elevated temperature, polyethylene (PE) and polypropylene (PP) undergo random scission and create radicals. The radicals then undergo β-scission to produce monomers, which stabilizes by intra-molecular or intermolecular hydrogen transfer. Successive β-scission reactions of the secondary radicals prompted the formation of olefins and dienes. On the other hand, the intermolecular hydrogen transfer leads to the formation of paraffins. At high temperature, the chances of successive β-scission with intramolecular hydrogen transfer was highly anticipated due to the abundance of hydrogen atom in the radical chain [145,146].

Based on the correlations given by Myers et al. [121,122] three important properties of the PDOs can be predicted by ^{1}H NMR data. Those are hydrogen-carbon (H/C)

ratio, iso-paraffin index and research octane number (RON), which can be predicted using Eq. (39) – (41). The ratio of H/C gives the burning quality of fuel. High H/C ratio means clean burning of fuel with less emission. Iso-paraffin index predicts the amount of branching in the hydrocarbon molecules present in the sample. The RON values give a cognate idea of the theoretical octane number of the liquid products. The H/C ratio, iso-paraffin index and research octane number (RON) of the PDO samples obtained from all the feed samples are summarised in Table 4.2. It was observed that the PDOs from PP has higher RON (>91) value compared to the oil produced from LDPE and HDPE. This is primarily due to the high olefin content, high isoparaffin index (more branching) of PDOs from PP (Fig. 4.3). The increase in olefin concentration with increase in temperature also attributes to higher values of iso-paraffin index and RON [147,148].

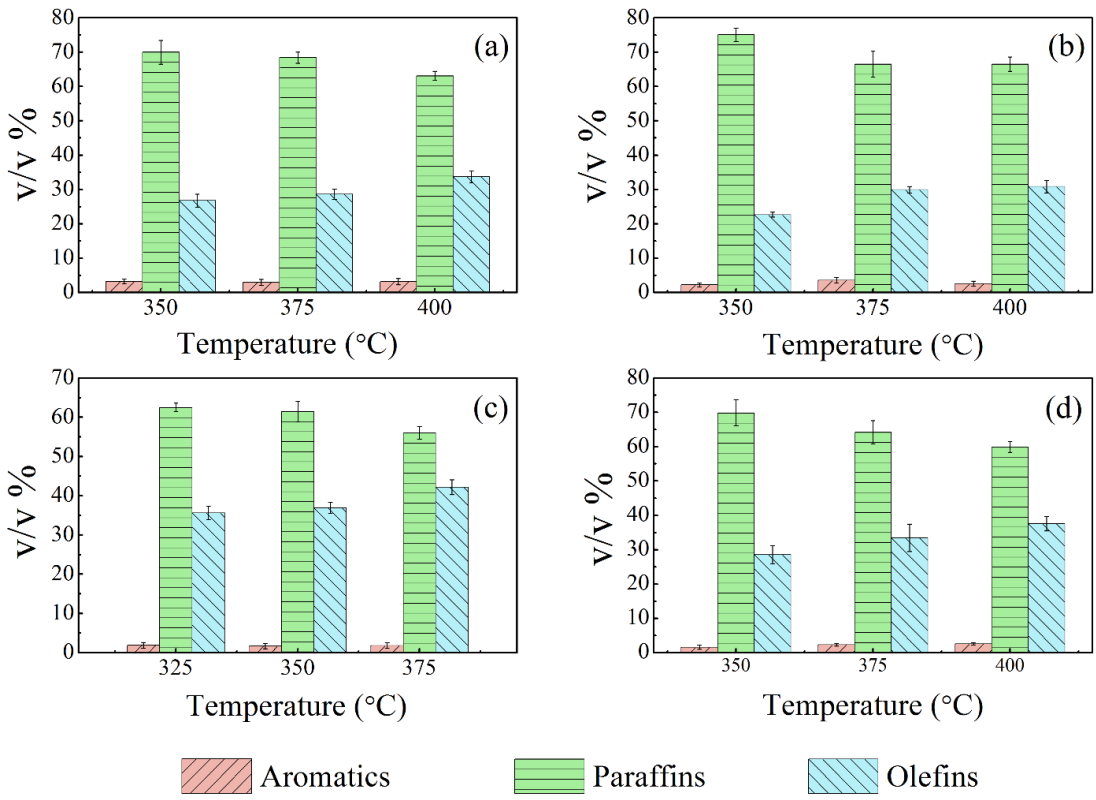

Fig. 4. 3 Volume fraction of paraffin, olefins and aromatics of the PDOs obtained from the isothermal slow pyrolysis of (a) LDPE, (b) HDPE, (c) PP and (d) RMIX

Table 4. 2: Iso-paraffin index, H/C ratio and RON calculated for PDOs by ^{1}H NMR analysis

Feed Material	Temperature, °C	Iso-paraffin index	H/C ratio	RON
LDPE	400	0.16	1.78	82.13
	375	0.18	1.81	82.27
	350	0.22	1.81	82.55
HDPE	400	0.16	1.81	82.14
	375	0.19	1.82	82.24
	350	0.21	1.85	81.99
PP	375	1.41	1.62	92.94
	350	1.31	1.64	91.21
	325	1.21	1.62	91.17
RMIX	400	0.37	1.73	83.73
	375	0.43	1.74	83.86
	350	0.63	1.75	86.01

Simulated distillation (SimDist) analysis of PDO

To determine the carbon number distribution and the boiling point range of the PDO samples, simulated distillation was carried out with the help of gas chromatography (GC). The procedure of analysis was explained in details in section 2.2.8. A profound effect of temperature on carbon number distribution was established. The chromatography spectra of PDOs obtained from RMIX along with the spectras of paraffin standards are shown in Fig. A.4 in Appendix A. Fig. A.5 of Appendix A, shows the carbon number distribution of PDOs in terms of wt% (weight equivalent to the peak areas of chromatogram). Similar analysis were performed for the other PDO samples from virgin plastics (LDPE, HDPE and PP). The oil fractions were grouped (by % wt) as light (C_6 - C_{11}), middle (C_{12} - C_{20}) and heavy (C_{21} - C_{32}) and obtained data are summarise in Table 4.3. Lighter fractions were more dominantly present in the PDOs obtained from low temperature pyrolysis. 92% of the PDO obtained at 350 °C have the carbon number range of C_6 – C_{20} (light and middle fraction). The amount of light and middle fractions decreased to 71% (for LDPE) when the pyrolysis temperature was 400 °C but the amount of heavy fraction increased as the pyrolysis temperature increased. The heavy fraction (>C_{20}) has the highest value at 400 °C, which amounted to be ~29%. In case of HDPE, the lighter fraction (C_6 – C_{11}) was maximum when the pyrolysis temperature was minimum at 350 °C and maximum yield of middle fraction (C_{12} – C_{20}) and heavy fraction (>C_{20}) were observed when the pyrolysis temperature was 400 °C. Due to lower degradation temperature, PP pyrolysis was carried out in the isothermal

temperatures of 325 °C, 350 °C, and 375 °C. More than 30% of lighter hydrocarbon fraction and around 60% of middle fractions were obtained in all the PDOs obtained from PP. For the feed RMIX (real waste) the lighter and middle fractions were highest at 350 °C and heavy fraction increased as the pyrolysis temperature increased to 400 °C.

The boiling point distribution curves with cumulative yield with respect to carbon number distribution (along with boiling point distribution of n-paraffin) for the PDOs obtained from the individual virgin plastics (LDPE, HDPE and PP) and real world waste plastic mix (RMIX) are shown in Fig. 4.4. The boiling point of n-paraffins (standards) are taken from the literature [149]. The corresponding values of the boiling point at each carbon number of n-paraffin was incorporated with the PDO sample. It can be observed that around 90% yield of the liquid have boiling point of 350 °C when the pyrolysis was carried out at the lowest temperature. Most conventional diesel fuel undergo evaporation with a 95% conversion at temperature 350 – 370 °C[150]. However, the yield decreased to 70% at 400 °C at that boiling point range. The pyrolysis experiments carried out for a long duration of 8 hours under low-temperature conditions selectively produce light to moderate liquid hydrocarbon (C_6 - C_{20}) product from the chosen plastic wastes composed of LDPE, HDPE and PP.

Table 4. 3: PDO fractions obtained from SimDist analysis

Feed material	Pyrolysis temperature (°C)	PDO fractions (%wt)**		
		Light (C_6-C_{11})	Middle (C_{12}-C_{20})	Heavy (C_{21}-C_{32})
LDPE (Virgin) (LDPE = 50 g)	350 °C	11.72	80.12	8.16
	375 °C	12.41	73.13	14.46
	400 °C	12.63	58.64	28.73
HDPE (Virgin) (HDPE = 50 g)	350 °C	29.52	66.8	3.68
	375 °C	17.6	73.7	8.7
	400 °C	12.32	76.37	11.3
PP (Virgin) (PP = 50 g)	325 °C	34.89	61.79	3.32
	350 °C	32.01	61.79	3.32
	375 °C	30.01	58.54	9.45
RMIX (from waste) (LDPE = 15 g ; HDPE = 15 g; PP = 20 g)	350 °C	27.24	69.04	3.72
	375 °C	26.54	62.84	10.62
	400 °C	12.44	60.39	27.08

** *The values were average values of minimum of three analysis with standard deviation <2%*

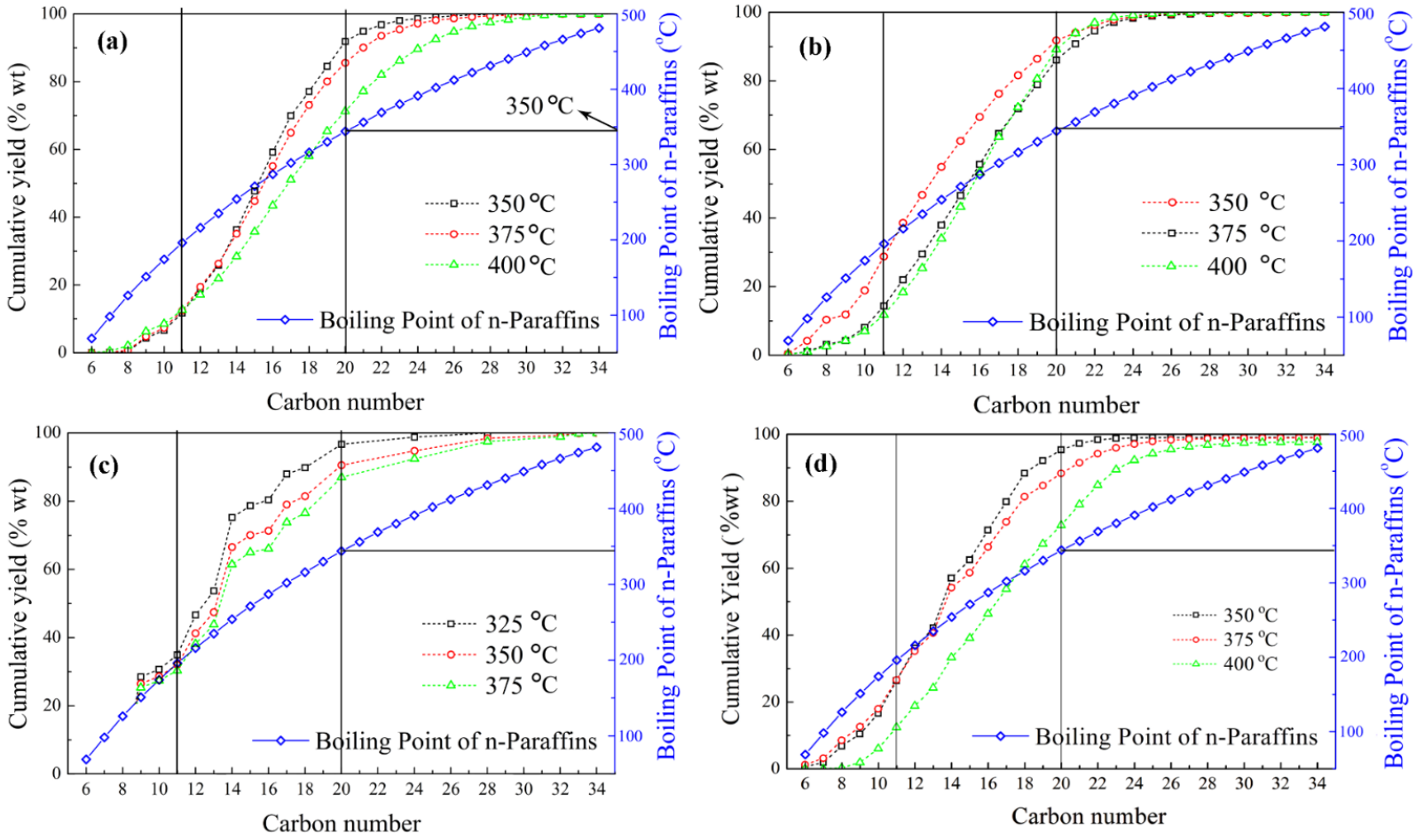

Fig. 4. 4: Cumulative yield (% wt) of hydrocarbons with respect to carbon number and the boiling range of n-paraffins and for PDO obtained at three temperature from the pyrolysis of (a) LDPE, (b) HDPE, (c) PP and (d) RMIX

4.1.2 ***Fuel properties of PDO***

The PDO samples obtained from the pyrolysis at various reaction conditions have some of the similar attributes like that of the existing refinery products such as gasoline and diesel (middle distillates). The fuel properties (using ASTM methods) of all the PDO samples along with gasoline and diesel are summarized in Table 4.4. The analysis where conducted 3 – 4 times and the average values are reported in Table 4.4. The pyrolysis temperature and feed quality have substantial influence on the fuel properties of the end products. High calorific values (>45 MJ/kg) were estimated for all the samples. The oils have low viscosity values and the viscosity of the PDO from all feed condition increased with the increase of pyrolysis temperature. At high temperature, the liquid products have higher percentage of long-chain hydrocarbons, due to which the obtained oil samples are more viscous and heavier. The PDO samples obtained from PP have low density, cloud point and pour point values. The high concentration of olefins in the oil makes the product less susceptible to form crystals at a lower temperature [151]. The liquid products from the mixed feed (RMIX) exhibited the characteristics of a middle distillate (diesel) petroleum product, having calorific value around 47 MJ/kg, viscosity as low as 0.09 cP (at pyrolysis temperature of 350 °C) and comparable pour point (-2 °C) and flash point (35 °C).

Conventional Indian diesel standard (Bharat Stage III) [152] has pour point values of 3°C (winter) and 15 °C (summer) and a flash point of 35 °C (Abel) and 66 °C

(Pensky Martens closed cup)[153]. The analysis of fuel properties indicated the fact that the PDOs from the plastic pyrolysis particularly when the feed is LDPE, HDPE or RMIX have characteristics similar to that of conventional diesel-like fuel. However, PDOs from PP are lighter, less viscous and with relatively high research octane number (RON) values (~92) (Table 4.3). Therefore, PDOs from PP notably obtained at low-temperature slow pyrolysis can be considered as a possible blend component for the gasoline. The common fuel properties of gasoline and diesel are incorporated in Table 4.4 for comparison with the different PDOs obtained from the pyrolysis of packaging plastics.

Therefore, by simply increasing the pyrolysis time at a moderate degradation temperature the plastics can be converted into alternative liquid fuels. Sharma, Moser et al. (2014) upgraded the fast pyrolysis liquid product from HDPE waste (grocery bags) by distillation. A direct comparison can be made between the slow pyrolysis end product and the fast pyrolysis distilled product as most of the properties like density, calorific value, cloud point, pour point and flash point etc. are closely identical and comparable to conventional liquid fuel such as gasoline and diesel.

Table 4. 4: Fuel properties of PDOs

Feed Material	Temperature, °C	Density, Kg/m³	Calorific value, MJ/kg	Viscosity, cP, at 25 °C	Cloud point (CP), °C	Pour point (PP), °C,	Flash point, °C	Fire point, °C
		Method of calculation						
		Pycnometer	*ASTM D4809*	Rheometer	*ASTM D97*	*ASTM D97*	*ASTM D92*	*ASTM D92*
LDPE	**400**	807	46.23	0.17	18.2	15	41	47
	375	804	46.29	0.16	9	5.6	39	44
	350	803	46.77	0.12	4	1	33	40
HDPE	**400**	810	46.43	0.17	4	0	37	41
	375	808	46.49	0.15	13.3	2	36	40
	350	804	46.81	0.13	15	4	32	38
PP	**375**	794	45.59	0.9	-15	-23	39	44
	350	790	45.92	0.7	-11	-17.5	35	40
	325	790	45.97	0.56	-5	-12	34	39
RMIX	**400**	802	46.37	0.31	8	4	37	41
	375	800	46.44	0.13	3	0	35	42
	350	801	46.79	0.09	1	-2	35	40
Gasoline*	**-**	720 – 775	46 – 48	0.5 – 1.0	<-40	<-70	-25 to -15	10 to -5
Diesel*	**-**	820 – 860	44 – 46	2.0 – 5.0	-5 to -20	-40	35	40 - 45

**The fuel values of gasoline and diesel were collected from literature[127]*

4.1.3 ***Pyrolysis gas analysis***

Plastics have carbon and hydrogen in their polymer backbone. Thermal degradation of plastics leads to the generation hydrocarbon gases. The uncondensed gases were analysed by gas chromatography. The detailed procedure of analysis was explained in section 2.2.8. The pyrolysis gas evolution pattern and its compositions demonstrated a comparative trend for all the feed. The gaseous products collected at the various interval during the pyrolysis of RMIX were identified and the average volume % are reported in Table 4.5. Similarly, for the other feeds (i.e. LDPE, HDPE and PP) the gas compositions are shown in Table A.1 to A.3 in Appendix A. Methane, ethane, ethylene, propane, propylene, n-butane, 1-butene and n-pentane were found in significant quantities. The hydrogen, carbon monoxide, and carbon dioxide were also found in trace amount, generation of these gases may be due to the presence of any impurity in the feed. The unsaturated hydrocarbons like ethene, propylene and butene and their derivatives were also observed, which actually produce due to random scission degradation mechanism of plastic followed by stabilization of the intermediate radicals. The concentrations of hydrogen, carbon dioxide and carbon monoxide decreased with pyrolysis temperature. Nitrogen-free gross calorific value (GCV) and net calorific value (NCV) of the gases from RMIX were found in the proximity of 105 MJ/m^3 and 96 MJ/m^3 respectively. The GCV value of the gas was found to be 120 MJ/m^3, when PP was pyrolyzed at 325 °C under isothermal condition. The increase of GCV value is due to the presence of

52% of n-pentane. The high calorific value of the gaseous product indicates that the evolved gases can be used as fuel gas.

Table 4. 5: Composition (% vol) and GCV and NCV of gas derived from pyrolysis of RMIX

Gas composition	From the pyrolysis of RMIX at		
	400° C	375 °C	350 °C
Methane	5.69	5.56	4.95
Ethane	8.85	8.02	11.03
Ethylene	3.24	2.54	2.36
Propane	6.69	7.9	6.78
Propylene	28.32	28.87	32.93
Propadiene	0.55	0.5	0.32
n-Butane	2.97	2.9	2.52
Trans-2-Butene	0.6	0.69	0.43
1-Butene	3.34	3.01	2.13
Isobutylene	8.11	8.04	8.52
Cis-2-butane	0.47	1.89	0.35
Isopentane	0.12	0.16	0.04
n-Pentane	28	27.8	26.44
Methyl Acetylene	0.37	0.49	0.22
Hydrogen	1.36	0.96	0.44
Carbon monoxide	0.44	0.16	0.17
Carbon-di-oxide	0.88	0.51	0.37
GCV (MJ/m^3)	105 ± 1.51	106.89 ± 2.08	105.67 ± 1.62
NCV (MJ/m^3)	96 ± 1.77	97.71±1.8	96.98 ± 2.06

4.2 General aspects of pyrolytic degradation mechanism of plastics

The thermal degradation mechanisms of plastics evolved from three general polymer chain reactions viz. polymeric chain scission, side group reaction and recombination reaction [154]. Under the influence of heat, the polymer chain breaks (end chain or random chain scission) at weak links (sp^3 bond) and forms radicals. According to Levine and Broadbelt [155] most of the scission reactions in polymer degradation take place at β- position of the polymer chain. The end chain β -scission requires less energy than random chain β -scission, hence at low temperature slow pyrolysis the production of gaseous hydrocarbon is high. Both random and end chain β -scission reactions are responsible for the lighter fractions (C_6 - C_{20}) of the liquid products while the formation of olefin is due to the radical recombination reactions followed by inter or intramolecular hydrogen shift. In addition to β-scission, the thermal degradation of plastics might undergo α-scission, methyl scission, or hydrogen scission. Scission of C – H (α – scission) bond under low-temperature pyrolysis is thermodynamically less favourable. The α–scission refers to the breaking of σ bond (sp^2 carbon). The dissociation energy of α – scission (83-94 kcal mol^{-1}) is more than β-scission (61.5 – 63 kcal mol^{-1})[145]. Hence, at low-temperature pyrolysis the β-scission reactions are more likely to occur. The pyrolysis at high temperature (~400 °C) may facilitate the α – scission reactions that may eventually lead to the formation heavy fraction of PDOs. The obtained results in the isothermal slow pyrolysis of plastics can be compared with the literature findings summarised in Table 4.6.

Table 4. 6: Comparison of %yield and liquid product quality obtained from the pyrolysis of various polyolefins (LDPE, HDPE and PP) and various mix plastic studied in various literature

Material	Process	Yield (% wt)			Liquid product quality	Reference
		Liquid	Gas	Residue		
LDPE	Fluidized bed reactor (*T = 500 °C, 3 g/batch, t = 15 s*)	89.2	10.8	0	Wax 49%; Oil 51%	Williams and Williams [53]
LDPE	Fixed bed reactor(*T = 700 °C, β = 25 °C/min*)	84.3	15.1	0	Wax	Williams and Williams [95]
LDPE	Spouted bed reactor (*T = 450 °C*)	80	20	0	Wax	Aguado, et al. [156]
HDPE	Microwave induced pyrolysis (*T = 500 °C*)	81	19.0	0	Oil/wax (C3-C56)	Ludlow-Palafox and Chase [157]
HDPE	Steam Fluidized bed reactor (*T = 600 °C, 3.4 Kg, t = 3 hour*)	41	31	28	87% aliphatic	Kaminsky, et al. [19]
HDPE	Batch autoclave reactor (*T = 500 °C, P = 19.2 MPa, t = 1 hour*)	93	7	0	Unknown	Williams and Slaney [158]
HDPE (Waste)	Batch reactor (*T = 440 °C, t = 2 hours*)	74	9	17	Crude	Sharma, et al. [96]
HDPE	Two stage free fall reactor (*T = 500 °C, 0.14 g/min, t = 20 min*)	97.4	1.8	0.8	Oil/wax; 97.36 % C5-C60, <0.05% Aromatic	Mastral, et al. [159]
HDPE	Fixed bed reactor (*T = 700 °C, β = 25 °C/min*)	79.7	18.0	0	Wax	Williams and Williams [95]
HDPE	Spouted bed reactor (*T = 450 °C*)	80	20	0	Wax	Aguado, et al. [160]
PP	Batch autoclave reactor (*T = 500 °C, P = 19.2 MPa, t = 1 hour*)	95	5	0	Unknown	Williams and Slaney [158]
PP	Fixed bed reactor (*T = 700 °C, β = 25 °C/min*)	84.4	15.3	0.2	Wax	Williams and Williams [95]
PP	Spouted bed reactor (*T = 450 °C*)	92	8	0	Wax	Aguado, et al. [160]
PP	Batch reactor (*T = 740 °C β = 10 °C/min*)	48.8	49.6	1.6	>40% olefins	Demirbas [31]
Real waste (PE, PP, PS, PET, PVC)	Batch reactor (*T = 500 °C, β = 20 °C/min, t = 30 min*)	40.9	25.6	33.5	93.4 % Aromatics	Adrados, et al. [20]
Simulated waste (PE, PP, PS, PET, PVC)	Batch reactor (*T = 500 °C, β = 20 °C/min, t = 30 min*)	65.2	34.0	0.8	73.9 % Aromatics	Adrados, et al. [20]
MIX (American plastic council)	Tubing bomb micro reactor (*T = 445 °C, P = 800 psig, t = 60 min*)	~85	~10	~5	Crude :55% Heavy HC (275 °C-FBP)	Shah, et al. [102]

T = pyrolysis temperature; P = reactor pressure; t = residence time or reaction time and β = heating rate

4.3 Summary

The low temperature pyrolysis of household plastic waste (RMIX) and individual samples of virgin LDPE, HDPE and PP were pyrolysed in a semibatch reactor. Liquid yield of ~82 % was achieved in case of virgin plastics at highest pyrolysis temperature considered in this study. The liquid products or the plastic derived oils (PDOs) mostly constitute of paraffins and olefins. Increasing the temperature increases the yield of PDO but produces heavier oil with long hydrocarbon chains ($>C_{20}$). On the other hand, the PDO obtained at lower temperature (350 °C) have superior fuel properties like high calorific value and low viscosity, pour point and flash point. Low temperature and long duration supported the polymer scission reaction (end chain and random) and leads to the production of lighter hydrocarbons. The data obtained in this chapter are useful in the context of utilization of pyrolysis process to produce targeted value added products like gasoline or diesel from plastic waste. More investigations with respect to streamlining the process condition, process design and prudent assessment are required to scale up the process. Nevertheless, to minimize the energy consumption in the pyrolysis process low-temperature slow pyrolysis will play a vital role in the near future in terms of process implementation. Plastic derived oil (PDO) produced under low-temperature pyrolysis from waste LDPE, HDPE and PP can address the demand for alternative fuels and utilization of plastic waste

Chapter 5

THE EFFECT OF SLOW PYROLYSIS ON THE CONVERSION OF PLASTIC WASTE INTO FUEL

Packaging plastic waste

Non-isothermal pyrolysis

Hydrocarbon distribution

Waste to fuel

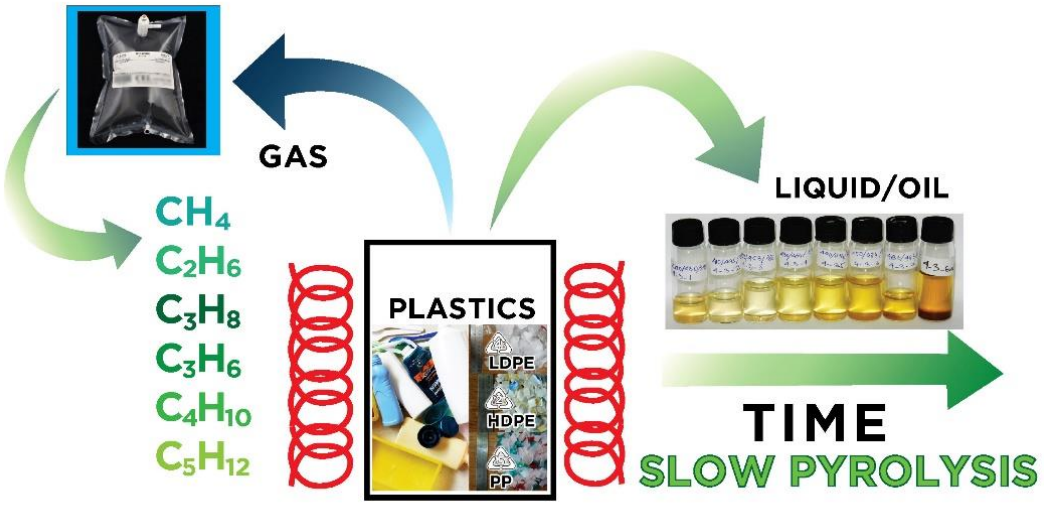

Work published at:

Pallab Das and Pankaj Tiwari, 'The effect of slow pyrolysis on the conversion of packaging waste plastics (PE and PP) into fuel,' *Waste Management*, vol-79 pp. 615-624 (2018). IF = 5.431

5 The effect of slow pyrolysis on the conversion of plastic waste into fuel

This chapter focuses on the effect of slow pyrolysis on the composition of the product throughout the pyrolysis process. Packaging plastic waste consisting of low and high-density polyethylene (LDPE and HDPE) and polypropylene (PP) as virgin as well as sample collected from the pyrolysis of household plastic waste were pyrolyzed in the lab scale semi-batch reactor at a very slow dynamic condition (1 °C/min) upto a temperature of 400 °C. Gaseous and liquid products were collected at regular intervals starting from their inception during the degradation process. Detailed analysis was carried out to estimate the properties and compositions of plastic derive oil (PDO) and gaseous products obtained at different stages of the pyrolysis process.

5.1 Thermogravimetric analysis and semi-batch pyrolysis yield

To determine the degradation range for non-isothermal slow pyrolysis of three plastic samples, TGA analysis was carried out at a very slow heating rate (1 °C/min). Fig. 5.1 shows the TGA and DTG profiles of virgin samples of LDPE, HDPE and PP. The rate of mass loss (DTG) increased with the temperature and passed through a maximum (Fig. 5.1) at peak degradation temperature (T_m).

The onset temperatures (T_o) or the point at which degradation were 330 °C, 340 °C and 275 °C for LDPE, HDPE and PP respectively. Similarly, PP has a lower value of peak degradation temperature of 405 °C than LDPE (430 °C) and HDPE. (435 °C) Clearly, PP has low degradation temperature than LDPE and HDPE and this

effected the pyrolysis product distribution when PP was in the feed. Values of degradation temperatures (T_o and T_m) and the rate of degradation are also function of heating rate [144]. A low onset point was achieved by lowering the heating rate to 1 °C/min. Detail explanation of thermal degradation and the TGA based kinetics of the plastic samples are explained elaborately in Chapter 3 of the thesis [144].

Lab-scale pyrolysis was carried out for virgin plastics (LDPE, HDPE, PP and VMIX) as well for the real plastic waste mixture (RMIX). Detailed experimental procedure for non-isothermal slow pyrolysis is explained in section 2.2.7. A slow heating rate of 1 °C/min was maintained to reach the final temperature of 400 °C. The condensed liquid product and uncontested gaseous products were collected at regular intervals (10 min) for analysis. Residue samples (char) were collected at the end of each experiment (after cooling) and weighed. Sum of the weight (g) of the liquid, gaseous product and solid residue from the non-isothermal pyrolysis are listed in Table 5.1 in terms of % yield. The cumulative yield of liquid product/plastic derived oil (PDO) with respect to time was shown in Fig. 5.2 for different feed condition. The % yield of PDO was around 75% for the real world waste and for all other feed condition (virgin plastics) the % yield was found to in the range of 82 - 83 %. Around 3.66% of the residue was collected for RMIX feed. Presence of impurities (traces of metals, plasticisers, flame-retardants and colours etc.) in the real waste sample (RMIX) may attributed to the high yield of solid residue [161]. The residue accumulation was <1% in other feed condition.

Table 5. 1: Overall product yield (w/w%) for non-isothermal pyrolysis**

Material	PDO w/w%	Gas w/w%	Residue w/w%
LDPE, virgin (50 g)	82.68	16.88	0.44
HDPE virgin (50 g)	82.66	16.78	0.56
PP virgin (50 g)	83.16	16.53	0.31
VMIX (50 g)	82.25	17.04	0.71
RMIX (50 g)	74.98	21.36	3.66

***The values reported here are average values of three (or more) runs with a standard deviation <5%*

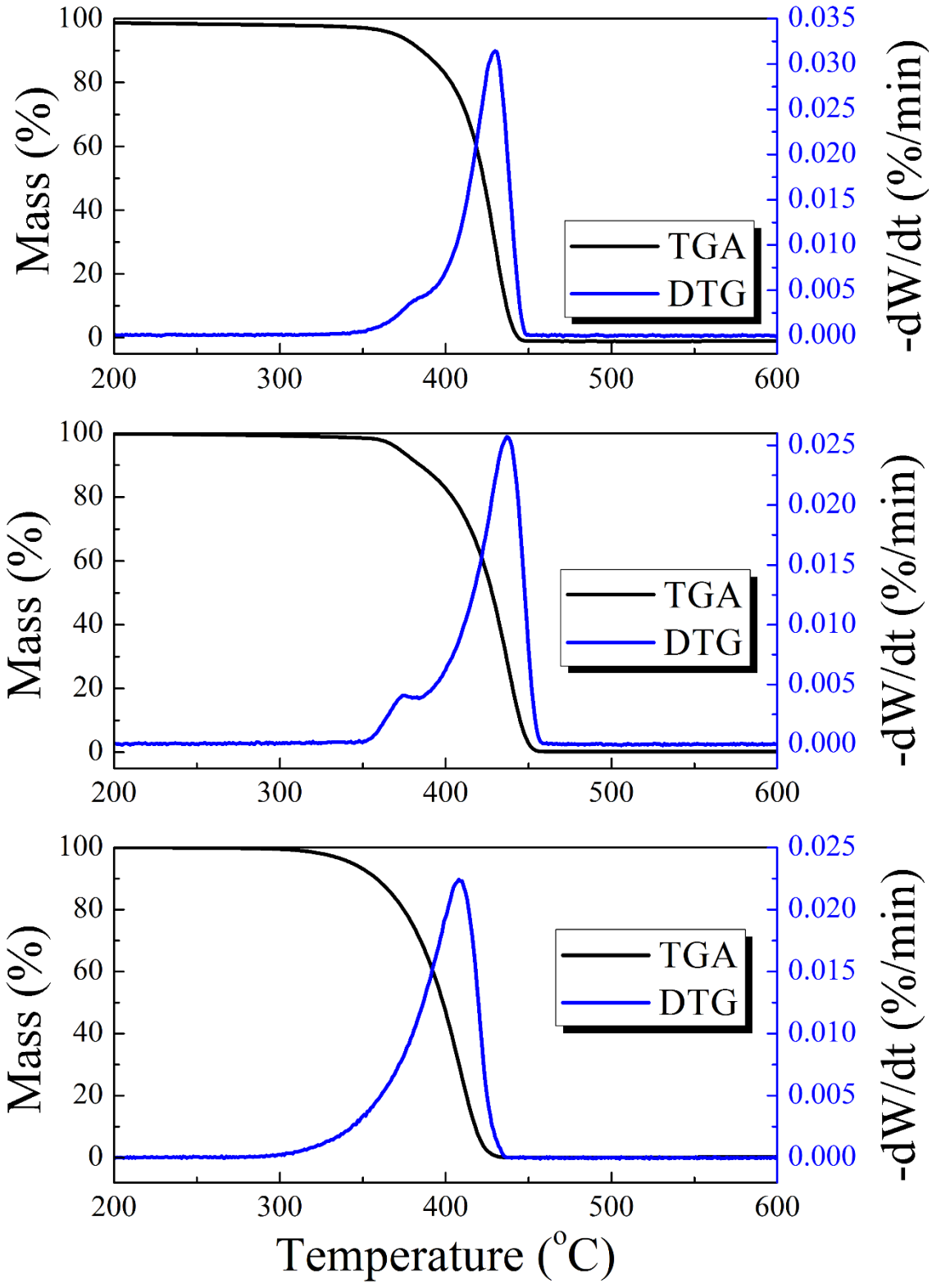

Fig. 5. 1: Non-isothermal (1 °C/min) TGA and DTG profiles of (a) LDPE, (b) HDPE and (c) PP

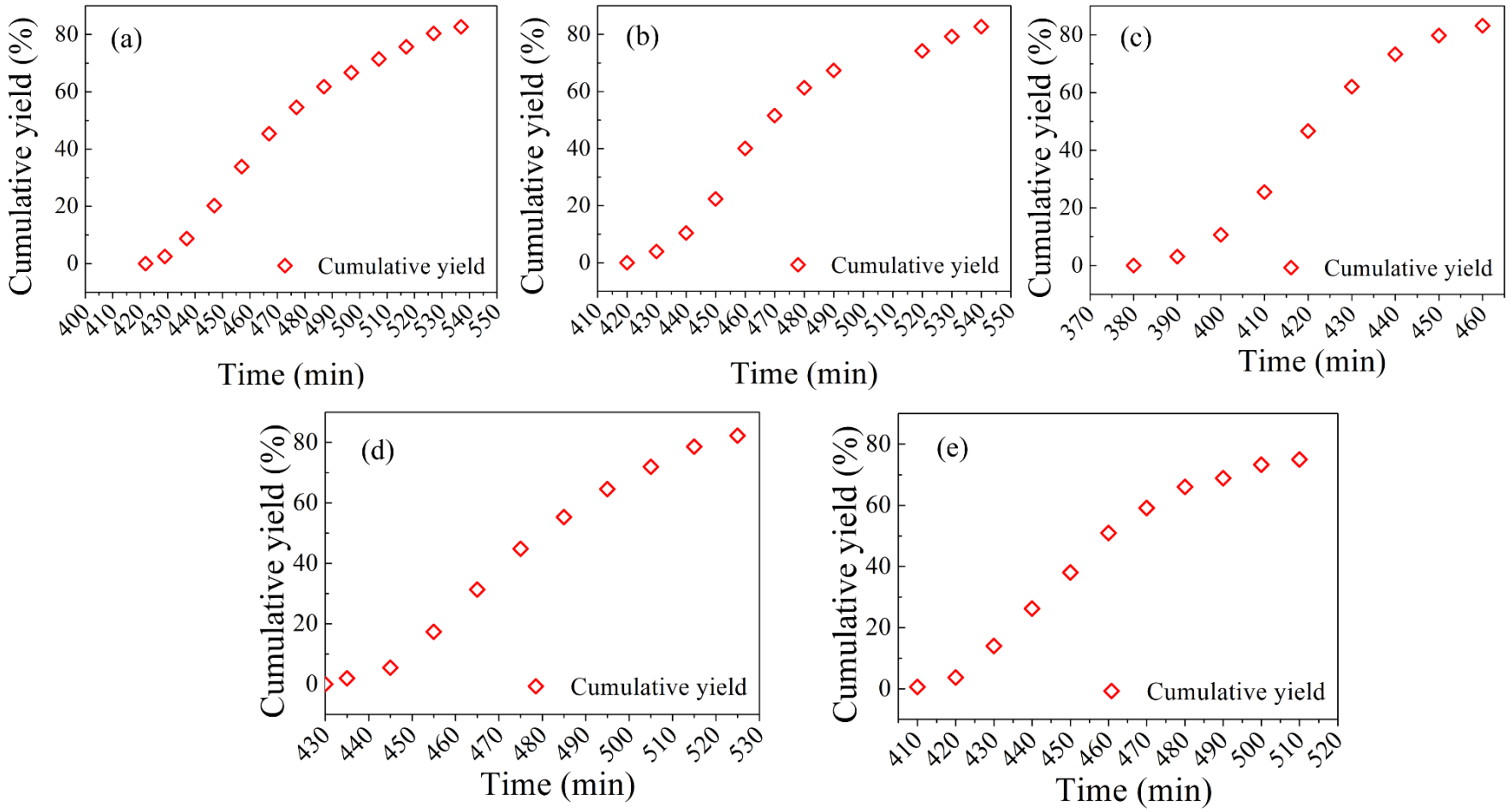

Fig. 5. 2 Cumulative oil yield in the region of oil formation period for (a) LDPE, (b) HDPE, (c) PP, (d) VMIX and (d) RMIX

5.2 Liquid product analysis

Plastic derived oil (PDO) or the liquid products were the major and targeted component of the pyrolysis products. The analysis was carried out for the individual samples collected at different intervals. The analytical techniques such as Fourier transform infrared spectroscopy with attenuated total reflection (FTIR-ATR), proton nuclear magnetic resonance spectroscopy (^{1}H NMR) and gas chromatography with simulated distillation (GC-SimDist) were used. The analytical processes are explained in section 2.2.8 of Chapter 2.

5.2.1 *FTIR and ^{1}HNMR analyses*

FTIR-ATR spectras of the PDOs are shown in Fig. 5.3. Functionalities of the IR peaks with respect to wavenumber are displayed in Fig. A.6 (Appendix A). Wavenumber range (s) of different hydrocarbon functionality is listed in Table A.4 (Appendix A). The IR spectra of the PDOs obtained at the various interval of non-isothermal pyrolysis was found similar to that of IR spectra of the PDOs obtained at isothermal pyrolysis, that is explained in Chapter 4 for the same type of feed.

The functionalities remained consistent with the progress of the pyrolysis at the dynamic heating condition. Oxygenated components were missing. However, quantitative variations of paraffin, olefins and aromatics with increasing reaction time (temperature) were observed by ^{1}H NMR analysis. Total paraffin, olefin and aromatic content of the PDOs are reported in Table 5.2. Aromatic hydrocarbon compositions were <5% and high aromaticity was observed for the samples collected

at higher temperatures. A slightly higher (7.4%) aromatic yield was obtained from the RMIX feed from the sample collected at 510 min. Mild aromatization occurred at higher temperatures. Aliphatic components were more dominant in the PDOs. Olefins concentration was higher in the PDOs obtained from PP feed. An increasing trend of olefins with the progress of the reaction (pyrolysis time/temperature) was noticed. A maximum yield of 55 v/v% olefin yield was found for the PDO collected at 390 min from PP pyrolysis. Paraffin fractions were found consistent as the reaction continued, except for a few samples obtained at higher temperatures, where paraffin yield was relatively high. For example, PDO obtained at 510 min from HDPE pyrolysis had shown a paraffin yield of 72.1 v/v%. The concentration of the paraffinic and olefinic components of PDOs was also examined for the multiple isothermal pyrolysis studies in Chapter 4[162]. Effect of reaction temperatures in the product distribution can be established from both studies. Adjusting pyrolysis temperature and heating rate may lead to target suitable hydrocarbons (paraffinic/olefinic) from the packaging plastic waste. Similar observation was reported by Marcilla et al.[104] under low temperature range of 360 – 385 °C and also emphasize that 1-olefin and n-paraffins were the major components from the LDPE and HDPE. Onwudili et al. [105] reported a decrease of aliphatic concentration at high temperature (500 °C) and high pressure (4.31 MPa) pyrolysis followed by occurrence of cyclization and aromatization reaction.

The table 5.2 also reported the values of H/C ratio, iso-paraffin index and research octane number (RON) values of PDOs calculated by Eq. (37) – (38). Higher values

of H/C ratio (>1) indicate less emission of greenhouse gases during burning if utilized as fuel alternatives [124]. PDOs from LDPE and HDPE had shown the higher H/C ratio and the H/C values apparently consistent with temperature. The isoparaffin index represents the proportion of branched to the normal paraffin[124]. The isoparaffin index was found to be higher in case of PDO from PP and the values had an increasing trend with the temperature (reaction time) in case of PP, whereas in other feed condition isoparaffin index decreased with the temperature. The elevated isoparaffin index (more branching) implies a high RON value. The RON values appeared to be higher for the initial (low temperature) PDO samples from LDPE, HDPE, VMIX and RMIX. The PP polymer chain has a methyl group attached with every other carbon atom, which helps in the formation of branched paraffins and olefins. According to Pinto et al. [97] the presence of extra methyl group in the PP polymer chain stabilizes the intermediate radicals by forming double bond between two carbon atoms. A qualitative explanation regarding the degradation mechanism of such polymers can be derived from various past studies [104,146,163,164]. At elevated temperature, polyolefins breaks down into radicals by scission reaction. These radicals undergo stabilization (propagation) by intra or inter molecular hydrogen transfer. Low temperature favours the intramolecular hydrogen transfer lead to the formation of olefins whereas increasing temperature shifts to inter molecular hydrogen transfer which results more paraffins. The high concentration of olefins in the oil sample have huge industrial application. The petrochemical olefins used to produce industrial organic chemicals like vinyl acetate,

acetaldehyde, and vinyl chloride. The unsaturated hydrocarbons (olefins) can undergo metathesis to produce cyclic and acyclic alkenes etc., which have greater industrial and commercial importance.

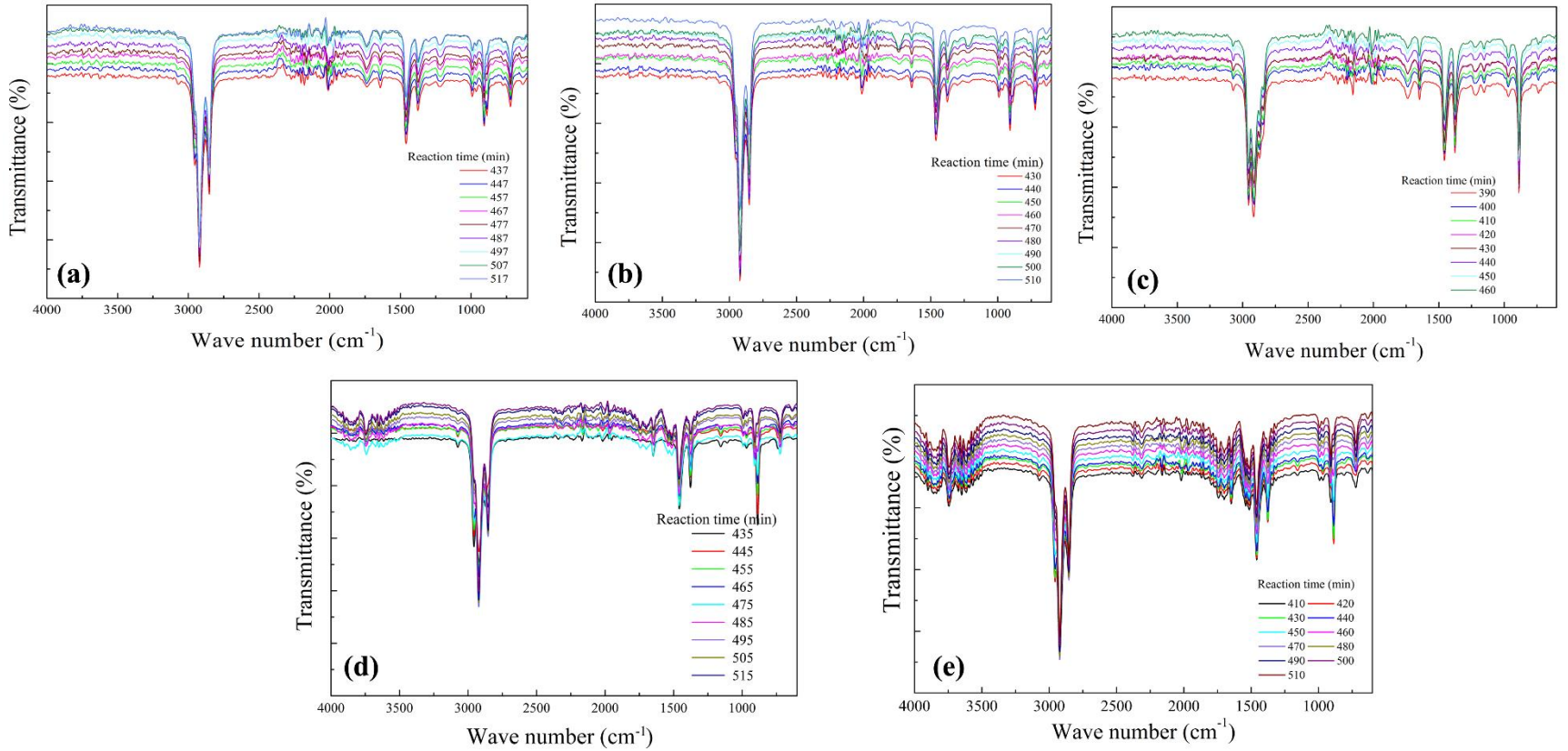

Fig. 5. 3 FTIR-ATR spectra of PDOs obtained at different time intervals from (a) LDPE, (b) HDPE, (c) PP, (d) VMIX and (e) RMIX

Table 5. 2: Volume fractions of paraffin, olefin and aromatic, H/C, isoparaffin index and RON values of the PDOs

Feed material	Pyrolysis time	Paraffin (v/v %)	Olefin (v/v %)	Aromatic (v/v %)	H/C	Isoparaffin index	RON
LDPE	437	65.58	32.09	2.33	1.82	0.24	82.55
	447	60	37.3	2.7	1.8	0.25	82.74
	457	62.9	34.24	2.86	1.8	0.21	82.38
	467	65.89	31.83	2.28	1.82	0.19	82.2
	477	68	29.55	2.45	1.83	0.19	82.15
	487	69.46	27.69	2.85	1.82	0.16	81.97
	497	70.46	27.02	2.52	1.83	0.17	81.99
	507	68.36	28.69	2.95	1.82	0.18	82.08
	517	65.62	30.65	3.73	1.78	0.16	82.07
HDPE	430	49.49	47.69	2.82	1.75	0.22	82.5
	440	63.26	33.85	2.89	1.8	0.19	82.22
	450	64.5	32.65	2.85	1.8	0.19	82.21
	460	66.24	30.8	2.96	1.83	0.17	82.03
	470	67.27	29.33	3.4	1.81	0.16	81.96
	480	67.9	29.15	2.95	1.8	0.16	81.95
	490	66	31.37	2.63	1.77	0.16	81.9
	500	68.2	28.9	2.9	1.8	0.15	81.86
	510	72.13	25.03	2.84	1.83	0.19	80.42
PP	390	43.9	55.27	0.83	1.33	0.59	85.55
	400	55.51	43.1	1.38	1.64	0.98	89.07
	410	61.34	37.5	1.2	1.66	1.23	91.25
	420	59.67	38.67	1.37	1.62	1.32	92.1
	430	59.1	39.28	1.6	1.6	1.3	92.03
	440	59.04	39.6	1.36	1.61	1.42	93.02
	450	57.54	40.25	2.21	1.6	1.23	91.44
	460	62.08	35.93	1.98	1.65	1.34	92.36
VMIX	435	51.3	47.2	1.5	1.68	0.9	88.3
	445	56.88	41.52	1.6	1.7	0.75	87
	455	60.44	37.9	1.65	1.7	0.6	85.4
	465	60.59	37.33	2.08	1.7	0.61	86
	475	52.88	44.06	3.06	1.8	0.28	83.01
	485	61.87	35.2	2.92	1.76	0.22	82.5
	495	61.55	34.8	3.65	1.77	0.2	82.4
	505	61.86	34.1	4.05	1.8	0.2	82.33
	515	65.54	31.01	3.44	1.75	0.2	82.4
RMIX	410	63.15	33.85	3	1.76	0.49	84.86
	420	60.76	37.46	1.78	1.7	0.65	86.18
	430	58.9	39.5	1.62	1.7	0.7	86.6
	440	59.65	38.17	2.46	1.7	0.54	85.3
	450	61.61	36.04	1.52	1.76	0.27	82.94
	460	63.36	33.92	2.71	1.76	0.27	82.95
	470	64.71	32.84	3.6	1.76	0.2	82.38
	480	66.62	30.3	3.1	1.8	0.21	82.38
	490	66.49	30.12	3.42	1.8	0.2	82.34
	500	66.6	29.28	4.8	1.75	0.18	82.3
	510	65.58	28.93	7.39	1.78	0.19	82.3

5.2.2 *Simulated distillation (SimDist) analysis of PDO*

Simulated distillation (analysis) of the PDO samples were carried out and weight equivalent of peak areas were determined and converted into weight percent to determine the carbon number distribution. Boiling point of normal n-paraffin standard fixed the boiling point range. Boiling point distribution for the respective carbon number was predicted from the boiling points of n-paraffins. The GC spectras are shown in Fig. A. 7 to Fig. A.11. The distributed weight fractions were classified into light (C_6 – C_{11}), middle (C_{12} – C_{20}) and heavy (C_{21} – C_{FBP}) fraction, which resemble the conventional petroleum fractions.

A difference in carbon number distribution with the increase of temperature was observed with the progress of the reaction. The boiling point distribution (carbon number) curve with cumulative yield for the PDOs obtained from mix waste sample (RMIX) is shown in Fig 5.4 for all the liquid samples collected along the progress of the reaction. The boiling point of normal paraffin for carbon number 20 (icosane) is around 350 °C (341.1 °C). It was observed in Fig 5.4, that the fraction of PDOs collected at the initial stages of the degradation process (at 410 min) have 95% liquid distilled (boiling point) before 350 °C. However, the fraction decreased to 75% for the PDO collected towards the end of the degradation process (510 min). Similar boiling point (carbon number) distribution profiles for the other feeds were shown in Fig. 5.5, and similar observation could be made.

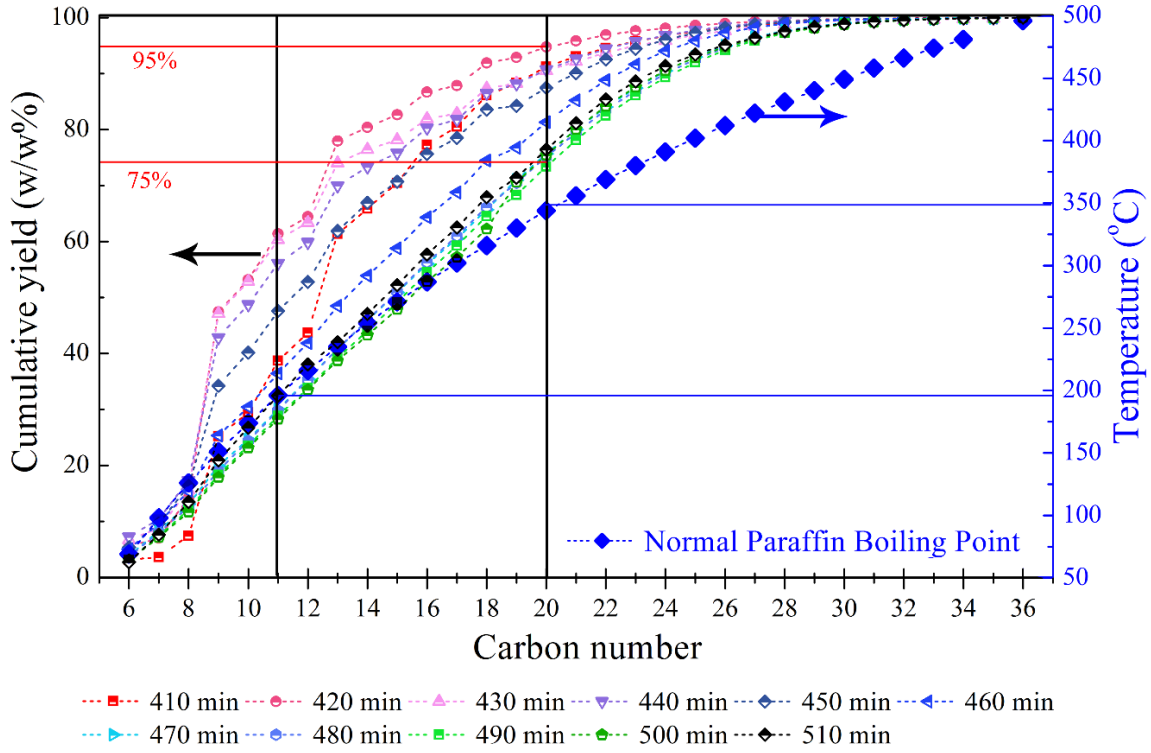

Fig. 5. 4 Cumulative yield (w/w%) of hydrocarbons with respect to carbon number and the boiling range of n-paraffins and for PDO obtained at various time interval of non-isothermal pyrolysis of RMIX sample

The variation of hydrocarbon fractions for each PDOs gathered at various intervals during the pyrolysis of each sample is shown in Fig. 5.6 and Fig. 5.7. Both Fig. 5.6 and 5.7 reflected a high yield of light fractions during the initial stages of plastic degradation, whereas the concentration of middle and heavy fractions increased as the process continued to a higher temperature. PDOs from PP were comparatively lighter than PDOs from other plastic feed (LDPE, HDPE, VMIX and RMIX) as the concentration of the lighter fractions maintained a yield of more than 40% throughout the process and maximum (62.8%) was obtained at 390 min (300 °C). Similarly, a maximum concentration of middle fraction (71.6 %) was obtained for the PDO from HDPE pyrolysis collected at 510 min. Similar distribution trends

were noticed for LDPE (Fig. 5.6(a)) and both the mixed plastic feeds (Fig. 5.7 (a) and (b)).

The highest concentration of lighter fraction was obtained at 445 min (310 °C) for VMIX and 420 min (305 °C) for RMIX. The yield of middle fractions was minimum (around 30%) at 445 min (310 °C) and 430 min (325 °C) for the VMIX and RMIX respectively. Simdist analysis of the PDOs obtained for the isothermal pyrolysis in Chapter 4 elucidate the similar observation like non-isothermal slow pyrolysis. It is evident that chosing a particular temperature for isothermal pyrolysis with long duration or slowing down the heating can influence the overall product distribution and properties of the liquid oil. A comparison table was prepared with respect to current results and the results obtained for non-isothermal plastic pyrolysis in the past studies and listed in Table 5.3. Similarity, in terms of product composition (paraffins/olefins) and the effect of increasing temperature is evident in most of the reported literature (Table 5.3). A common conclusion that can be drawn by comparing the limited literature (slow pyrolysis) and the current study. It is very evident that by lowering the speed (heating rate) of the pyrolysis of packaging plastics gives a better control over the process to target a certain value added products like light/middle distillates of petroleum.

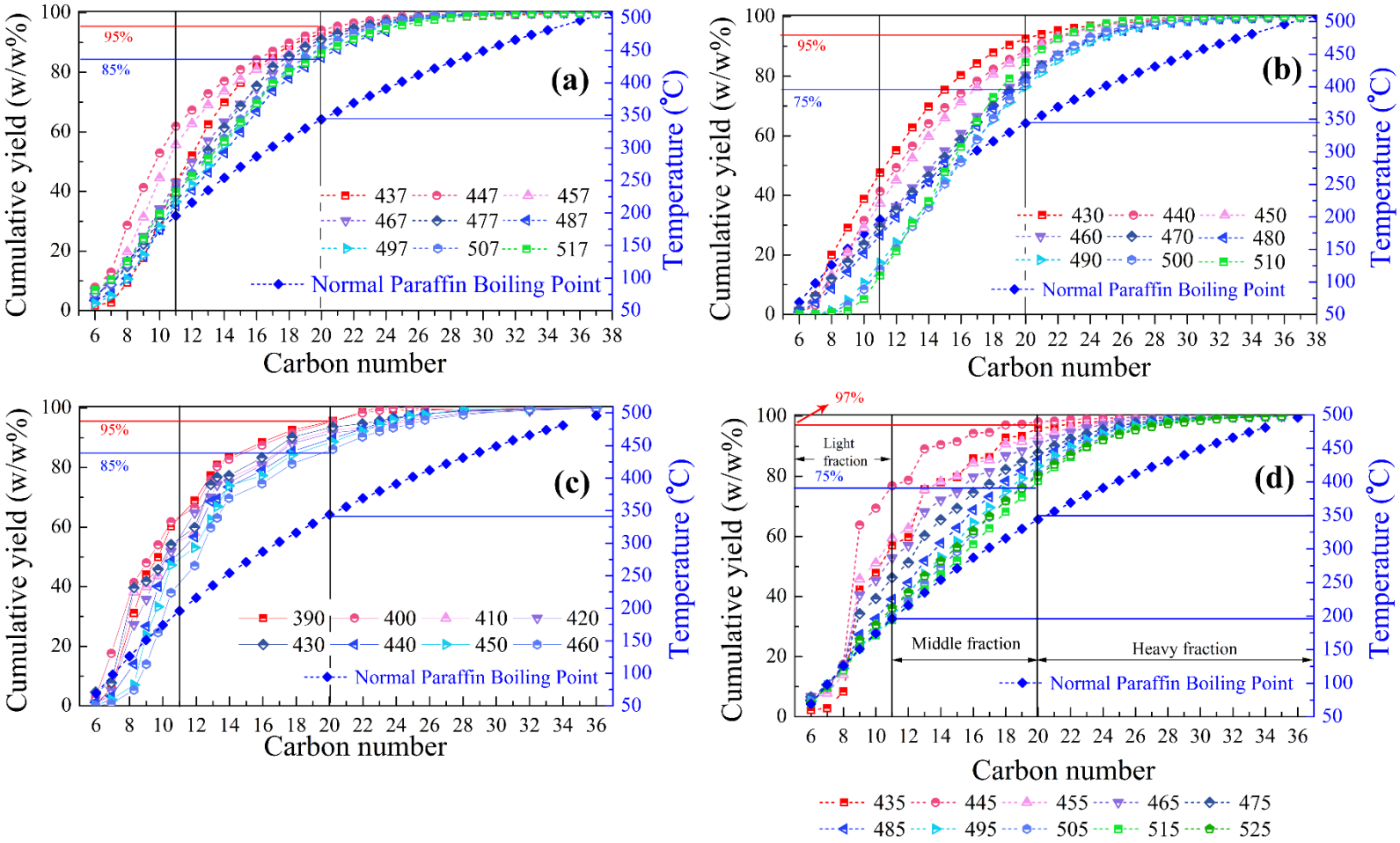

Fig. 5. 5 Cumulative yield (w/w%) of hydrocarbons with respect to carbon number and the boiling range of n-paraffins and for PDO obtained at various time interval of non-isothermal pyrolysis of (a) LDPE, (b) HDPE, (c) PP and (d) VMIX

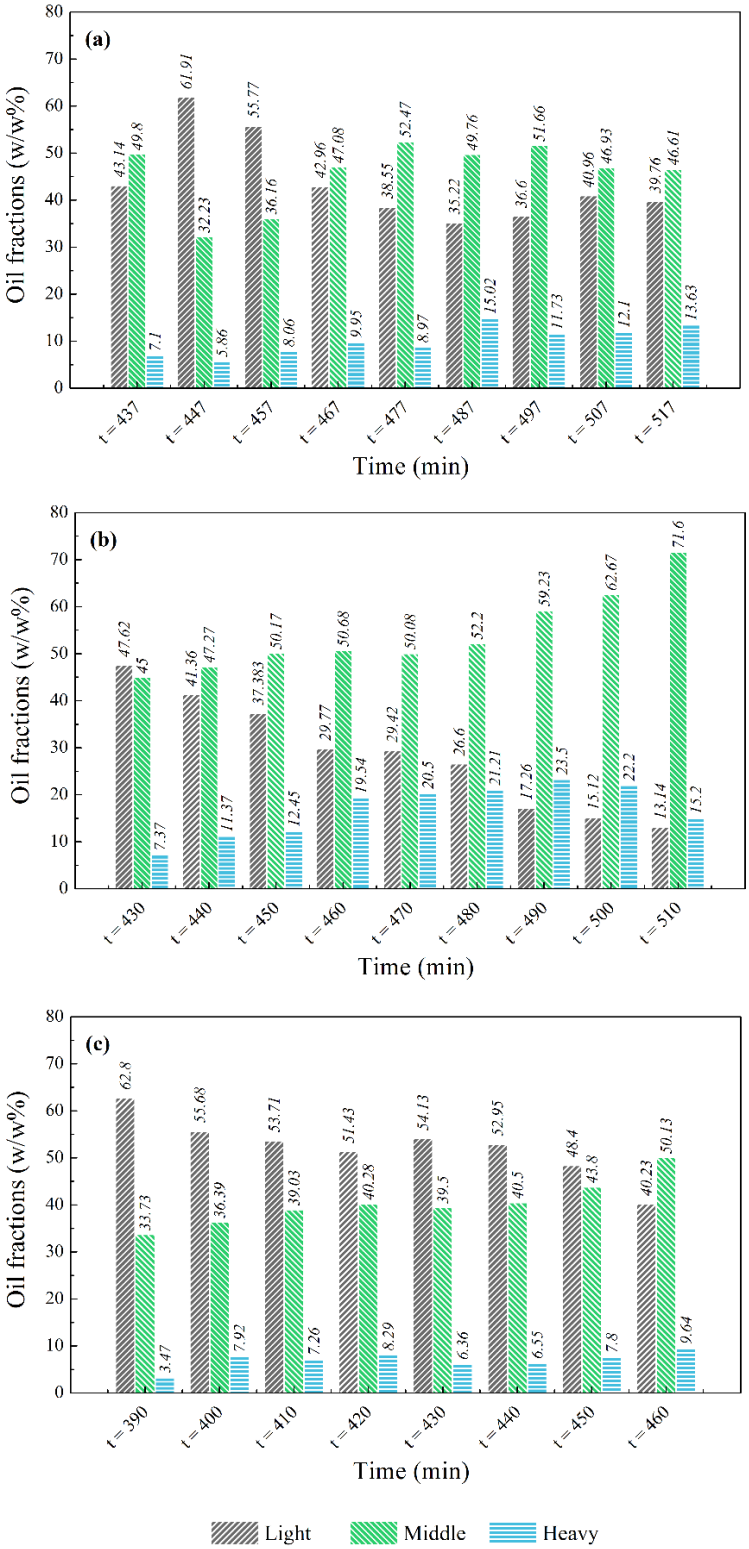

Fig. 5. 6 Fractional distribution of PDOs obtained at different pyrolysis interval for (a) LDPE, (b) HDPE and (c) PP as feed

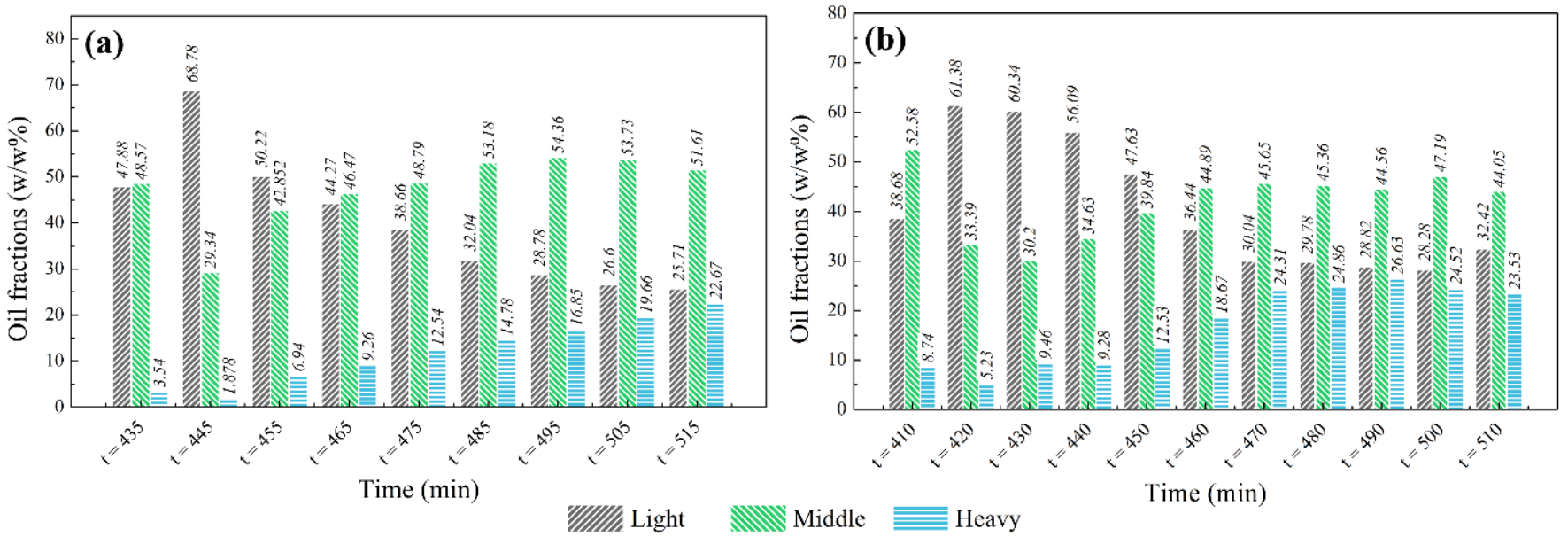

Fig. 5. 7 Fractional distribution of PDOs obtained at different pyrolysis interval for (a) VMIX and (b) RMIX

5.3 Pyrolysis gas analysis

The composition of evolved gases during plastic pyrolysis with temperature rise is a relevant information required for sustainable implementation of the pyrolysis process of plastics. The evolved gases from pyrolysis of plastics (polyolefins) composed of hydrocarbon gases such as methane, ethane, ethylene, propane, propylene, propadiene, acetylene, n-butane, trans-2-butene, 1-butene, isobutylene, cis-2-butene, isopentane, n-pentane, methyl acetylene, including trace amount of inorganic gases like H_2, CO_2 and CO etc. Presence of these hydrocarbon gases in the off gases exhibited their potential use as fuel gas due to their high calorific value [162]. The variation in gas concentration (v/v %) of major gaseous components present in the evolve gases with respect to pyrolysis time is shown in Fig. 5.8 and 5.9, for both the individual plastics (LDPE, HDPE and PP) and mix feeds (VMIX and RMIX) respectively. It was observed from Fig 5.8 and 5.9 that the gas evolution increased as pyrolysis temperature increased and went through a maximum value. The gas evolution certainly decreased as the condensation of long chain hydrocarbons started. Propylene concentration was found to be dominating (maximum around 22 – 25 v/v %) among other hydrocarbon gases in all the feed condition throughout the gas generation period. Other major gases like ethane, propane, butane and ethylene were major in case of LDPE and HDPE as feed [Fig. 5.8(a) and Fig 5.8 (b)], whereas isobutylene and pentane concentrations were higher when PP was in the feed [Fig 5.8 (c)]. Similar evolution pattern was also observed for virgin plastic mix feed (VMIX) (Fig. 5.9) but in case of real world waste mix (RMIX) the methane,

concentration was slightly higher at various stages of the process [Fig 5.9(b)]. The evolution of methane, ethane, ethylene, propane, and n-butane was also reported by Singh and Ruj [106] in the pyrolysis of municipal plastic waste at isothermal condition (450 – 600 °C). Marcilla et al. [104] observed a higher yield of C_3 components (propane and propylene) as compared to other hydrocarbon gases.

The variation of evolved gas composition with the temperature rise and different plastic feed under the slow dynamic condition was observed. This is a piece of valuable information, which can be utilized in the process optimization to enhance the production of certain hydrocarbon gases such as propane, propylene, pentane etc.

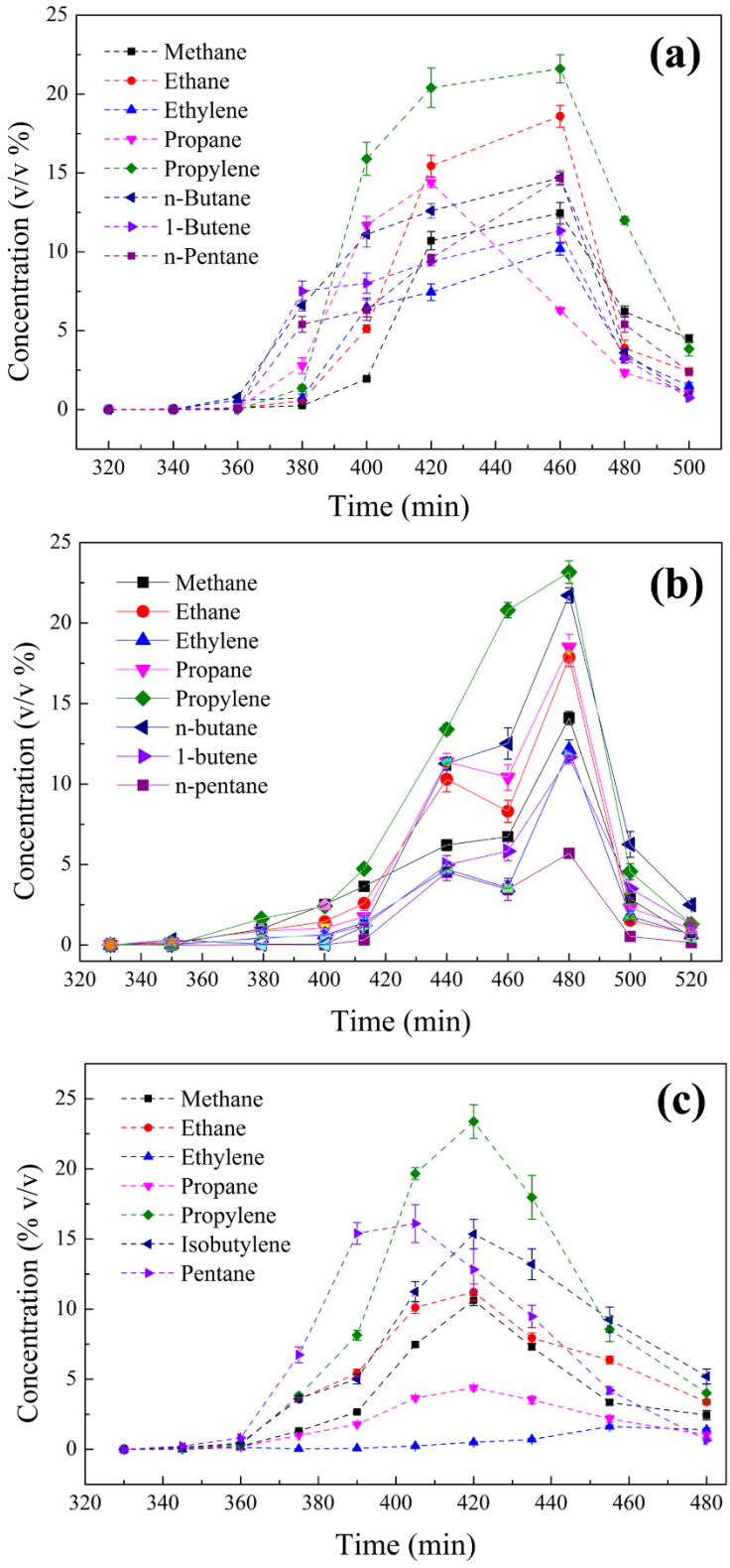

Fig. 5. 8 Distribution of hydrocarbon gases over various interval of slow pyrolysis for (a) LDPE; (b) HDPE and (c) PP

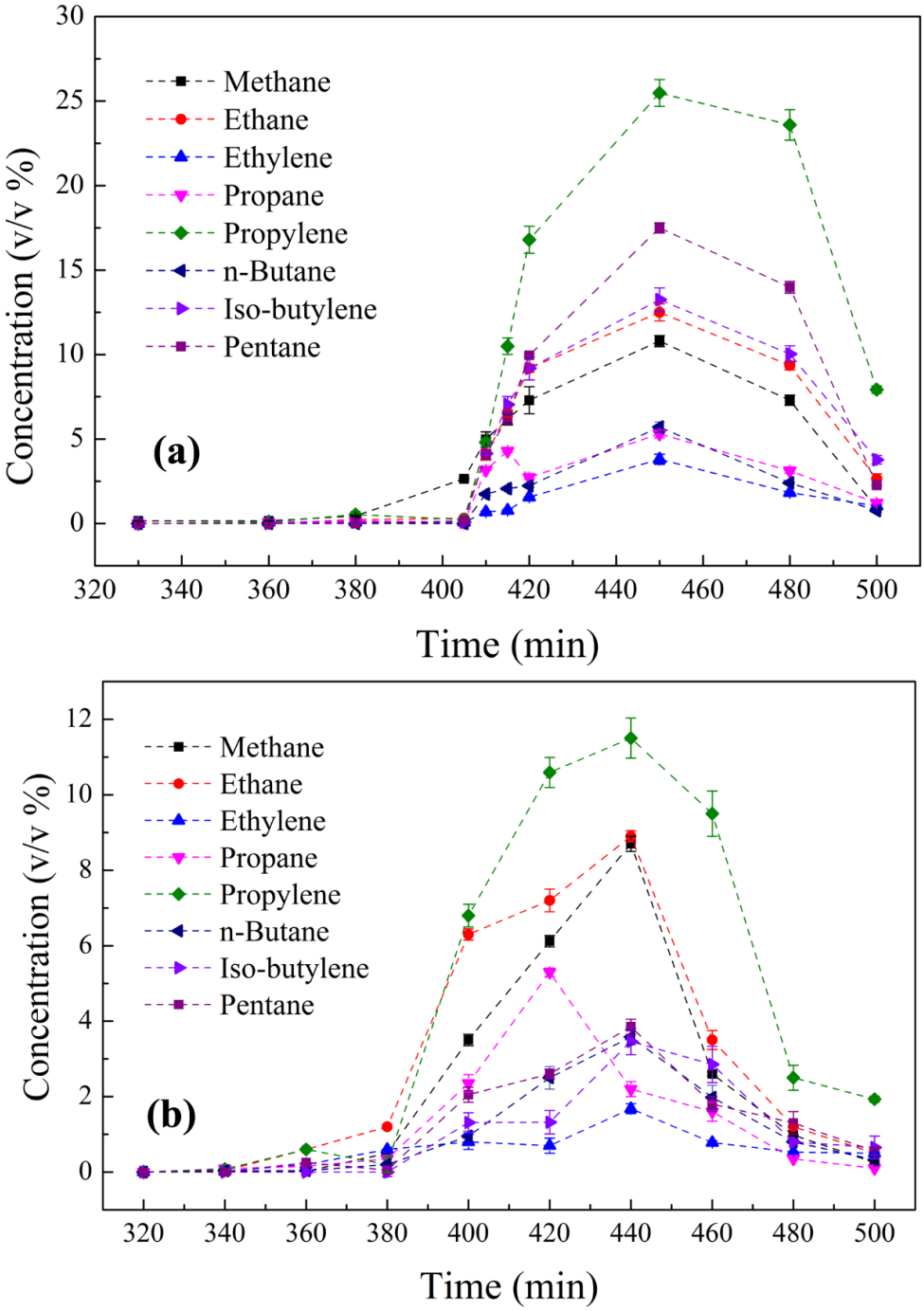

Fig. 5. 9: Distribution of hydrocarbon gases over various interval of slow pyrolysis for (a) VMIX and (b) RMIX

Table 5. 3: Comparison of current study with other works considering slow pyrolysis of packaging plastics

References	Material	Reactor type	Pyrolysis condition	Liquid yield/quality
Williams and Slaney [158]	Simulated plastic mixture with HDPE as major component	Pressurized batch autoclave	β= 5 °C/min; T_f = 500 °C; t_h = 1 h; under N_2 and H_2 gas; P_0 = 0.2 MPa	48.7% (N_2); Paraffin concentration is more
Marcilla, et al. [104]	LDPE; HDPE (virgin powder form)	Batch reactor	β= 5 °C/min; T_f = 550 °C; N_2 flow rate = 150 ml/min;	Paraffin and olefins are major component but %yield of most components pass through a maximum as temperature increases
Onwudili, et al. [105]	LDPE; PS	Pressurised batch autoclave	B = 10 °C/min; T_f = 350 – 500 °C; t_h = 1 h;	At 425 °C; 44 wt% paraffin and 11.6 wt% olefins
Grieco and Baldi [165]	LDPE; beech sawdust; paper	Stainless steel capsule in oven	β= 1 °C/min and 0.1 °C/min	86.2% tar at 1 °C/min and 90.9% tar at 0.1 °C $\cdot$ min^{-1} (from pure LDPE)
Zanella, et al. [166]	PP; coffee	Fixed bed reactor	β= 5 °C/min; T_f = 360 – 480 °C; t_h = 3 h (inert gas: Ar/N_2)	Heavy fraction increases with the increase of temperature
Current study	LDPE; HDPE; PP and their mixture (virgin/real waste)	Semi-batch pyrolysis reactor	β= 1 °C/min; T_f = 400 °C (reactor); t_h = 1 h;	Liquid yield at low temperatures have short chain hydrocarbons with high octane number and RON.

β= heating rate; T_f = final temperature; t_h = isothermal holding time; P_0 = initial pressure and PS = polystyrene

5.4 **Summary**

The ultimate aim to do the non-isothermal slow pyrolysis was to find out the pyrolysis condition, which can enhance the chance of producing a particular value added products such as light (C_6 – C_{11}) and middle distillates (C_{12} – C_{20}) of hydrocarbon liquid fractions as oil and hydrocarbon gases like propane, propylene, butane, pentane etc. Detailed analysis was carried out for the product obtained at different interval of pyrolysis process. The distribution of product in terms of functionality and carbon number range varies with the reaction temperature as the reactor temperature rises from ambient to final temperature. The effect of heating also observed in the gas evolution pattern. Propylene was found in excess amount compared to other hydrocarbon gases. Results obtained ensures the effect of slow pyrolysis in the product distribution. Manipulating the reaction-heating rate and temperature can enhance certain targeted product. However, rigorous experimentation and in depth study is needed for the large-scale application of the process.

Chapter 6

CONCLUSION AND FUTURE WORK

Summary of the dissertation

Future scope

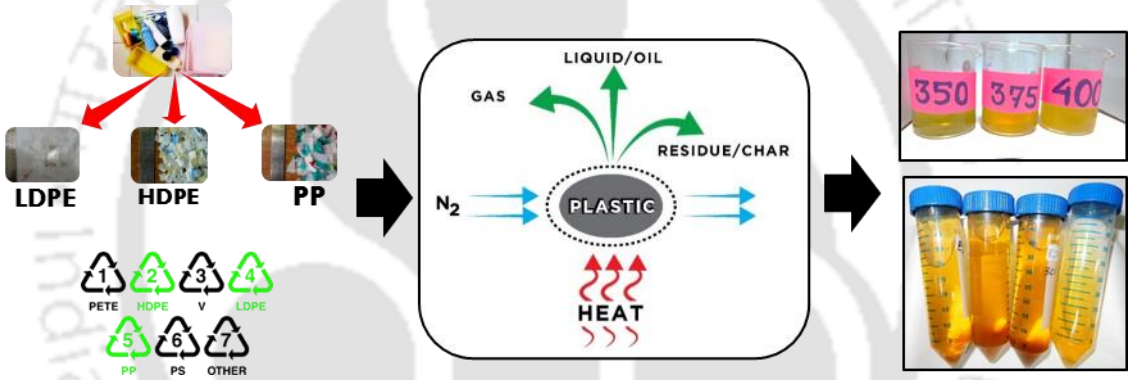

6 Conclusion and future work

This chapter summarises the significant outcomes acquired in the present dissertation and conclude the overall achievement of the study with regard to its relevance to science and technology. In addition to that, a few recommendations for future work has been made for further study and implementations.

6.1 Overall conclusion of the thesis

The application of process engineering to recover energy and resource material from waste and at the same time protecting the environment with maximum capacity is fundamental to sustainable development. Utilizing minimum energy with maximum yield of desired product and lowering the overall carbon footprint is the basic idea of any green technology. This can be achieved by rigorous experimentation and theoretical evaluation of existing process to develop suitable process conditions and design optimization. Utilization of resources at optimum condition is the sole purpose of resource management. Effective waste management should entails business driven techniques that targets recovery of value added products.

In this current study, an elaborate TGA based kinetic study was carried out for the packaging plastics. On the other hand, the recovery of plastic derived oil (PDO) was successfully carried out from the packaging plastic wastes those made up of LDPE, HDPE and PP. The characterisation of oil indicates the similarity of PDOs with conventional fuels such as gasoline and diesel.

The degradation kinetic study was carried out based on the mass loss data recorded from TGA of the plastic samples that was performed under nitrogen atmosphere in both non-isothermal and isothermal conditions. The degradation profiles from non-isothermal TGA, gave the degradation temperatures (onset, peak and end) at different heating rates (5, 10, 15, 20, 30, 40, 50 °C/min). The degradation temperature increases with the heating rates, which is due to time and temperature history subjected to the materials. The shape of the TGA curve also remain consistent with the heating rates. The sole peak of the DTG plot confirmed that the degradation takes place in a single step which is comprise of many series and parallel reactions.

The kinetic study based on TGA data was carried out to investigate the degradation characteristic during pyrolysis and to determine the kinetic parameters. The variable activation energy values of the samples were calculated by using mathematical models derived from Arrhenius kinetic theory using isoconversional principle for multi heating rates data. Out of various models, advance isoconversional method (AIC) was found to be best suited as it integrate the TGA data numerically and optimize the values of activation energy at various stages of the reaction. The distribution of activation energy from AIC method was found in the range of 170 – 232 kJ/mol for LDPE, 143 – 231 kJ/mol for HDPE, 133 – 173 kJ/mol for PP, 99 – 116 kJ/mol for PLA and 99 – 116 kJ/mol for PET-SDB. Values of activation energy for the degradation reactions of the plastics are due to the difference in their molecular structure. The variation of activation energy over the various stages of

the reaction indicates the possible degradation mechanism of the plastic. Low value of activation energy at the initial stages refers to the initiation of degradation reaction at the weaker links of the polymer chain mostly follows side chain scission. In later stages of degradation (high temperature) the random scission and mid-chain scission occurs, which is indicated by higher values of activation energy.

The reaction model *f(α)* was calculated with the help of Criados' masterplot technique, which compares the theoretical masterplots $\left(z(\alpha)/z(0.5)\right)$ of known models with experimental masterplots. The reaction models for LDPE, HDPE, PP, PLA and PET-SDB found to be R2, R2, R3, R2 and F1 respectively. Both R2 and R3 are geometrical contracting models and assume that the rate of degradation starts at the surface and rate is controlled by the interface reaction progress toward the centre. The R2 and R3 models are different from each other based on the particle shape associated during degradation. The R2 and R3 models refer to the degradation of particle by contracting cylinder and sphere respectively. The F1 model is the first order model also known as Mampel first order model, for which the order of the reaction is 1. The variable pre-exponential factor was calculated from the linear relationship between the logarithmic form of pre-exponential values and activation energy applying isoconversional principle for multiple heating rates. It was also found that isothermal degradation data collected at multiple temperatures can be used to calculate variable activation energy for any non-isothermal system. The TG-FTIR analysis was carried out for the five samples to understand the evolved gas pattern and the environmental impact due to harmful emission.

Detailed lab scale pyrolysis was conducted for three types of packaging plastics such as LDPE, HDPE and PP as virgin sample and their mixture, which was collected from household waste (RMIX) with proper plastic identity. Pyrolysis experiments were conducted in the isothermal temperature range between 300 – 400 °C with 8 h of holding time. A liquid oil yield of 82 – 83% was achieved. The liquid product or plastic derived oil (PDO) mostly contains paraffins and olefins. At higher temperature the PDOs get heavier with higher carbon ($>C_{20}$) number hydrocarbon fractions. PDOs obtained at low temperature pyrolysis have superior fuel properties having high calorific value, low viscosity, pour point and flash point. It is evident from the results that low temperature and long duration supports the polymer scission reaction (end chain and random) and leads to the production of lighter fractions of hydrocarbon liquid which have similar characteristic like that of conventional fossil fuels like gasoline and diesel.

The non-isothermal slow pyrolysis of the polyolefins (LDPE, HDPE and PP) provides a detail understanding of the influence of reaction temperature on the product distribution at different stages of the process. NMR analysis of the PDOs obtained from PP has shown encouraging prospects of producing gasoline blend components with a very high RON value (~92). High values of H/C ratio of the PDOs ensures clean burning if use as liquid fuel. PDO samples obtained at low temperatures have higher percentage of lighter fractions (C_6 – C_{11}). However, the yield of both middle (C_{12} – C_{20}) and heavy (C_{21} – C_{FBP}) fractions increases as the reaction proceeds to higher temperature. The evolution of hydrocarbon gas also

varies as process progresses, due to the effect of temperature on gas formation. The overall gas yield ($<C_6$) decreases with the initiation of gas condensation. Major components of hydrocarbon gases were methane, ethane, ethylene, propane, propylene, butane and pentane etc. Propylene concentration was higher compare to the other gases. The gas evolved during pyrolysis will play a significant role in the implementation of the process as most of these gases have high calorific value and can be a fuel source for pyrolyser heating. The solid or residue product is negligible when the virgin sample was considered. A small amount of residue was collected when real plastic waste mixture (RMIX) was in the feed, which can be attributed to the impurities and other inorganic additives present in the waste.

Both isothermal and non-isothermal pyrolysis provided significant input to the slow pyrolysis process of packaging plastic waste to produce liquid fuel. It was evident in the isothermal pyrolysis that the higher pyrolysis temperature yields more liquid product but liquid quality is heavier than that was obtained in the low temperature. On the other hand, the non-isothermal pyrolysis can produce array of hydrocarbon liquid from lighter to heavier in a single run. Therefore, to enhance the yield of a certain fraction of hydrocarbon liquid both non-isothermal and isothermal slow pyrolysis can be utilize simultaneously. The slow pyrolysis parameters can be change with the increase of sample quantity or in the scale up processes. For, industrial purpose the continuous and fast processes are preferred mostly. In such case, high mixing efficiency of the feed sample inside the reactor will facilitate uniform heat distribution and will reduced the time required for the degradation. Therefore, screw

kiln reactors are recommended for slow pyrolysis of packaging plastic waste for continuous processes.

A more in depth research is necessary in terms of large-scale implementation of the slow pyrolysis. The knowledge obtained in this study will provide valuable insights in designing and optimization of pyrolysis process plant to convert packaging plastic waste into valuable fuel utilizing slow heating rate or low temperature (long duration) slow pyrolysis.

6.2 Future work and recommendation

The successful implementation of isoconversional methods to determine kinetic parameters and utilizing low temperature slow pyrolysis to convert plastic waste into value added products unfold new horizon of research in the area waste plastic disposal through thermal means. Following recommendations can be made for the future work:

1. The relationship between the kinetic parameters obtained from non-isothermal TGA and isothermal TGA can be derived with rigorous mathematical, numerical evaluation and a theoretical interpretation of the degradation mechanism can be made.
2. Effect of other pyrolysis conditions such as variation of pressure (high/vacuum pressure), reactor design, presence of catalyst and co-pyrolysis with carbonaceous materials like biomass or coal can be studied in detail.

3. The non-distilled PDOs obtained from the packaging plastic waste by slow pyrolysis can be sent directly for the engine test to investigate its viability of using as locomotive engine oil or motor oil.
4. Detail study of the fuel upgradation (distillation/reforming) of the liquid products obtained by the slow pyrolysis of packaging plastics.
5. Cost optimization of the pyrolysis system considering slow pyrolysis and various reactor size and design is a promising topic for the future research.
6. Pilot plant study can be done to scale up the slow pyrolysis process by using complicated advance reactor system with process intensification to make the technology economically more viable.

References

[1] A. L. Andray, *Plastics and the environment*, John Willey and Sons Publication, 2003, p.

[2] S. Perry, J. Klemeš and I. Bulatov, *Energy*, 33, (2008) 1489.

[3] R. Kothari, V. V. Tyagi and A. Pathak, *Renewable and Sustainable Energy Reviews*, 14, (2010) 3164.

[4] D. Hoornweg and P. Bhada-Tata, in U.d. series (Ed.), *What a Waste : A Global Review of Solid Waste Management*, World bank, Washington DC, 2012.

[5] in, TERI Press, New Delhi, 2010, p. 333.

[6] J. S. Kamyotra and D. Sinha, in, Central Pollution Control Board, Delhi, 2016, p. 20.

[7] D. Lazarevic, E. Aoustin, N. Buclet and N. Brandt, *Resources, Conservation and Recycling*, 55, (2010) 246.

[8] J. R. Jambeck, R. Geyer, C. Wilcox, T. R. Siegler, M. Perryman, A. Andrady, R. Narayan and K. L. Law, *Science*, 347, (2015) 768.

[9] K. A. Kalyani and K. K. Pandey, *Renewable and Sustainable Energy Reviews*, 31, (2014) 113.

[10] R. C. Mebane, T. R. Rybolt and A. Matsick, *Plastics and Polymers*, Twenty-First Century Books, 1995, p.

[11] R. Geyer, J. R. Jambeck and K. L. Law, *Science Advances*, 3, (2017).

[12] A. Buekens, in, John Wiley & Sons, Ltd, 2006, p. 1.

[13] L. C. M. Lebreton, J. van der Zwet, J.-W. Damsteeg, B. Slat, A. Andrady and J. Reisser, *Nature Communications*, 8, (2017) 15611.

[14] R. Joshi and S. Ahmed, *Cogent Environmental Science*, 2, (2016).

[15] S. M. Al-Salem, P. Lettieri and J. Baeyens, *Waste Manag*, 29, (2009) 2625.

[16] D. S. Achilias, C. Roupakias, P. Megalokonomos, A. A. Lappas and E. V. Antonakou, *Journal of Hazardous materials*, 149, (2007) 536.

[17] E. Yildirir, J. A. Onwudili and P. T. Williams, *The Journal of Supercritical Fluids*, 92, (2014) 107.

[18] C. Zhou, W. Fang, W. Xu, A. Cao and R. Wang, *Journal of Cleaner Production*, (2014).

[19] W. Kaminsky, B. Schlesselmann and C. Simon, *Journal of Analytical and Applied Pyrolysis*, 32, (1995) 19.

[20] A. Adrados, I. de Marco, B. M. Caballero, A. Lopez, M. F. Laresgoiti and A. Torres, *Waste Manag*, 32, (2012) 826.

[21] M. Lackner, Á. Palotás and F. Winter, *Combustion: from basics to applications*, John Wiley & Sons, 2013, p.

[22] S.-C. Oh, D.-G. Lee, H. Kwak and S.-Y. Bae, *Environmental Engineering Research*, 11, (2006) 250.

[23] S. D. Anuar Sharuddin, F. Abnisa, W. M. A. Wan Daud and M. K. Aroua, *Energy Conversion and Management*, 115, (2016) 308.

[24] A. K. Panda, R. K. Singh and D. K. Mishra, *Renewable and Sustainable Energy Reviews*, 14, (2010) 233.

[25] M. He, B. Xiao, Z. Hu, S. Liu, X. Guo and S. Luo, *International Journal of Hydrogen Energy*, 34, (2009) 1342.

[26] J. A. Conesa, R. Font, A. Marcilla and A. N. Garcia, *Energy & Fuels*, 8, (1994) 1238.

[27] F. Xu, B. Wang, D. Yang, J. Hao, Y. Qiao and Y. Tian, *Energy Conversion and Management*, 171, (2018) 1106.

[28] V. Sinha, M. R. Patel and J. V. Patel, *Journal of Polymers and the Environment*, 18, (2010) 8.

[29] Z. Zhibo, S. Nishio, Y. Morioka, A. Ueno, H. Ohkita, Y. Tochihara, T. Mizushima and N. Kakuta, *Catalysis Today*, 29, (1996) 303.

[30] S. F. Sodero, F. Berruti and L. A. Behie, *Chemical Engineering Science*, 51, (1996) 2805.

[31] A. Demirbas, *Journal of Analytical and Applied Pyrolysis*, 72, (2004) 97.

[32] J. Scheirs and W. Kaminsky, *Feedstock recycling and pyrolysis of waste plastics: converting waste plastics into diesel and other fuels*, J. Wiley & Sons, 2006, p.

[33] A. López, I. de Marco, B. M. Caballero, M. F. Laresgoiti and A. Adrados, *Chemical Engineering Journal*, 173, (2011) 62.

[34] S. Kumar, S. R. Smith, G. Fowler, C. Velis, S. J. Kumar, S. Arya, Rena, R. Kumar and C. Cheeseman, *Royal Society Open Science*, 4, (2017).

[35] E. A. Williams and P. T. Williams, *Journal of Analytical and Applied Pyrolysis*, 40 - 41, (1997) 347.

[36] R. Moliner, M. Lazaro and I. Suelves, *Energy & Fuels*, 11, (1997) 1165.

[37] J. D. Nixon, P. K. Dey and S. K. Ghosh, *Sustainable Energy Technologies and Assessments*, 21, (2017) 23.

[38] J. Thorneycroft, J. Orr, P. Savoikar and R. J. Ball, *Construction and Building Materials*, 161, (2018) 63.

[39] E. A. Williams and P. T. Williams, *Journal of Chemical Technology and Biotechnology*, 70, (1997) 9.

[40] P. N. Sharratt, Y. H. Lin, A. A. Garforth and J. Dwyer, *Industrial & Engineering Chemistry Research*, 36, (1997) 5118.

[41] W. Kaminsky, M. Predel and A. Sadiki, *Polymer Degradation and Stability*, 85, (2004) 1045.

[42] A. Lopez-Urionabarrenechea, I. de Marco, B. M. Caballero, M. F. Laresgoiti and A. Adrados, *Journal of Analytical and Applied Pyrolysis*, 96, (2012) 54.

[43] J. Aguado, D. Serrano, J. Escola and E. Garagorri, *Catalysis Today*, 75, (2002) 257.

[44] A. Demirbas, *Applied Energy*, 88, (2011) 17.

[45] D. Vamvuka, *International Journal of Energy Research*, 35, (2011) 835.

[46] P. C. F. Pinto, I. Gulyurtlu, I. Cabrita, *Journal of Analytical and Applied Pyrolysis*, 51, (1999) 39.

[47] A. De Stefanis, P. Cafarelli, F. Gallese, E. Borsella, A. Nana and G. Perez, *Journal of Analytical and Applied Pyrolysis*, (2013).

[48] M. Brebu, T. Bhaskar, K. Murai, A. Muto, Y. Sakata and M. A. Uddin, *Polymer Degradation and Stability*, 87, (2005) 225.

[49] A. G. George Manos, and John Dwyer, *Industrial & Engineering Chemistry Research*, 39, (2000) 1198.

[50] P. T. W. Ranbir Bagri, *Journal of Analytical and Applied Pyrolysis*, 63, (2002) 29.

[51] A. López, I. de Marco, B. M. Caballero, M. F. Laresgoiti, A. Adrados and A. Aranzabal, *Applied Catalysis B: Environmental*, 104, (2011) 211.

[52] A. De Stefanis, P. Cafarelli, F. Gallese, E. Borsella, A. Nana and G. Perez, *Journal of Analytical and Applied Pyrolysis*, 104, (2013) 479.

[53] P. T. Williams and E. A. Williams, *Journal of Analytical and Applied Pyrolysis*, 51, (1999) 107.

[54] P. T. W. Elizabeth A. Williams, *Journal of Analytical and Applied Pyrolysis*, 40 - 41, (1997) 347.

[55] A. Undri, S. Meini, L. Rosi, M. Frediani and P. Frediani, *Journal of Analytical and Applied Pyrolysis*, 103, (2013) 149.

[56] H. Cheng and Y. Hu, *Bioresource Technology*, 101, (2010) 3816.

[57] D. P. Serrano, J. Aguado, J. M. Escola and E. Garagorri, *Applied Catalysis B: Environmental*, 44, (2003) 95.

[58] J. Aguado, D. P. Serrano, J. M. Escola and E. Garagorri, *Catalysis Today*, 75, (2002) 257.

[59] M. Uchimiya, I. M. Lima, K. T. Klasson and L. H. Wartelle, *Chemosphere*, 80, (2010) 935.

[60] D. Mikociak, A. Magiera, G. Labojko and S. Blazewicz, *Journal of Analytical and Applied Pyrolysis*, 107, (2014) 191.

[61] C. H. Wu, C. Y. Chang, J. L. Hor, S. M. Shin, L. W. Chen and F. W. Chang, *Waste Management*, 13, (1993) 221.

[62] Y. B. Yang, A. N. Phan, C. Ryu, V. Sharifi and J. Swithenbank, *Fuel*, 86, (2007) 169.

[63] S. Zhou, B. Pecha, M. van Kuppevelt, A. G. McDonald and M. Garcia-Perez, *Biomass and Bioenergy*, 66, (2014) 398.

[64] O. Onay and O. M. Kockar, *Renewable Energy*, 28, (2003) 2417.

[65] U. Hujuri, A. K. Ghoshal and S. Gumma, *Polymer Degradation and Stability*, 93, (2008) 1832.

[66] M. Erceg, T. Kovačić and I. Klarić, *Polymer Degradation and Stability*, 90, (2005) 86.

[67] V. B. Carmona, A. de Campos, J. Marconcini and L. H. C. Mattoso, *Journal of Thermal Analysis and Calorimetry*, 115, (2013) 153.

[68] J. W. Bujak, *Energy*, 90, (2015) 1468.

[69] M. E. Brown, M. Maciejewski, S. Vyazovkin, R. Nomen, J. Sempere, A. K. Burnham, J. Opfermann, R. Strey, H. L. Anderson, A. Kemmler, R. Keuleers, J. Janssens, H. O. Desseyn, C. Li, T. B. Tang, B. Roduit, J. Malek and T. Mitsuhashi, *Thermochimica Acta*, 355, (2000) 125.

[70] A. K. Burnham, *Thermochimica Acta*, 355, (2000) 165.

[71] M. Maciejewski, *Thermochimica Acta*, 355, (2000) 145.

[72] S. Vyazovkin, *Thermochimica Acta*, 355, (2000) 155.

[73] S. Vyazovkin, A. K. Burnham, J. M. Criado, L. A. Pérez-Maqueda, C. Popescud and N. Sbirrazzuolie, *Thermochimica Acta*, 520, (2011) 1.

[74] S. Vyazovkin, *Thermochimica Acta*, 397, (2003) 269.

[75] H. L. Friedman, *Journal of Polymer Science: Part C*, 6, (1964) 183.

[76] J. H. Flynn and L. A. Wall, *Journal of Research of the National Bureau of Standards-A. Physics and Chemistry*, 70A, (1966) 487.

[77] T. Ozawa, *Bulletin of the Chemical Society of Japan*, 38, (1965) 1881.

[78] T. Akahira and T. Sunose, *Research Report China Institute of Technology (Science Technology)*, 16, (1971) 22.

[79] M. J. Starink, *Thermochimica Acta*, 404, (2003) 163.

[80] B. Janković, L. Kolar-Anić, I. Smičiklas, S. Dimović and D. Aranđelović, *Thermochimica Acta*, 495, (2009) 129.

[81] R. Valapa, G. Pugazhenthi and V. Katiyar, *International Journal of Biological Macromolecules*, 65, (2014) 275.

[82] S. Vyazovkin and C. A. Wight, *Analytical Chemistry*, 72, (2000) 3171.

[83] J. D. Peterson, S. Vyazovkin and C. A. Wight, *Macromolecular Chemistry and Physics*, 202, (2001) 775.

[84] S. Vyazovkin and N. Sbirrazzuoli, *Macromolecular Rapid Communications*, 27, (2006) 1515.

[85] B. Saha and A. K. Ghoshal, *Thermochimica Acta*, 451, (2006) 27.

[86] S. Khedri and S. Elyasi, *Polymer Degradation and Stability*, 129, (2016) 306.

[87] B. Saha and A. K. Ghoshal, *Thermochimica Acta*, 460, (2007) 77.

[88] C. He, Y. Wang, Y. Luo, L. Kong and Z. Peng, *Journal of polymer engineering* 33, (2013) 331.

[89] G. Mishra and T. Bhaskar, *Bioresource Technology*, 169, (2014) 614.

[90] L. N. Samuelsson, M. U. Babler and R. Moriana, *Fuel*, 161, (2015) 59.

[91] A. A. Jain, A. Mehraa and V. V. Ranade, *Fuel*, 165, (2016) 490.

[92] L. N. Samuelsson, R. Moriana, M. U. Babler, M. Ek and K. Engvall, *Fuel*, 143, (2015) 438.

[93] A. Zotti, A. Borriello, M. Ricciardi, V. Antonucci, M. Giordano and M. Zarrelli, *Composites Part B: Engineering*, 73, (2015) 139.

[94] P. Rajeshwari and T. K. Dey, *Journal of Thermal Analysis and Calorimetry*, 125, (2016) 369.

[95] P. T. Williams and E. A. Williams, *Energy and Fuels*, 13, (1999) 188.

[96] B. K. Sharma, B. R. Moser, K. E. Vermillion, K. M. Doll and N. Rajagopalan, *Fuel Processing Technology*, 122, (2014) 79.

[97] F. Pinto, P. Costa, I. Gulyurtlu and I. Cabrita, *Journal of Analytical and Applied Pyrolysis*, 51, (1999) 39.

[98] M. N. Siddiqui and H. H. Redhwi, *Fuel Processing Technology*, 90, (2009) 545.

[99] V. Goodship, *Introduction to Plastics Recycling*, Smithers Rapra, 2007, p.

[100] L. Ballice, M. Yüksel, M. Sağlam, R. Reimert and H. Schulz, *Energy & Fuels*, 12, (1998) 925.

[101] P. K. Ramdoss and A. R. Tarrer, *Fuel*, 77, (1998) 293.

[102] N. Shah, J. Rockwell and G. P. Huffman, *Energy & Fuels*, 13, (1999) 832.

[103] H. Wong and L. J. Broadbelt, *Industrial Engineerin Chemistry Research*, 40, (2001) 4716.

[104] A. Marcilla, M. I. Beltrán and R. Navarro, *Journal of Analytical and Applied Pyrolysis*, 86, (2009) 14.

[105] J. A. Onwudili, N. Insura and P. T. Williams, *Journal of Analytical and Applied Pyrolysis*, 86, (2009) 293.

[106] R. K. Singh and B. Ruj, *Fuel*, 174, (2016) 164.

[107] J. A. Brydson, *Plastics Materials*, Butterworth-Heinemann, 2013, p.

[108] A. Aboulkas, K. El harfi and A. El Bouadili, *Energy Conversion and Management*, 51, (2010) 1363.

[109] S. Vyazovkin and C. A. Wight, *Annual Reveiws Physics Chemistry*, 48, (1997) 125.

[110] J. Fahrenfort, *Spectrochimica Acta*, 17, (1961) 698.

[111] S. Vyazovkin, A. K. Burnham, J. M. Criado, L. A. Pérez-Maqueda, C. Popescu and N. Sbirrazzuoli, *Thermochimica Acta*, 520, (2011) 1.

[112] R. Atkinson, *Chemical Reviews*, 85, (1986) 69.

[113] S. M. Lomakin, S. Z. Rogovina, A. V. Grachev, E. V. Prut and C. V. Alexanyan, *Thermochimica Acta*, 521, (2011) 66.

[114] C. D. Doyle, *Journal of Applied Polymer Science*, 6, (1962) 639.

[115] M. H. Levitt, *Spin Dynamics: Basics of Nuclear Magnetic Resonance*, Wiley, 2001, p.

[116] S. Vyazovkin and C. A. Wight, *International Reviews in Physical Chemistry*, 17, (1998) 407.

[117] J. M. Criado, *Thermochimica Acta*, 24, (1978) 186.

[118] F. H. Constable, *Proceedings of Royal Society of London*, 108, (1923) 355.

[119] D. J. T. Hill, L. Dong, J. H. O'Donnell, G. George and P. Pomery, *Polymer Degradation and Stability*, 40, (1993) 143.

[120] J. R. MacCallum, *Comprehensive polymer science*, Pergamon, Oxford 1989, p.

[121] M. E. Myers, J. Stollstelmer and A. M. Wims, *Analytical Chemistry*, 47, (1975) 2010.

[122] M. E. Myers, J. Stollstelmer and A. M. Wims, *Analytical Chemistry*, 47, (1975) 2301.

[123] H. S. Joo and J. A. Guin, *Fuel Processing Technology*, 57, (1998) 25.

[124] A. Sinag, M. Sungur, M. Gullu and M. Canel, *Energy & Fuels*, 20, (2006) 2093.

[125] T. A. Albahri, *Industrial Engineering Chemistry Research*, 42, (2003) 657.

[126] N. Pasadakis, V. Gaganis and C. Foteinopoulos, *Fuel Processing Technology*, 87, (2006) 505.

[127] J. G. Speight, *Handbook of Petroleum Product Analysis*, Wiley, 2015, p.

[128] L. Turnbull, J. J. Liggat and W. A. MacDonald, *Polymer Degradation and Stability*, 98, (2013) 2244.

[129] T. Ozawa, *Journal of thermal analysis*, 2, (1970) 301.

[130] A. C. K. Chowlu, P. K. Reddy and A. K. Ghoshal, *Thermochimica Acta*, 485, (2009) 20.

[131] İ. Kayacan and Ö. M. Doğan, *Energy Sources, Part A: Recovery, Utilization, and Environmental Effects*, 30, (2008) 385.

[132] J. H. Chan and S. T. Balke, *Polymer Degradation and Stability*, 57, (1997) 135.

[133] B. Saha, A. K. Maiti and A. K. Ghoshal, *Thermochimica Acta*, 444, (2006) 46.

[134] I. C. McNeill and H. A. Leiper, *Polymer Degradation and Stability*, 11, (1985) 309.

[135] I. C. McNeill and H. A. Leiper, *Polymer Degradation and Stability*, 11, (1985) 267.

[136] B. Saha and A. Ghoshal, *Chemical Engineering Journal*, 111, (2005) 39.

[137] A. Khawam and D. R. Flanagan, *J. Phys. Chem. B*, 110, (2006) 17315.

[138] O. Gutiérrez and H. Palza, *Polymer Degradation and Stability*, 120, (2015) 122.

[139] J. Yang, R. Miranda and C. Roy, *Polymer Degradation and Stability*, 73, (2001) 455.

[140] H. Zou, C. Yi, L. Wang, H. Liu and W. Xu, *Journal of Thermal Analysis and Calorimetry*, 97, (2009) 929.

[141] J. Li, W. Zheng, L. Li, Y. Zheng and X. Lou, *Thermochimica Acta*, 493, (2009) 90.

[142] W. Gang and L. Aimin, *Chinese Journal of Chemical Engineering*, 16, (2008) 929.

[143] B. J. Holland and J. N. Hay, *Polymer*, 43, (2002) 1835.

[144] P. Das and P. Tiwari, *Thermochimica Acta*, 654, (2017) 191.

[145] Y. R. Luo, *Handbook of bond dissociation energies in organic compounds*, CRC Press, 2002, p.

[146] R. Simha, L. A. Wall and J. Bram, *The Journal of Chemical Physics*, 29, (1958) 894.

[147] H. H. Mooiweer, K. P. de Jong, B. Kraushaar-Czarnetzki, W. H. J. Stork and B. C. H. Krutzen, in J. Weitkamp, H.G. Karge, H. Pfeifer and W. Hölderich (Eds.), *Studies in Surface Science and Catalysis*, Elsevier, 1994, p. 2327.

[148] N. Rankovic, G. Bourhis, M. Loos and R. Dauphin, *Fuel*, 150, (2015) 41.

[149] A. C. D.-o. P. Products and Lubricants, *Manual on Hydrocarbon Analysis*, American Society for Testing and Materials, 1963, p.

[150] B. Kunwar, H. N. Cheng, S. R. Chandrashekaran and B. K. Sharma, *Renewable and Sustainable Energy Reviews*, 54, (2016) 421.

[151] W. M. Sweeney, in, Google Patents, 1970.

[152] S. K. Guttikunda and D. Mohan, *Energy Policy*, 68, (2014) 556.

[153] R. C. Lance, A. J. Barnard and J. E. Hooyman, *Journal of Hazardous materials*, 3, (1979) 107.

[154] S. C. Moldoveanu, *Analytical pyrolysis of synthetic organic polymers*, Elsevier, 2005, p.

[155] S. E. Levine and L. J. Broadbelt, *Polymer Degradation and Stability*, 94, (2009) 810.

[156] R. Aguado, M. Olazar, B. Gaisan, R. Prieto and J. Bilbao, *Industrial Enfineerin Chemistry Research*, 41, (2002) 4559.

[157] C. Ludlow-Palafox and H. A. Chase, *Industrial Enfineerin Chemistry Research*, 40, (2001) 4749.

[158] P. T. Williams and E. Slaney, *Resources, Conservation and Recycling*, 51, (2007) 754.

[159] J. F. Mastral, C. Berrueco and J. Ceamanos, *Energy & Fuels*, 20, (2006) 1365.

[160] R. Aguado, M. Olazar, M. J. San José, B. Gaisán and J. Bilbao, *Energy & Fuels*, 16, (2002) 1429.

[161] L. Zhao, Z. H. Wang, D. Z. Chen, X. B. Ma and J. Luan, *Huan Jing Ke Xue*, 33, (2012) 329.

[162] P. Das and P. Tiwari, *Resources, Conservation and Recycling*, 128, (2018) 69.

[163] L. A. Wall, S. L. Madorsky, D. W. Brown, S. Straus and R. Simha, *Journal of the American Chemical Society*, 76, (1954) 3430.

[164] B. Singh and N. Sharma, *Polymer Degradation and Stability*, 93, (2008) 561.

[165] E. M. Grieco and G. Baldi, *Waste Manag*, 32, (2012) 833.

[166] E. Zanella, M. Della Zassa, L. Navarini and P. Canu, *Energy & Fuels*, 27, (2013) 1357.

Appendix

Appendix A

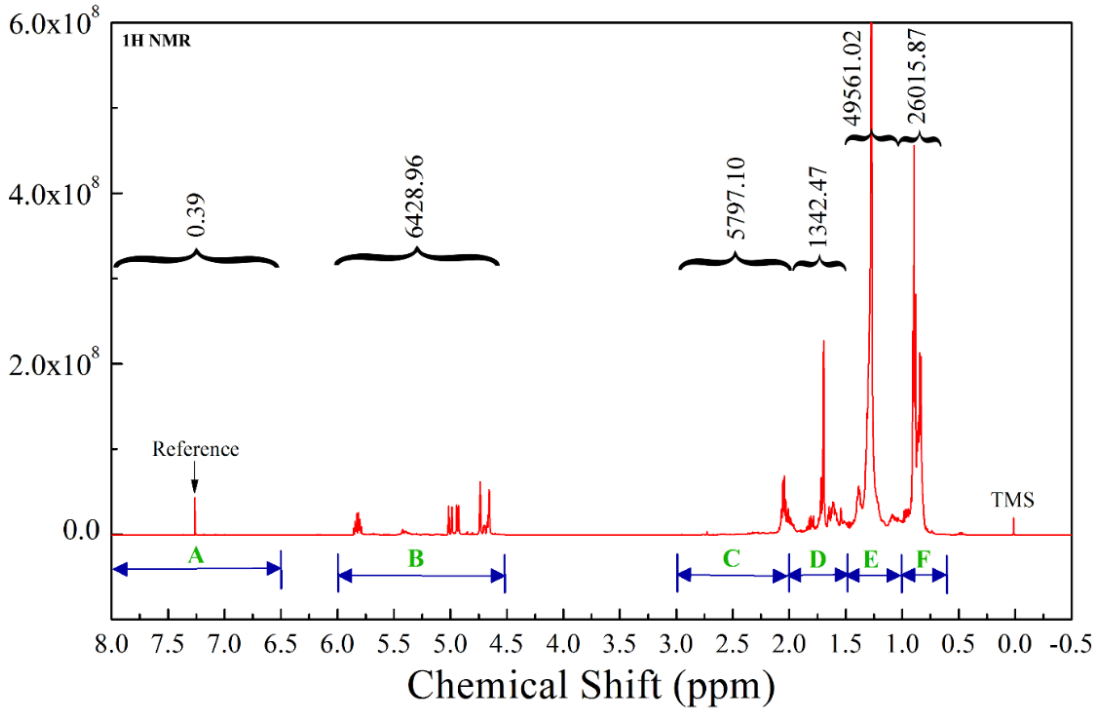

Fig. A. 1: ^{1}H NMR spectra with different spectral region (A – F) and the integrated area under the curves (for PDO obtained at 400 °C from LDPE)

Fig. A.1 is the proton NMR spectra of PDO obtained at 400 °C for LDPE (virgin) pyrolysis. The spectral regions (A, B, C, D, E and F etc.) are measured in terms of the integral area under the peaks. Similar calculations were carried out for other PDOs mentioned in Chapter 3 and Chapter 4.

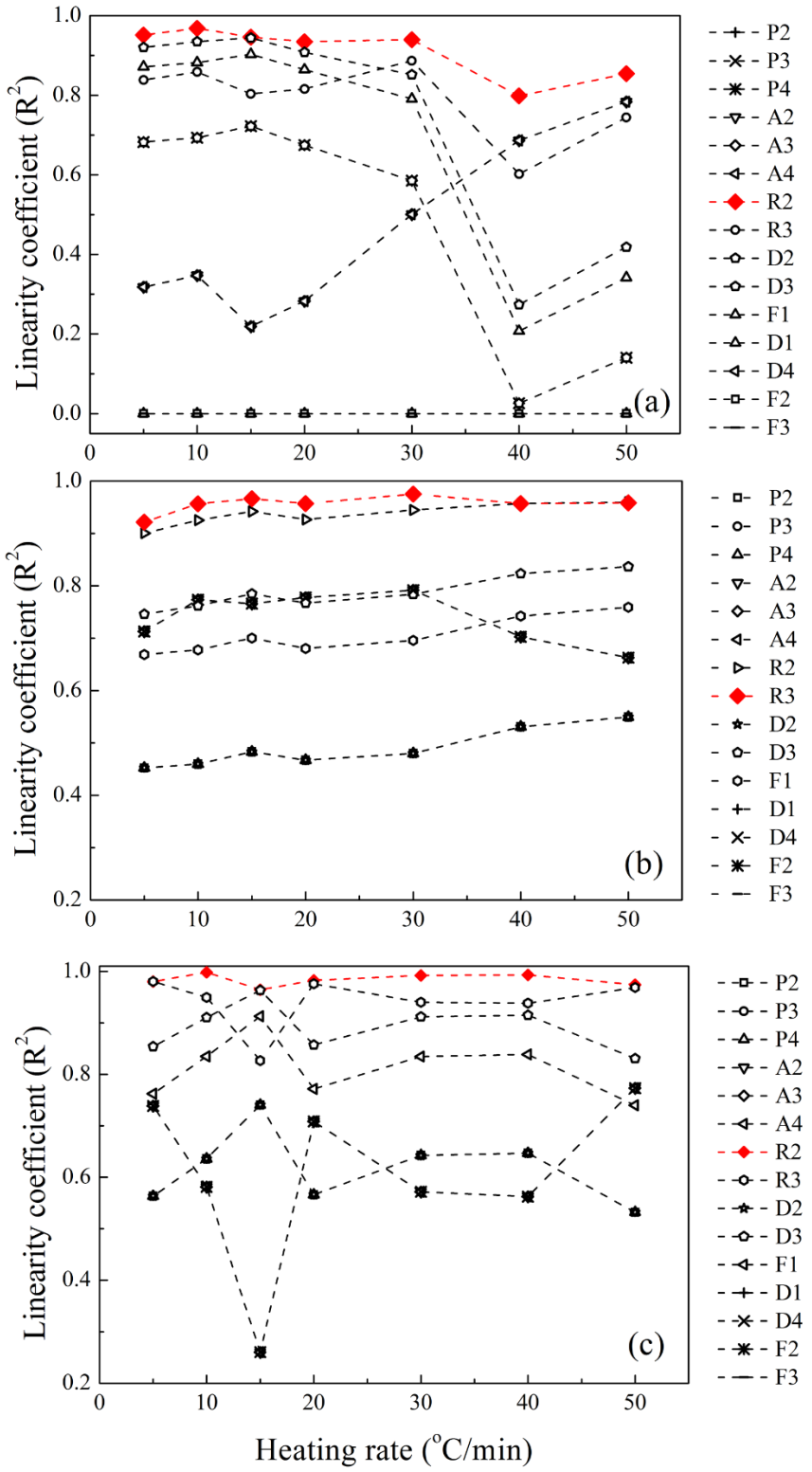

Fig. A. 2: Linearity coefficient (R^2) between the theoretical and experimental masterplots obtained by Criados' masterplots technique for the determination of the reaction model $f(\alpha)$ for the materials (a) HDPE, (b) PP and (c) PLA

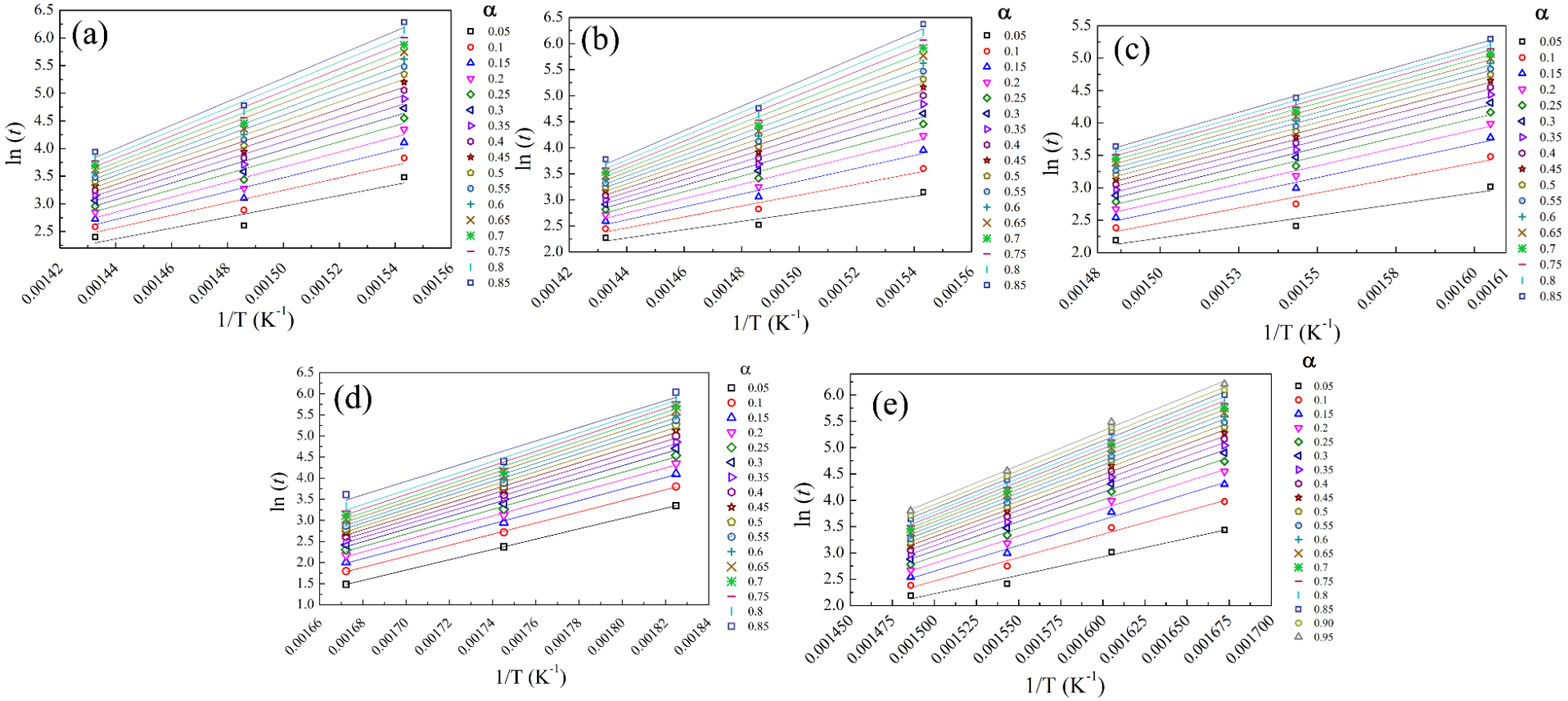

Fig. A. 3: Plots of ln(t) vs 1/T of isothermal TGA analysis of (a)LDPE, (b) HDPE, (c) PP, (d) PLA and (e)PET-SDB

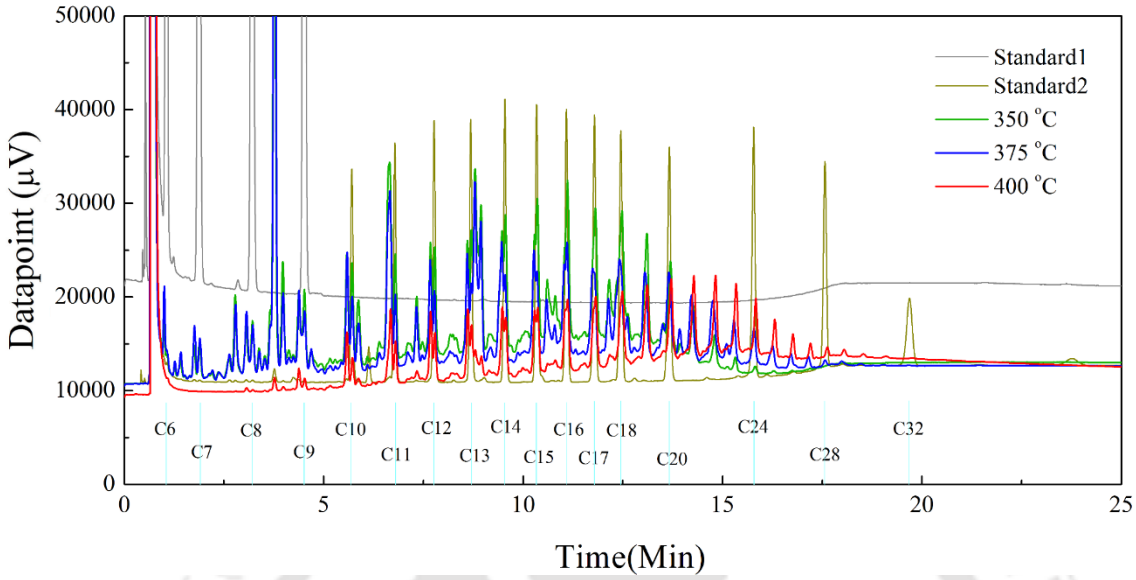

Fig. A. 4: SimDist GC spectra of paraffin standard 1 (C_6-C_9) and standard 2 (C_{10}-C_{32}) and three PDO obtained at three temperatures from the pyrolysis of RMIX sample

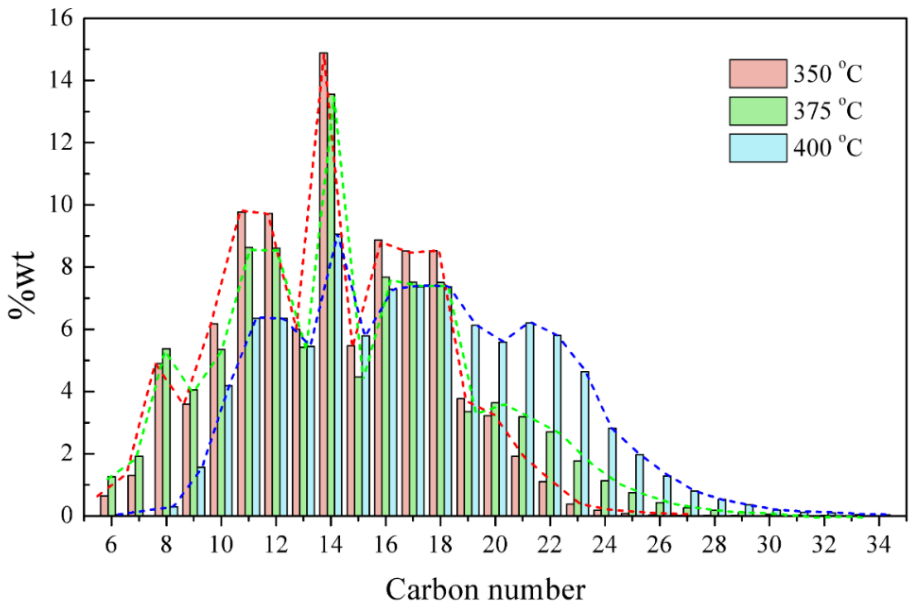

Fig. A. 5: Carbon number distribution acquired from SimDist analysis of PDO samples obtained at three-pyrolysis temperature from pyrolysis of RMIX sample

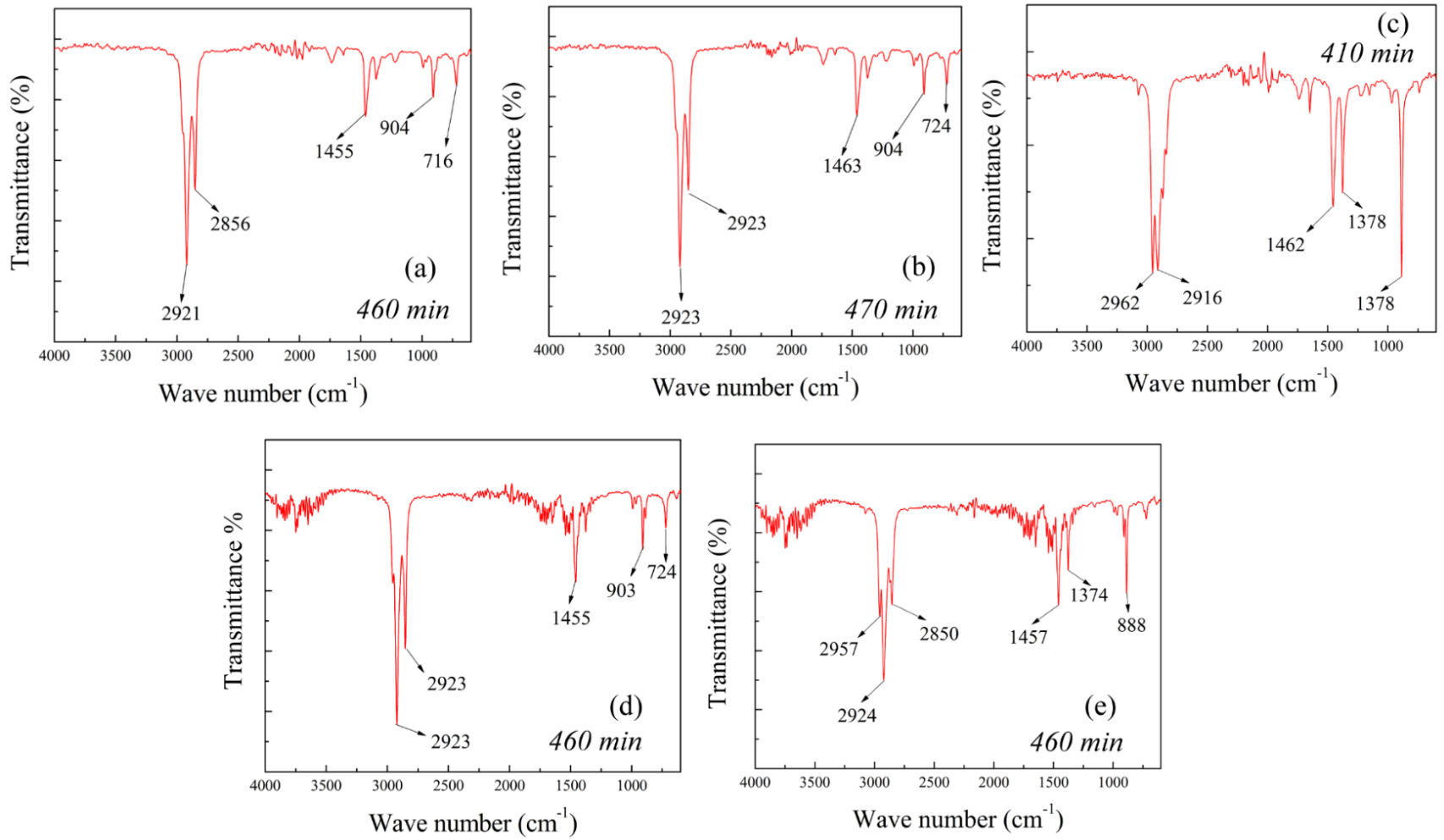

Fig. A. 6: FTIR-ATR spectra with notable peaks (wave number) of (a) LDPE, (b) HDPE, (c) PP and (e) VMIX and (d) RMIX

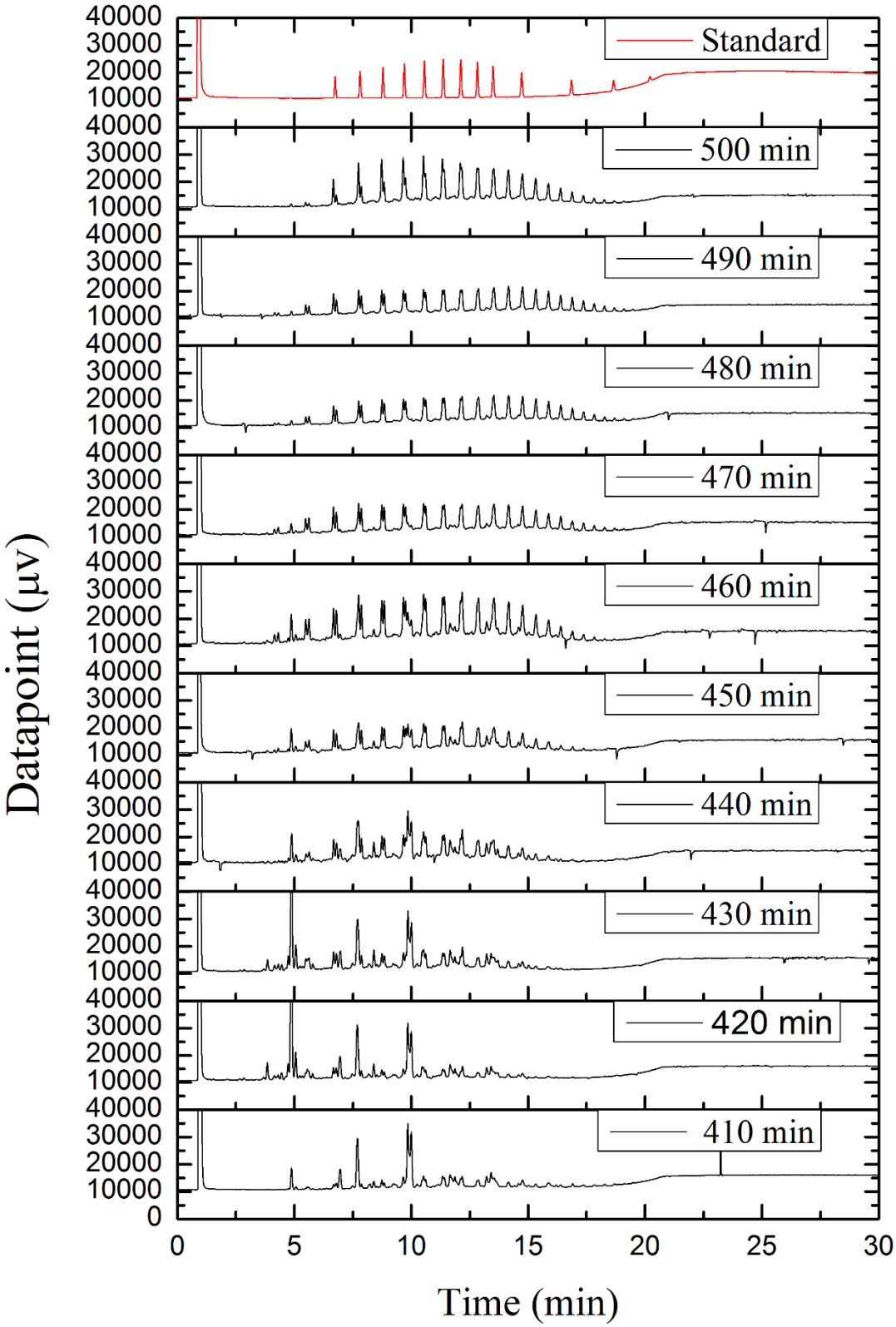

Fig. A. 7: GC (SimDist) spectra of PDOs obtained at different intervals of non-isothermal slow pyrolysis of RMIX sample (-) and standard paraffin sample (-)

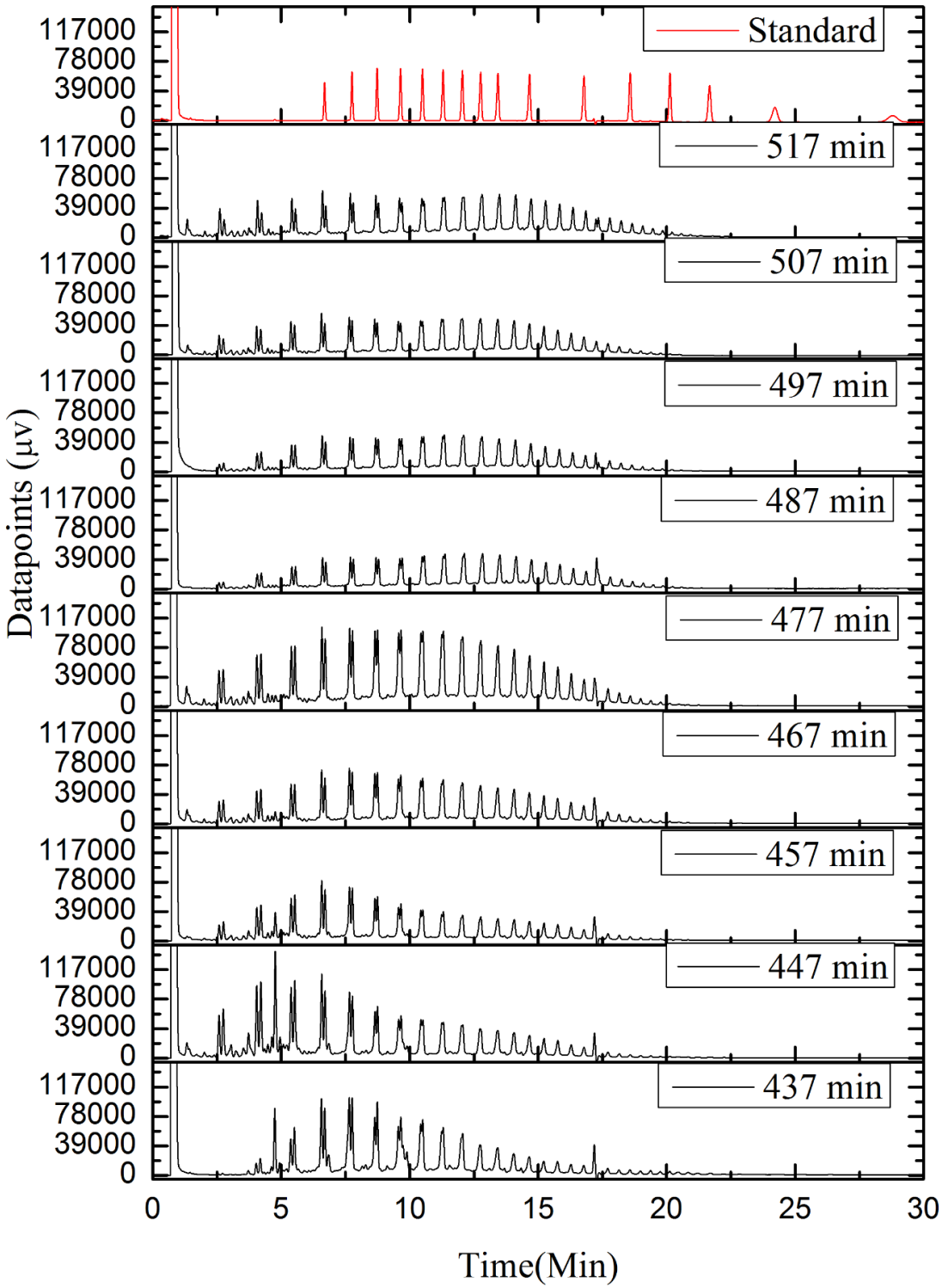

Fig. A. 8: GC (SimDist) spectra of PDOs obtained at different intervals of non-isothermal slow pyrolysis of virgin LDPE plastics (-) and standard paraffin sample (-)

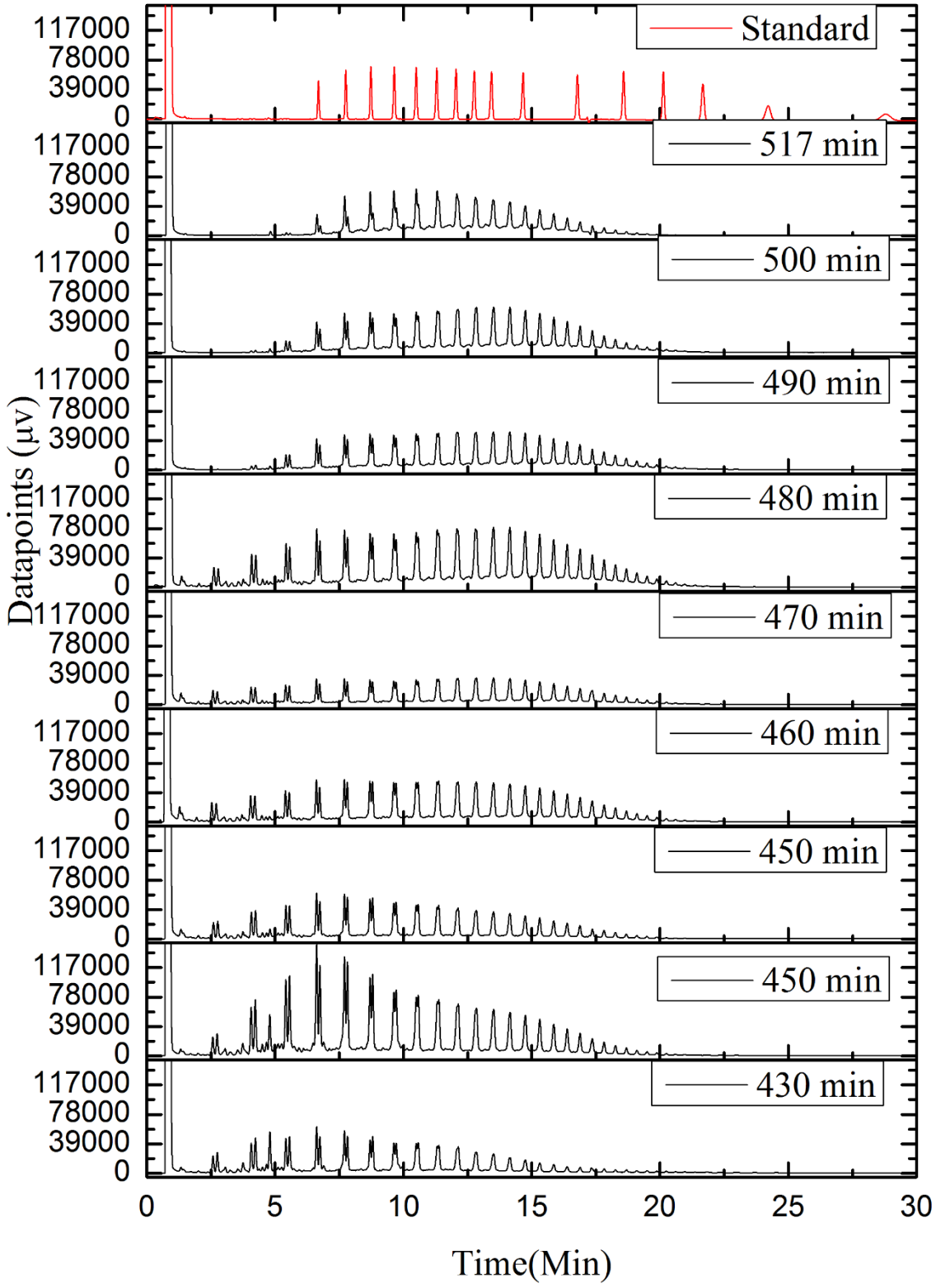

Fig. A. 9: GC (SimDist) spectra of PDOs obtained at different intervals of non-isothermal slow pyrolysis of virgin HDPE plastics (-) and standard paraffin sample (-)

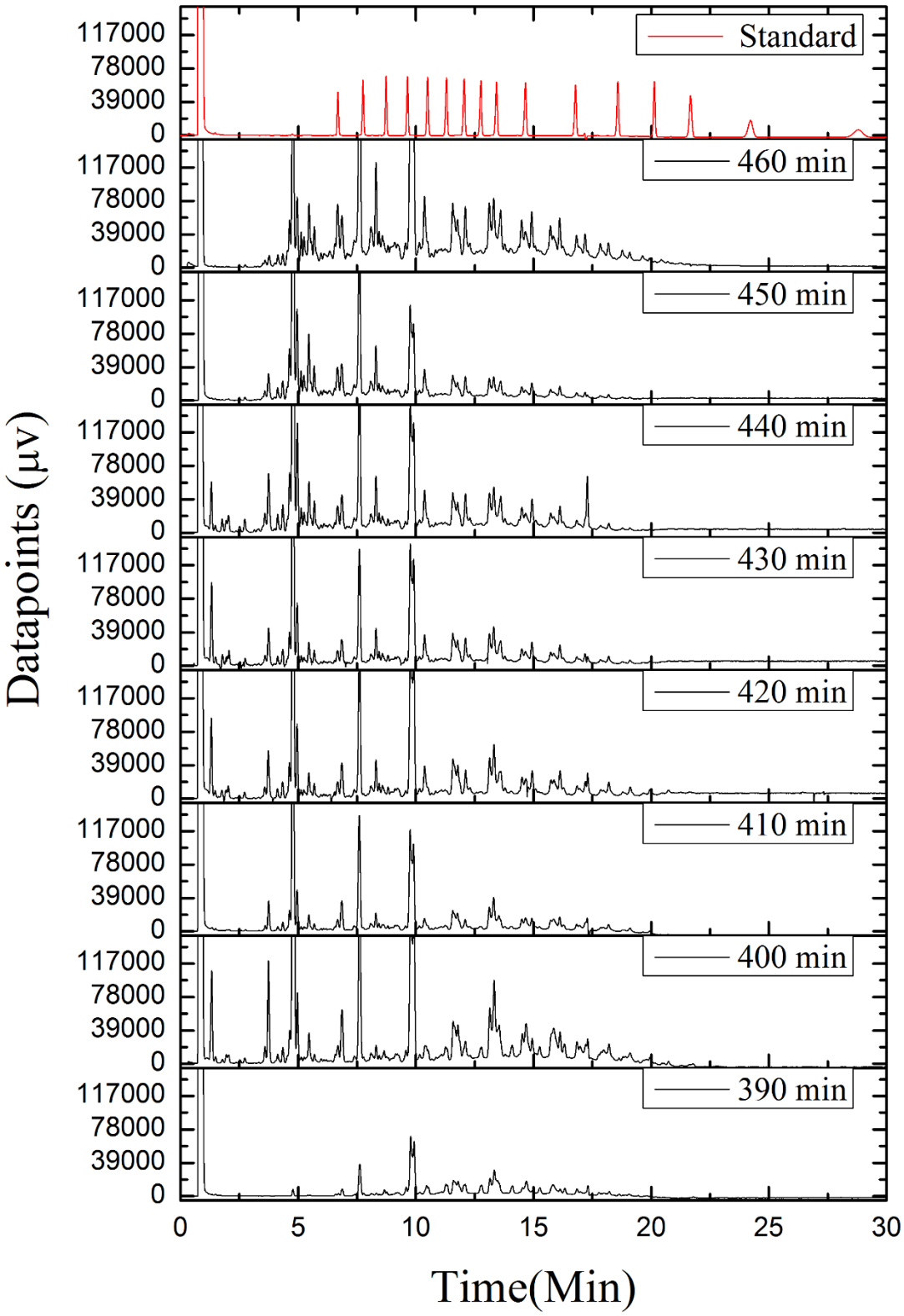

Fig. A. 10: GC (SimDist) spectra of PDOs obtained at different intervals of non-isothermal slow pyrolysis of virgin PP plastics (-) and standard paraffin sample (-)

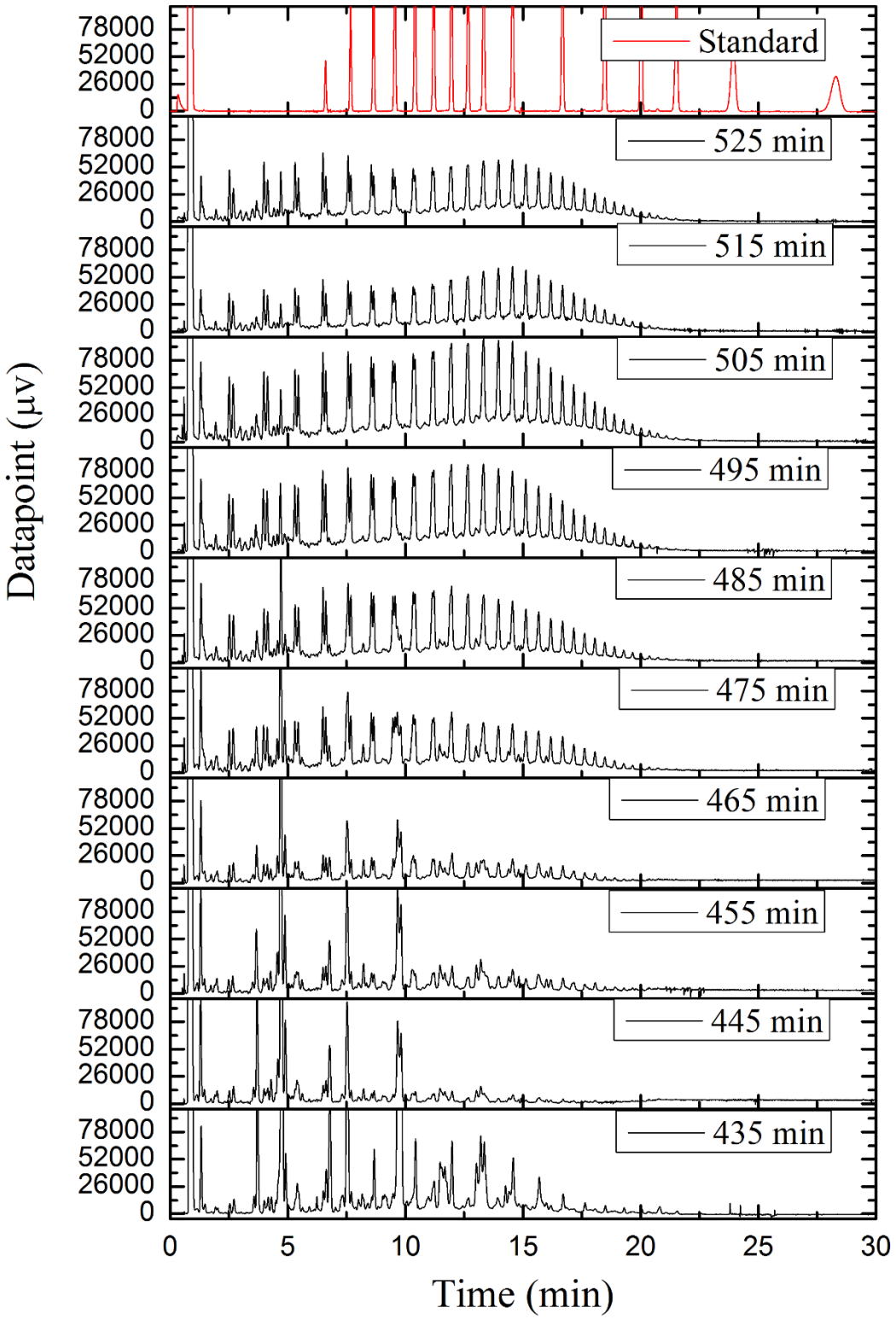

Fig. A. 11: GC (SimDist) spectra of PDOs obtained at different intervals of non-isothermal slow pyrolysis of VMIX sample (-) and standard paraffin sample (-)

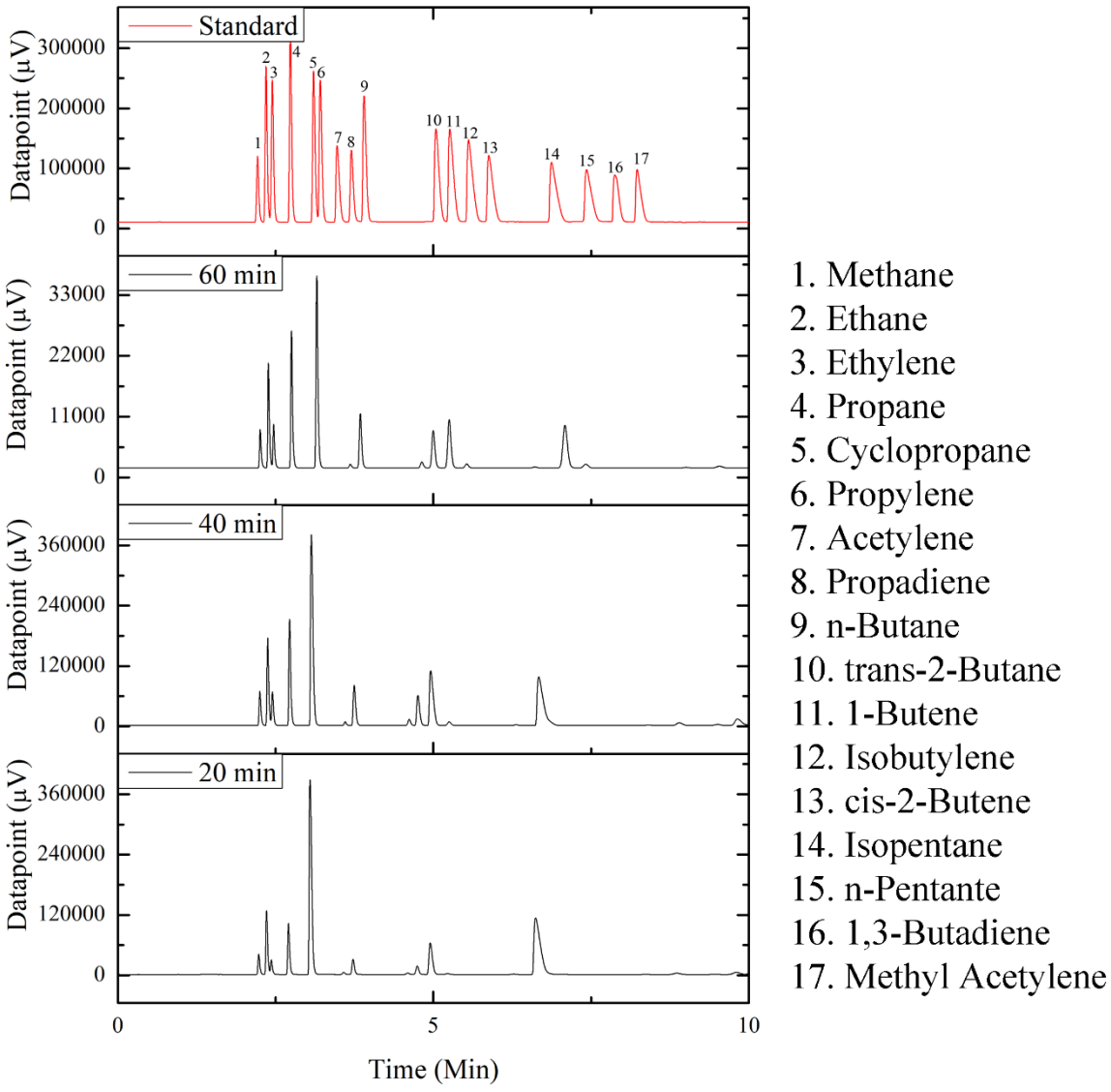

Fig. A. 12: Gas chromatographic spectra (FID) of the collected gases during the pyrolysis of RMIX at 375 °C along with the standard gas

Table A. 1: Composition (% vol) and GCV and NCV of gas derived from the pyrolysis of LDPE (virgin)

Gas components	400 °C	375 °C	350 °C
Methane	12.00	11.11	10.23
Ethane	14.23	15.57	16.92
Ethylene	7.40	6.46	5.522
Propane	13.20	12.31	11.41
Propylene	19.94	19.85	19.77
Propadiene	0.26	0.28	0.30
n-Butane	8.05	7.60	7.15
Trans-2-Butene	1.68	1.65	1.62
1-Butene	7.97	6.77	5.56
Isobutylene	2.25	2.93	3.60
cis-2-Butene	1.39	1.60	1.81
Isopentane	0.14	0.17	0.20
n-Pentane	7.19	10.63	14.08
Methyl Acetylene	1.46	0.99	0.51
Hydrogen	1.53	1.03	0.53
Carbon monoxide	0.22	0.27	0.32
Carbon-di-oxide	1.00	0.70	0.40
GCV (MJ/m^3)	91 ±1.05	93 ± 1.21	96 ± 0.92
NCV (MJ/m^3)	81 ±0.8	83 ± 0.68	86 ± 1.5

Table A. 2: Composition (% vol) and GCV and NCV of gas derived from the pyrolysis of HDPE (virgin)

Gas components	**400 °C**	**375 °C**	**350 °C**
Methane	6.73	7.69	8.65
Ethane	11.50	14.12	16.74
Ethylene	7.00	5.90	4.81
Propane	14.21	14.45	14.69
Propylene	23.28	20.99	18.71
Propadiene	0.29	0.25	0.21
n-Butane	9.41	7.41	5.41
Trans-2-Butene	2.17	1.47	0.77
1-Butene	8.68	5.83	2.98
Isobutylene	2.88	3.87	4.85
cis-2-Butene	1.76	1.20	0.63
Isopentane	0.15	0.02	-0.11
n-Pentane	9.50	11.46	13.41
Methyl Acetylene	1.02	0.62	0.21
Hydrogen	1.05	2.35	3.64
Carbon monoxide	0.10	0.76	1.42
Carbon-di-oxide	0.16	1.55	2.93
GCV (MJ/m^3)	98 ± 0.35	93 ± 1.8	89 ± 1.44
NCV (MJ/m^3)	89 ± 0.4	85 ± 0.66	80 ± 0.78

Table A. 3: Composition (% vol) and GCV and NCV of gas derived from the pyrolysis of PP (virgin)

Gas components	400 °C	375 °C	350 °C
Methane	3.40	3.38	3.36
Ethane	6.75	6.18	5.61
Ethylene	0.18	0.14	0.09
Propane	3.40	2.74	2.08
Propylene	50.47	39.67	28.88
Propadiene	0.45	0.36	0.27
n-Butane	0.32	0.23	0.14
Trans-2-Butene	0.004	0.01	0.02
1-Butene	0.24	0.18	0.12
Isobutylene	12.2	9.78	7.36
cis-2-Butene	0.002	0.004	0.01
Isopentane	0	0.04	0.07
n-Pentane	22.16	36.76	51.37
Methyl Acetylene	0.004	0.003	0.002
Hydrogen	0	0	0
Carbon monoxide	0.06	0.1	0.14
Carbon-di-oxide	0.33	0.39	0.45
GCV (MJ/m^3)	105 ± 1.22	112 ± 3.5	120 ± 5.41
NCV (MJ/m^3)	97 ± 0.77	103 ± 2.8	107 ±4.6

Table A. 4: Functional groups of the major peaks for hydrocarbons arrived in FTIR spectra

Wave number (cm-1)		bond		Gruoup	
3333-3267	strong	C-H	stretching	Alkyne	
3100-3000	medium	C-H	stretching	Alkene	
3000-2840	medium	C-H	stretching	Alkane	
2830-2695	medium	C-H	stretching	Aldehyde	doublet
2000-1650	weak	C-H	bending	aromatic compound	overtone
1678-1668	weak	C=C	stretching	Alkene	disubstituted
1675-1665	weak	C=C	stretching	Alkene	trisubstituted
1675-1665	weak	C=C	stretching	Alkene	tetrasubstituted
1662-1626	medium	C=C	stretching	Alkene	disubstituted (cis)
658-1648	medium	C=C	stretching	Alkene	vinylidene
1650-1600	medium	C=C	stretching	conjugated alken	
1650-1566	medium	C=C	stretching	cyclic alkene	
1648-1638	strong	C=C	stretching	Alkene	monosubstituted
1620-1610	strong	C=C	stretching	α,β-unsaturated ketone	
1465	medium	C-H	bending	Alkane	methylene group
1450 1375	medium	C-H	bending	Alkane	methyl group
1390-1380	medium	C-H	bending	Aldehyde	
1385-1380	medium	C-H	bending	Alkane	gem dimethyl
880 ± 20	strong	C-H	bending	1,2,4-trisubstituted	
880 ± 20	strong	C-H	bending	1,3-disubstituted	
810 ± 20	strong	C-H	bending	1,4-disubstituted or 1,2,3,4-tetrasubstituted	
780 ± 20 and (700 ± 20)	strong	C-H	bending	1,2,3-trisubstituted	

Publications

Journal publication:

i. Pallab Das and Pankaj Tiwari, 'Thermal degradation kinetics of plastics and model selection', Thermochimica Acta, Vol. 654, pp. 191-202 (2017).

ii. Pallab Das and Pankaj Tiwari, 'Valorization of packaging plastic waste by slow pyrolysis,' Resources, Conservation and Recycling, vol. 128, pp. 69-77 (2018).

iii. Pallab Das and Pankaj Tiwari, 'The effect of slow pyrolysis on the conversion of packaging waste plastics (PE and PP) into fuel,' Waste Management 79: 615-624 (2018).

iv. Pallab Das and Pankaj Tiwari, 'Thermal degradation study of Polyethylene terephthalate from waste soft drink bottles, under inert and oxidative environments,' Thermochimica Acta, 178340

Conference participation (national/international)

i. Pallab Das and Pankaj Tiwari, Experimental study of waste plastic pyrolysis. **Chemcon-2014**, Punjab University, Chandigarh, Punjab, India. (International)

ii. Pallab Das and Pankaj Tiwari. Valorization of packaging waste plastic by pyrolysis process in an experimental and model based study. **Chemcon-2015**, IIT Guwahati, Assam, India. (International)

iii. Pallab Das and Pankaj Tiwari. Pyrolysis of three common plastics and optimization of process parameters targeting value added hydrocarbon products. **MRSI symposium-2016**, CSIR-NEIST, Jorhat, Assam, India (International)

iv. Pallab Das and Pankaj Tiwari. Conversion of Plastic Waste into Fuel by Slow Pyrolysis. **Advances and Challenges in Energy Technologies**, RGIPT, Raebareli, UP, India (International)

v. Pallab Das and Pankaj Tiwari. Kinetics of thermal degradation of plastic waste and their conversion into liquid fuel by slow pyrolysis, Symposium on Advances in Sustainable Polymers 2017 (**ASP 2017**), IIT Guwahati, Assam, India (International)

vi. Pallab Das and Pankaj Tiwari. Valorisation of packaging plastic waste by slow pyrolysis. **National conference on non-conventional energy: Harvesting technology and its challenges**, 2017, Assam Engineering College, Guwahati, Assam, India (National)

vii. Pallab Das and Pankaj Tiwari, "Waste plastics: Thermal degradation kinetics and lab scale pyrolysis," **ISCRE**, Florence, Italy, 2018 (International)